

Broken Lefschetz Fibrations, Lagrangian matching invariants and Ozsváth-Szabó Invariants

by

Yankı Lekili

Bachelor of Arts, Bilkent University (2004)

Maîtrise, École Normale Supérieure de Lyon (2005)

Submitted to the Department of Mathematics
in partial fulfillment of the requirements for the degree of

Doctor of Philosophy

at the

MASSACHUSETTS INSTITUTE OF TECHNOLOGY

June 2009

© Yankı Lekili, MMIX. All rights reserved.

The author hereby grants to MIT permission to reproduce and to distribute publicly paper and electronic copies of this thesis document in whole or in part in any medium now known or hereafter created.

Author.....

Department of Mathematics

April 27, 2009

Certified by.....

Denis Auroux

Associate Professor of Mathematics

Thesis Supervisor

Accepted by.....

David S. Jerison

Chairman, Department Committee on Graduate Students

Broken Lefschetz Fibrations, Lagrangian matching invariants and Ozsváth-Szabó Invariants

by

Yankı Lekili

Submitted to the Department of Mathematics
on April 27, 2009, in partial fulfillment of the
requirements for the degree of
Doctor of Philosophy

Abstract

Broken Lefschetz fibrations are a new way to depict smooth 4-manifolds and to investigate their topology; for instance, Perutz defines invariants of 4-manifolds by counting J-holomorphic sections of these fibrations. The first part of this thesis is about the calculus of these objects. In particular, based on earlier results we prove the existence of broken Lefschetz fibrations on any smooth oriented closed 4-manifold and describe certain topological manipulations of these objects, to construct new broken Lefschetz fibration, e.g. with better properties from other ones.

The second part is about Perutz's invariants for broken Lefschetz fibrations, the corresponding invariants for 3-manifolds mapping to S^1 , and relating these invariants to Ozsváth-Szabó's 3 and 4-manifold invariants. Specifically, we prove an isomorphism between two 3-manifold invariants, namely Perutz's quilted Floer homology and Ozsváth-Szabó's Heegaard Floer homology for certain spin^c structures. This yields interesting and in a sense simplified geometric interpretations of Ozsváth-Szabó invariants. In particular, we give new calculations of these invariants and other applications, e.g. a proof of Floer's excision theorem in the context of Heegaard Floer homology.

Thesis Supervisor: Denis Auroux
Title: Associate Professor of Mathematics

Acknowledgements

Foremost, I would like to thank my supervisor Denis Auroux for his generosity with time and ideas throughout the past three years. I am also indebted to Matthew Hedden, Robert Lipshitz, Peter Ozsváth and Tim Perutz for valuable discussions at various points during the completion of this thesis.

On a broader level, I would like to thank Peter Kronheimer, Tomasz Mrowka, Paul Seidel and Katrin Wehrheim for their contributions to my knowledge of mathematics and fellow students Andrew Cotton-Clay, Sheel Ganatra, Maksim Lipyanskiy, Maksim Maydanskiy and James Pascaleff for invaluable informal discussions.

I cannot end without thanking my family, on whose constant encouragement and support I have relied throughout my life. Finally, I am grateful to Nadia for all the necessary distractions.

Contents

1	Introduction	7
2	Broken Lefschetz fibrations	9
2.1	Introduction	9
2.1.1	Near-symplectic manifolds	9
2.1.2	Wrinkled fibrations	11
2.1.3	Seiberg–Witten invariants and Lagrangian matching invariants	17
2.2	A local modification on wrinkled fibrations	19
2.3	A set of deformations on wrinkled fibrations	24
2.4	Generic deformations of wrinkled fibrations and $(1, 1)$ –stability	38
2.5	The corresponding deformations on near-symplectic manifolds	41
2.6	Applications	48
2.7	A summary of moves and further questions	55
3	Heegaard Floer homology of broken fibrations over the circle	57
3.1	Introduction	57
3.1.1	(Perturbed) Heegaard Floer homology	59
3.1.2	Quilted Floer homology of a 3–manifold	61

3.2	Heegaard diagram for a circle-valued broken fibrations on Y	64
3.2.1	A standard Heegaard diagram	64
3.2.2	Splitting the Heegaard diagram	72
3.2.3	Calculations for fibred 3-manifolds and C_{right}	77
3.3	The isomorphism	84
3.3.1	A variant of Heegaard Floer homology for broken fibrations over the circle	85
3.3.2	Isomorphism between $QFH'(Y, f; \Lambda)$ and $HF^+(Y, f, \gamma_w)$. . .	88
3.3.3	An application to sutured Floer homology	96
3.4	Isomorphism between $QFH(Y, f; \Lambda)$ and $QFH'(Y, f; \Lambda)$	99
3.4.1	Heegaard tori as composition of Lagrangian correspondences .	100
3.4.2	Floer's excision theorem	108
3.4.3	4-manifold invariants	110
A	Classification of $(1, 1)$-stable unfoldings	112
B	Heegaard tori as compositions of Lagrangian correspondences	117

List of Figures

2-1	Local modification	20
2-2	Handle decomposition of the total space	22
2-3	Creation of a circle singularity along with two point singularities . . .	25
2-4	Merging singular circles	27
2-5	Flipping	29
2-6	Wrinkling	32
2-7	The fibre as a double branched cover	33
2-8	Local Deformation	35
2-9	Reference fibres	37
2-10	Merging of zero-circles along the path α	50
2-11	Making the fibres connected	51
2-12	Table of Moves	56
3-1	Heegaard surface for a broken fibration	65
3-2	The curves $(\bar{\xi}_{2i-1}, \bar{\xi}_{2i}), (\bar{\eta}_{2i-1}, \bar{\eta}_{2i})$	67
3-3	Torus bundles	79

Chapter 1

Introduction

Over the past 20 years, low-dimensional topology has seen an explosion of activity due to its relevance to gauge theory in physics, the study of local symmetries of quantum fields. Donaldson constructed invariants of smooth four-manifolds in his pioneering work on Yang-Mills theory. In the subsequent years, several related invariants were constructed, notably Seiberg-Witten invariants, Heegaard Floer invariants and Hutchings's embedded contact homology proved to be very powerful in answering many long standing conjectures in low-dimensional topology. Although much is developed in each of these theories, which are all conjectured to be isomorphic, a deeper understanding of the interplay between them has only recently become accessible. In particular, one of the most recent results in this direction is Taubes's construction of an isomorphism between Seiberg-Witten-Floer homology and embedded contact homology. Each theory elucidates different aspects of low dimensional topology, thus an isomorphism between them allows us to use the power of both theories to prove new theorems. In this thesis, we study another such Floer theoretic invariant developed

by Donaldson and Smith for symplectic manifolds and later generalized by Perutz to the more general spaces where the above theories apply. The crucial difference of this theory is the emphasis on symplectic techniques. The main protagonists in this approach are (suitably generalized) Lefschetz fibrations and pseudoholomorphic curves. The main result of this thesis is an isomorphism between the 3-manifold invariants associated to this theory and their counterparts in Heegaard Floer theory for certain spin^c structures. This reveals new features of Heegaard Floer theory and implies strong relations between Heegaard Floer theory and Periodic Floer homology, which itself is isomorphic to Seiberg-Witten-Floer homology (this follows from an extension of the above mentioned theorem of Taubes). As a prologue to this main result, we have also done more foundational work on broken Lefschetz fibrations and their Floer theoretic invariants.

In Chapter 2, we study topological aspects of broken Lefschetz fibrations. The main theorem we prove is that every smooth 4-manifold admits a broken Lefschetz fibration. We further give a set of moves which allows one to relate two different broken Lefschetz fibrations on a given 4-manifolds.

In Chapter 3, we study broken fibrations on a 3-manifold and a Floer theoretical invariant of three-manifolds associated with such a fibration, which we call *quilted Floer homology*. The main theorem that we prove is an isomorphism between quilted Floer homology and Heegaard Floer homology for certain spin^c structures.

Furthermore, the proofs of some of the more technically involved results are provided in Appendix A and B.

Chapter 2

Broken Lefschetz fibrations

2.1 Introduction

2.1.1 Near-symplectic manifolds

Let X be a smooth, oriented 4-manifold. Then a closed 2-form ω is called *near-symplectic* if $\omega^2 \geq 0$ and there is a metric g such that ω is self-dual harmonic and transverse to the 0-section of Λ^+ . Equivalently, without referring to any metric, one could define a closed 2-form ω to be near-symplectic if for any point $x \in X$ either $\omega_x^2 > 0$, or $\omega_x = 0$, and the intrinsic gradient $(\nabla\omega)_x: T_x X \rightarrow \Lambda^2 T_x^* X$ has maximal rank, which is 3. The zero-set Z of such a 2-form is a 1-dimensional submanifold of X . If X is compact and $b_2^+(X) > 0$ then Hodge theory gives a near-symplectic form ω on X . Clearly, in this case Z is just a collection of disjoint circles. Furthermore, by deforming ω , one can show that on any near-symplectic manifold, one can reduce the number of circles to 1, this was proved in [30]. We give a new

proof of this result in Theorem 2.6.1 as an application of the techniques developed in this chapter. Of course, the last circle cannot be removed unless the underlying manifold is symplectic.

Interesting topological information about X is captured by the natural decomposition of the normal bundle of these circles, provided by the near-symplectic form. More precisely, transversality of ω implies that $\nabla\omega: N_Z \rightarrow \Lambda^+X$ is an isomorphism, where N_Z is the normal bundle to the zero-set of ω . This enables us to orient the zero-set Z . Now consider the quadratic form $N_Z \rightarrow \mathbb{R}, v \rightarrow \langle \iota(z)\nabla_v\omega, v \rangle$, where z is a non-vanishing oriented vector field on Z . As $dw = 0$, this quadratic form is symmetric and has trace zero. It follows that, it has three real eigenvalues everywhere, where two are positive and one is negative. Then $N_Z = L^+ \oplus L^-$, where L^\pm are the positive and negative eigen-subbundles respectively. In particular, this allows us to divide the zero-set into two pieces, the even circles where the line bundle L^- is orientable, and the odd circles where L^- is not orientable. This definition is motivated by the following result of Gompf that the number of even circles is equal to $1 - b_1 + b_2^+$ modulo 2 [30]. In particular, observe that if there is only one zero circle which is even, the manifold X cannot be symplectic.

In this chapter, we will be interested in local deformations of near-symplectic forms on a 4-manifold. An important such deformation is provided by the Luttinger–Simpson model given on $D^4 \subset \mathbb{R}^4$ where the birth (or death) of a circle can be observed explicitly [30]:

$$\begin{aligned} \omega_s &= 3\epsilon(x^2 + t^2 - s)(dt \wedge dx + dy \wedge dz) + 6\epsilon y(tdt \wedge dz + xdx \wedge dz) \\ &\quad - 2z(dx \wedge dy + dt \wedge dz) + 2y(dt \wedge dy + dz \wedge dx) \end{aligned}$$

for $\epsilon \leq \frac{1}{6}$.

We will see that this is not the only type of deformation of near-symplectic forms. One of the goals of this chapter is to identify such deformations and interpret them in terms of the singular fibrations associated to them.

2.1.2 Wrinkled fibrations

A *broken fibration* on a closed 4-manifold X is a smooth map to a closed surface with singular set $A \sqcup B$, where A is a finite set of singularities of Lefschetz type where around a point in A the fibration is locally modeled in oriented charts by the complex map $(w, z) \rightarrow w^2 + z^2$, and B is a 1-dimensional submanifold along which the singularity of the fibration is locally modeled by the real map $(t, x, y, z) \rightarrow (t, x^2 + y^2 - z^2)$, B corresponding to $t = 0$. We remark here that we do not require the broken fibrations to be embeddings when restricted to their critical point set. In particular, this means that the critical value set may include double points.

There have been two different approaches to constructions of broken fibrations on 4-manifolds. The first approach is by Auroux, Donaldson and Katzarkov [4] based on approximately holomorphic techniques, generalizing the construction of Lefschetz pencils on symplectic manifolds. The more recent approach is due to Gay and Kirby [10], where the fibration structure is constructed explicitly in two pieces in the form of open books, and then Eliashberg's classification of overtwisted contact structures as well as Giroux's theorem of stabilization of open books are invoked to glue these two pieces together to form an achiral broken fibration. Achiral here refers to the existence of finitely many Lefschetz type singularities with the opposite orientation on the domain, namely the singularity is modeled by the complex map $(w, z) \rightarrow$

$$\bar{w}^2 + z^2.$$

There is a correspondence between broken fibrations and near-symplectic manifolds up to blow-up, in analogy with the correspondence between Lefschetz fibrations and symplectic manifolds up to blow-up. More precisely, given a broken fibration on a 4-manifold X with the property that there is a class $h \in H^2(X)$ such that $h(F) > 0$ for every component F of every fibre, it is possible to find a near-symplectic form on X such that the regular fibres are symplectic and the zero-set of the near-symplectic form is the same as the 1-dimensional critical point set of the broken fibration. This is an adaptation due to Auroux, Donaldson and Katzarkov of Gompf's generalization of Thurston's argument used in finding a symplectic form on a Lefschetz fibration. Conversely, in [4], it is proven that on every 4-manifold with $b_2^+(X) > 0$ (recall that this is equivalent to X being near-symplectic), there exists a broken fibration if we blow up enough. One of the questions of interest that remains to be answered is to determine how unique this broken fibration is. In particular, we would like to find a set of moves on broken fibrations relating two different broken fibrations on a given 4-manifold. One of the main themes of this chapter is the discussion of a set of moves which allows one to pass from one broken fibration structure to another.

In this chapter, we will consider a slightly more general type of fibration, where we will allow cuspidal singularities on the critical value set of the fibration. These type of fibrations occur naturally when one considers deformations of the broken fibrations. We will also discuss a local modification of a cuspidal singularity (without changing the diffeomorphism type of the underlying manifold structure) in order to get a broken fibration. Therefore, one can first deform a broken fibration to obtain a wrinkled fibration, then apply certain moves to this wrinkled fibration, and finally modify the wrinkled fibration in a neighborhood of cuspidal singularities to get a

genuine broken fibration. In this way, one obtains a set of moves on broken fibrations on a given 4–manifold.

Let X be a closed 4–manifold, and Σ be a 2–dimensional surface. We say that a map $f: X \rightarrow \Sigma$ has a *cuspl singularity* at a point $p \in X$, if around p , f is locally modeled in oriented charts by the map $(t, x, y, z) \rightarrow (t, x^3 - 3xt + y^2 - z^2)$. This is what is known as the Whitney tuck mapping, the critical point set is a smooth arc, $\{x^2 = t, y = 0, z = 0\}$, whereas the critical value set is a cusp, namely it is given by $C = \{(t, s): 4t^3 = s^2\}$. This is the generic model for a family of functions $\{f_t\}$, which are Morse except for finitely many values of t [3]. The signs of the terms y^2 and z^2 are chosen so that the functions f_t have only index 1 or 2 critical points. More precisely, if $f: \mathbb{R}^3 \rightarrow \mathbb{R}$ is a Morse function with only index 1 or 2 critical points, then $F: \mathbb{R}^4 \rightarrow \mathbb{R}^2$ given by $(t, x, y, z) \rightarrow (t, f(x, y, z))$ is a broken fibration with critical set in correspondence with the critical points of f . Notice that the functions $f_t(x, y, z) = x^3 - 3xt + y^2 - z^2$ are Morse except at $t = 0$, where a birth of critical points occur.

Definition 2.1.1. *A wrinkled fibration on a closed 4–manifold X is a smooth map f to a closed surface which is a broken fibration when restricted to $X \setminus C$, where C is a finite set such that around each point in C , f has cuspl singularities. We say that a fibration is purely wrinkled if it has no isolated Lefschetz-type singularities.*

It might be more appropriate to call these fibrations “broken fibrations with cusps”, to avoid confusion with the terminology introduced by Eliashberg-Mishachev [9]. The reason for our choice of terminology is that wrinkled fibrations can typically be obtained from broken Lefschetz fibrations by applying wrinkling moves (see move 4 in Section 2.3) which eliminates a Lefschetz type singularity and introduces a

wrinkled fibration structure. Conversely, as mentioned above, it is possible to locally modify a wrinkled fibration by smoothing out the cusp singularity at the expense of introducing a Lefschetz type singularity and hence get a broken fibration.

Theorem 2.1.2.

- a) *Every wrinkled fibration is homotopic to a broken fibration by a homotopy supported near cusp singularities.*
- b) *Every broken fibration is homotopic to a purely wrinkled fibration by a homotopy supported near Lefschetz singularities.*

The first part of this chapter is concentrated on a set of moves on wrinkled fibrations and corresponding moves on broken fibrations. All of these moves keep the diffeomorphism type of the total space unchanged. We remark here that as will be explained below these moves occur as deformations of wrinkled fibrations and not as deformations of broken fibrations. To be more precise, by a *deformation* of wrinkled fibrations we mean a one-parameter family of maps which is a wrinkled fibration for all but finitely many values of the parameter. In fact, as we will see, an infinitesimal deformation of a broken fibration gives a wrinkled fibration whereas the wrinkled fibrations are stable under infinitesimal deformations. This is indeed the main reason for extending the definition of the broken fibrations to wrinkled fibrations.

In the second part, using techniques from singularity theory, we prove that our list of moves is complete in the sense that any generic infinitesimal deformation of a wrinkled fibration which does not have any Lefschetz type singularity is given by one of the moves that we exhibited in Section 2.3. Furthermore, as we will see in Section 2.3, it is always possible to deform a wrinkled fibration infinitesimally so that the Lefschetz type singularities are eliminated.

Theorem 2.1.3.

- a) *Any one-parameter family deformation of a purely wrinkled fibration is homotopic rel endpoints to one which realizes a sequence of births, merges, flips, their inverses and isotopies staying within the class of purely wrinkled fibrations.*
- b) *Given two broken fibrations, suppose that after perturbing them to purely wrinkled fibrations, the resulting fibrations are deformation equivalent. Then one can get from one broken fibration to the other one by a sequence of birth, merging, flipping and wrinkling moves, their inverses and isotopies staying within the class of broken fibrations.*

As in the case of broken fibrations, one can define a wrinkled pencil on X to be a wrinkled fibration $f: X \setminus P \rightarrow \Sigma$, where P is a finite set and around a point in P , the fibration is locally modeled in oriented charts by the complex map $(w, z) \rightarrow w/z$. Note that, after blowing up X at the points P , one can get a wrinkled fibration. It is possible to construct a natural near-symplectic form that is “adapted” to a given wrinkled pencil. The key property of this form is that it should restrict to a symplectic form on the smooth fibres of the given wrinkled fibration. Therefore, we can equip every wrinkled pencil with a well-defined deformation class of near-symplectic forms, it is natural thus to study what happens to this class after each move that was described on the previous paragraph. This will be discussed Section 2.5 of this chapter.

In Section 2.6, we give a number of applications of our moves on broken fibrations. Notably, by considering the mirror image of the wrinkling move, we prove that we can turn an achiral Lefschetz singularity into a wrinkled map and then into a bro-

ken fibration, without losing equatoriality of the round handles. This provides the following simplification of the result of Gay and Kirby in [10]:

Theorem 2.1.4. *Let X be an arbitrary closed 4-manifold and let F be a closed surface in X with $F \cdot F = 0$. Then there exists a broken Lefschetz fibration from X to S^2 with embedded singular locus, and having F as a fibre. Furthermore, one can arrange so that the singular set on the base consists of circles parallel to the equator with the genera of the fibres in increasing order from one pole to the other.*

We remark that this disproves the conjecture 1.2 of Gay and Kirby in [10] about the essentialness of including achiral Lefschetz singularities for broken fibrations on arbitrary closed 4-manifolds.

After the first writing of this chapter, an earlier result of a similar nature, but allowing the set of critical values of the fibration to be immersed rather than embedded, has been obtained by Baykur in [5]. Namely, Baykur proved an existence theorem for broken fibrations with immersed critical value set by combining the following two ingredients: (1) a result of Saeki [37] which says that any continuous map from a closed 4-manifold $X \rightarrow S^2$ is homotopic to a stable map without definite folds, i.e. in our terminology, a purely wrinkled fibration with immersed critical value set, (2) the cusp modification described in Section 2.2 of this chapter.

Another recent development that took place after the writing of this chapter is worth mentioning here: Akbulut and Karakurt [2] came up with a new proof of the existence theorem stated above by refining the construction of Gay and Kirby. The difference between Akbulut and Karakurt's result and ours is that they directly construct a broken fibration on any 4-manifold, whereas we describe a way to modify achiral Lefschetz singularities into broken and Lefschetz singularities.

Finally, here we would like to discuss our main motivation for studying the particular structure of broken fibrations and their deformations, the wrinkled fibrations.

2.1.3 Seiberg–Witten invariants and Lagrangian matching invariants

In [8], Donaldson and Smith define an invariant of a symplectic manifold X by counting holomorphic sections of a relative Hilbert scheme that is constructed from a Lefschetz fibration on a blow-up of X . More precisely, by Donaldson’s celebrated theorem, there exists a Lefschetz fibration $f: X' \rightarrow S^2$, where X' is some blow-up of X . Then, for any natural number r , Donaldson and Smith give a construction of a relative Hilbert scheme $F: X_r(f) \rightarrow S^2$, where the fibre over a regular value p of f is the symmetric product $\Sigma^r(f^{-1}(p))$. In fact, $X_r(f)$ is a resolution of singularities for the relative symmetric product, which is the fibration obtained by taking the r^{th} symmetric product of each fibre. They then define their standard surface count, which is some Gromov invariant counting pseudoholomorphic sections of $X_r(f)$. Usher, in [42], proves that this invariant is the Gromov invariant of the underlying symplectic 4–manifold X . Finally, we know that this is in turn equal to the Seiberg-Witten invariant of X by the seminal work of Taubes [41]. Therefore, one obtains a geometric formulation of the Seiberg-Witten invariant for a symplectic manifold X on a Lefschetz fibration structure associated to X , which also shows in particular that this invariant is independent of the Lefschetz fibration structure.

A similar but technically not so straightforward generalization of this method of getting an invariant from a Lefschetz fibration is described in [31] for the case of broken fibrations, thus giving an invariant for all smooth 4–manifolds with $b_2^+(X) >$

0. These are called Lagrangian matching invariants. Here we give a quick sketch of the definition of these invariants.

Suppose X is a near-symplectic manifold with only one zero circle Z , and $f: X \rightarrow S^2$ is a broken fibration with one circle of singularity along the equator of S^2 . Take out a thin annulus neighborhood of the equator and write N and S for the closed discs that contain the north pole and the south pole respectively. Let $X^N = f^{-1}(N)$ and $X^S = f^{-1}(S)$, suppose the fibre genus of X^N is g and the fibre genus of X^S is $g - 1$. Consider the relative Hilbert schemes $\text{Hilb}_N^r(X^N)$ and $\text{Hilb}_S^{r-1}(X^S)$. These are symplectic manifolds with boundaries $Y_r^N = \Sigma_{S^1}^r(\partial X^N)$ and $Y_{r-1}^S = \Sigma_{S^1}^{r-1}(\partial X^S)$, respectively.

Perutz then constructs a sub-fibre bundle \mathcal{Q} of the fibre product $Y_r^N \times_{S^1} Y_{r-1}^S \rightarrow S^1$ which constitutes the Lagrangian boundary conditions for the pairs of pseudoholomorphic sections of $\text{Hilb}_N^r(X^N)$ and $\text{Hilb}_S^{r-1}(X^S)$ in the following sense : One defines $\mathcal{L}_{X,f}$ to be a Gromov invariant for pairs (u_N, u_S) of pseudoholomorphic sections of $\text{Hilb}_N^r(X^N)$ and $\text{Hilb}_S^{r-1}(X^S)$ such that the boundary values $(u_N|_{\partial N}, u_S|_{\partial S})$ lie in \mathcal{Q} .

Now, the big conjecture in this field is of course the conjecture that Lagrangian matching invariants equal the Seiberg-Witten invariants. This has been verified by Perutz, [31], in several cases, notably in the case of symplectic manifolds as mentioned above, and when the underlying manifold is of the form $S^1 \times M^3$, for any M which is a \mathbb{Z} -homology- $(S^1 \times S^2)$ and for connected sums.

An important problem to be explored is that the Lagrangian matching invariant is not yet known to be an invariant of the given 4-manifold. In other words, it is an invariant of the near-symplectic manifold together with a given broken fibration

structure. Our next task in this field will be to show that the Lagrangian matching invariant stays an invariant under the set of moves that we describe in this chapter. We believe that our set of moves will be enough to pass from a given broken fibration structure on a manifold to any other broken fibration structure on the same manifold under suitable hypotheses on the homotopy type of the fibration map. We have strong evidence for this since, as was mentioned above, the set of moves that we discuss in this chapter are sufficient to pass from a given broken fibration to any one-parameter deformation of it. These two hypotheses would imply that the Lagrangian matching invariant is really an invariant of the underlying manifold. We believe that these steps will play an important role in proving the big conjecture mentioned above.

2.2 A local modification on wrinkled fibrations

Recall from the introduction that a cusp singularity is given locally by the map $F: \mathbb{R}^4 \rightarrow \mathbb{R}^2$ given by:

$$(t, x, y, z) \rightarrow (t, x^3 - 3xt + y^2 - z^2)$$

The critical point set is a smooth arc, $\{x^2 = t, y = 0, z = 0\}$, whereas the critical value set is a cusp, namely it is given by $C = \{(t, s): 4t^3 = s^2\}$.

The idea is to modify a neighborhood of the singular point of the cusp with an allowed model for broken fibrations without changing the topology. We will do this by surgering out a neighborhood of the cuspidal singularity and gluing back in a neighborhood of an arc together with a Lefschetz type singular point as shown in Figure 1. The issue is to make sure that the fibration structures match outside the

neighborhood.

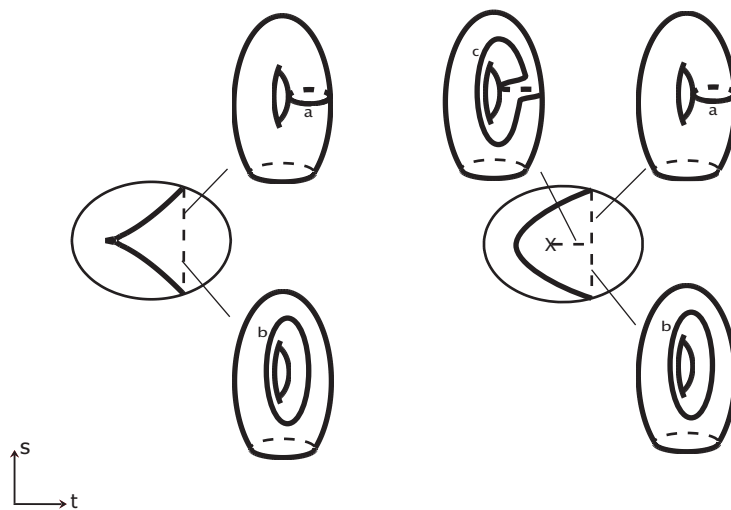


Figure 2-1: Local modification

Restricting to a neighborhood of the origin, we get a map $F: D^4 \rightarrow D^2$ and C divides the image into two regions, where the fibres above the “interior region” are punctured tori, whereas the fibres above the “exterior region” are discs, as shown in Figure 1. Furthermore, looking above the line $\{t = \frac{1}{2}\}$, one sees that as the parameter s converges to C from below, $s \rightarrow \frac{1}{\sqrt{2}}$, one of the generating loops of the homology of the torus collapses to a point, and as s converges to C from above, $s \rightarrow -\frac{1}{\sqrt{2}}$ the other generator collapses to a point. This is evident from the fact that $f_{1/2}(x, y, z) = x^3 - \frac{3}{2}x + y^2 - z^2$ restricted to the preimage of $\{t = \frac{1}{2}\}$ is a Morse function on D^3 with 2 critical points of indices 1 and 2 which cancel each other.

Now consider the D^2 -valued broken fibration structure described on the right of Figure 1. Let us denote this fibration by $p: X \rightarrow D^2$. This fibration is cooked up so that it matches above a neighborhood of the boundary of D^2 with the fibre structure of the map F . On the other hand, by introducing a Lefschetz type singularity, we are

able to have a broken fibration structure, where the vanishing cycles are described on the right of the Figure 1. In order to perform a local surgery to pass from the map F to the described broken fibration p , it remains to show that the total space X is diffeomorphic to D^4 . This will be accomplished by giving a handle decomposition of X , and showing that it is in fact obtained by attaching one 1–handle and one 2–handle to D^4 , in such a way that they can be cancelled.

Let us now describe X explicitly. Denote the standard loops generating homology of a regular fibre by a and b . As shown in Figure 1, restricting to the line $\{t = \frac{1}{2}\}$, as s approaches to C from below, a collapses to a point and as s approaches to C from above, b collapses. (This is to be consistent with the fibre structure of F .) Now the monodromy around the Lefschetz type singularity must be the Dehn twist along $c = a - b$, denoted by τ_{a-b} so that $\tau_{a-b}(a) = b$, where we oriented a and b so that $a \cdot b = -1$. Therefore, restricting to the line $s = 0$, as t approaches to the singularity $a - b$ collapses to a point. (Here by $c = a - b$ we really denote an embedded loop c which is equal to $[a - b]$ as a homology class.) We remark here that, just as in Lefschetz fibrations, a diagram indicating the fibre structure and vanishing cycles along relevant paths is enough to determine a broken (or wrinkled) fibration uniquely on a disc. We now have an explicit understanding of the various vanishing cycles for X . Next we proceed to describe the corresponding handle diagram. We first restrict to the preimage of the region shown in Figure 2. This is clearly diffeomorphic to the total space X . Now divide this region into 3 parts as shown in Figure 2. The preimage of region 0 is just $D^2 \times D^2 = D^4$. We claim that the preimage of regions 0 and 1 together is $D^4 \cup 1$ –handle, and the preimage of all three regions is $D^4 \cup 1$ –handle \cup 2–handle in such a way that the attaching sphere of the 2–handle intersects the belt sphere of the 1–handle transversely at a single point, so that these two handles

can be cancelled.

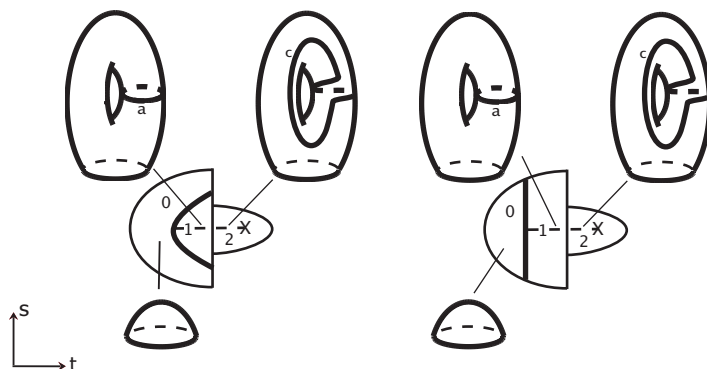


Figure 2-2: Handle decomposition of the total space

In this picture, it is more convenient to fix the reference fibre above a point which lies between regions 1 and 2 as shown in the Figure 2. Just for simplicity, we can choose an identification of this reference fibre with the previous choice using the parallel transport along a simple arc above the Lefschetz singularity so that the vanishing cycles in this new reference fibre are given as shown. Finally, observe that we can isotope the base so that the 1-dimensional singular set is straightened to a line.

Next, we are in a position to see the handle decomposition very explicitly. In fact, the preimage of the regions 0 and 1 can be thought as $(D^3 \cup 1\text{-handle}) \times D^1$, where the D^1 is the s direction. The belt circle of this 3-dimensional 1-handle corresponds to the vanishing cycle a on a regular fibre above the region 1, to be precise, fix the regular fibre F above a point p in region 1, say p lies on the $s = 0$ line. Now $(D^3 \cup 1\text{-handle}) \times D^1 = D^4 \cup 1\text{-handle}$ where the belt sphere of this latter 4-dimensional 1-handle intersects F at a . Now, by construction starting from F as one approaches to Lefschetz singularity the loop c collapses to a point. It is a standard fact of Lefschetz fibrations that gluing the preimage of region 2 corresponds to a 2-dimensional handle attachment with attaching circle being the loop c on F

[11]. (In fact, if one considers the local model $(z, w) \rightarrow z^2 + w^2$, then $Re(z^2 + w^2)$ is a Morse function with one critical point of index 2 at the origin.) Therefore, we conclude that $X = D^4 \cup 1\text{-handle} \cup 2\text{-handle}$ with belt sphere of the 1-handle intersects the attaching circle of the 2-handle transversely at exactly one point, and this intersection point is precisely the intersection of the loop a and the loop c on F . Finally, applying the cancellation theorem of handle attachments, we conclude that $X = D^4$ as required.

It is of interest to note that one could as well replace a cusp singularity with a broken arc singularity and an achiral Lefschetz singularity, where vanishing cycles for the cusp are given by a and b as before, and the vanishing cycle for the achiral Lefschetz singularity is given by $c = a + b$ (since one must now have $\tau_c^{-1}(a) = -b$). The difference between a Lefschetz singularity and an achiral Lefschetz singularity with the same vanishing cycle is in the framing of the corresponding 2-handle attachment. Namely, a Lefschetz singularity corresponds to -1 -framing with respect to the fibre framing whereas an achiral Lefschetz singularity corresponds to $+1$ -framing. The cancellation theorem of handle attachments does not see the framings, therefore the proof is verbatim.

We remark here that the local modification described in this section is not given as a deformation, in the sense that we have not explained how to give a one-parameter family of wrinkled fibrations which starts from the fibration depicted on the left side of Figure 1 and ends at the fibration given on the right side of Figure 1. We will actually give such a family in the next section, which will in fact give yet another way of proving the validity of the above move. However, we chose to present the above proof first, as it is considerably simpler and in fact this enabled the author to discover more complicated modifications described in Section 2.3, which come equipped

with deformations. Afterwards, we were able to recover the above modification as a composition of these deformations.

2.3 A set of deformations on wrinkled fibrations

In this section, we describe a set of moves on wrinkled fibrations. We first give three such moves which are deformations of wrinkled fibrations and the corresponding deformations which end up being broken fibrations are obtained by applying the modification described in Section 2.2, which as was mentioned there, is indeed a deformation. Note that this was not proved in the previous section. This will be accomplished after we describe the last move which enables us to turn a Lefschetz singularity into three cusp singularities.

Move 1 (Birth) : Consider the wrinkling map $F_s : \mathbb{R} \times \mathbb{R}^3 \rightarrow \mathbb{R}^2$, as defined in [9] :

$$(t, x, y, z) \rightarrow (t, x^3 + 3(t^2 - s)x + y^2 - z^2)$$

For $s < 0$, this is a genuine fibre bundle, i.e., there is no singularity. At $s = 0$, the only singularity is at the origin. This is a degenerate map, which is not an allowed singularity for a wrinkled fibration. For $s > 0$, the critical point set of F_s is the circle $\{x^2 + t^2 = s, y = z = 0\}$, whereas the critical value set C_s is a *wrinkle* shown on the left of Figure 3. This is clearly a wrinkled map. Therefore, we have a deformation of wrinkled maps, the only subtle change being at $s = 0$, where birth of the wrinkle happens.

Now, fix $s = 1$. Considering the wrinkle as obtained from gluing two cusps together,

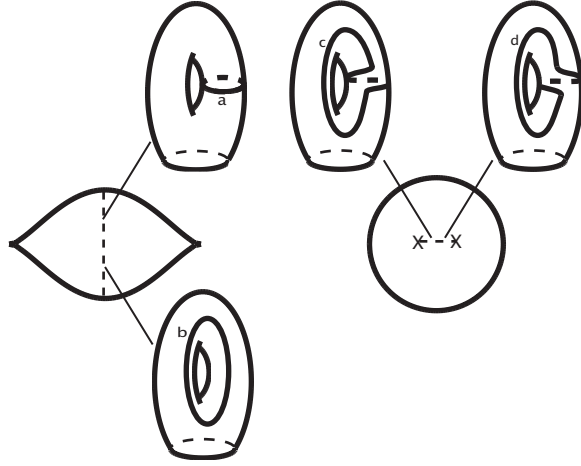


Figure 2-3: Creation of a circle singularity along with two point singularities

we can apply the local modification of Section 2.2 to obtain a broken fibration on \mathbb{R}^4 with singular set a circle together with two point singularities as shown on the right of Figure 3. Note that one has to check that the configuration of the vanishing cycles matches the model in Section 2.2. Conveniently, we can check this on the vertical line $t = 0$. Then the map becomes $(0, x, y, z) \rightarrow (0, x^3 - 3x + y^2 - z^2)$, and this is the same map that was used in Section 2.2, therefore the configuration of the vanishing cycles matches the model in Section 2.2. Namely, on $t = 0$, the two vanishing cycles obtained from approaching to C from below and from above starting from the origin, intersect transversely at a point.

Thus, given a broken fibration on any 4-manifold, we can restrict the fibration to a D^2 on the base where the fibration is regular, and also restrict the fibres to obtain $D^2 \times D^2$. Then, apply the move just described to obtain a new fibration, where the singular set is changed by an addition of a circle and two points. Furthermore, the fibre genus above the points in the interior of this new singular circle increases by 1.

We remark that this move on broken fibrations was first observed by Perutz in proposition 1.4 of [31], where he proves that the total space of the closed fibre case of the fibration on the right of Figure 3 is diffeomorphic to $S^2 \times S^2$. Here, we were able to divide this move into two pieces by allowing cusp singularities, which indicates that the local move of Section 2.2 is a more basic move.

Move 2 (Merging) : Let us now describe another move which corresponds to merging two singular circles to obtain one circle together with two Lefschetz type singularities. We begin with the local picture described on the left side of Figure 4. The lines which separate regions on the base indicate the critical value set. The vanishing cycles obtained from moving towards the upper line and moving towards the lower line are assumed to intersect transversely at a singular point. The standard model for such a broken fibration $F: \mathbb{R}^4 \rightarrow \mathbb{R}^2$ is given by the map $(t, x, y, z) \rightarrow (t, x^3 - 3x + y^2 - z^2)$. The critical value set of this map is given by two horizontal lines, and the configuration of the vanishing cycles is as described. Now consider the map $F_s: \mathbb{R} \times \mathbb{R}^3 \rightarrow \mathbb{R}$ defined by:

$$(t, x, y, z) \rightarrow (t, x^3 + 3(s - t^2)x + y^2 - z^2)$$

Then for $s < 0$, F_s is isotopic to F , with the critical value set being $C = \{(t, u) : 4(t^2 - s)^3 = u^2\}$. For $s < 0$, C consists of two simple curves and is isotopic to the left side of Figure 4. At $s = 0$, as before, we have a more degenerate map. This is where a subtle change in the fibration structure occurs. For $s > 0$, we get a wrinkled map with critical value set, including two cusp singularities, isotopic to the model depicted in the middle part of Figure 4. Note that the picture on Figure 4 is drawn

so that the maps are equal outside of a neighborhood of the origin, to ensure that when restricted to D^4 , the maps agree on a neighborhood of the boundary. Finally, we apply the local modification model from Section 2.2 to each cuspidal singularity to get a new broken fibration. Therefore, we obtain a move of broken fibrations, namely whenever one has the configuration described on the left side of Figure 4, one can surger out a D^4 and glue in the right side of Figure 4 to obtain a new configuration.

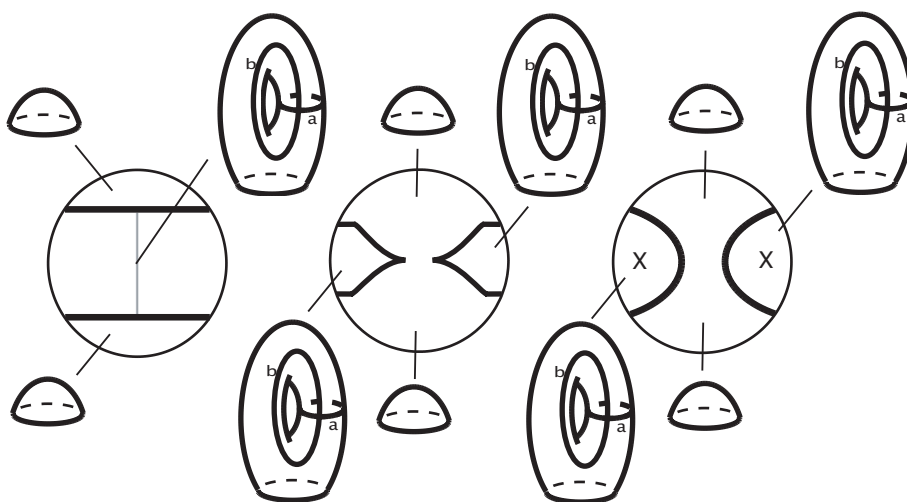


Figure 2-4: Merging singular circles

We remark here that to apply a merging move, one needs a configuration as in the left side of Figure 4, in particular it is necessary that the vanishing cycles intersect transversely at a unique point. On the other hand, to apply an inverse merging move the following two conditions are necessary. Referring to the right part of Figure 4, one needs to make sure that, fixing a reference fibre halfway along a path connecting the Lefschetz singularity and the broken singularity on the left, the vanishing cycles for the Lefschetz singularity and the broken singularities should intersect transversely at a point. Exactly the same configuration is required on the right side of the fibration.

However, we would like to point out that there is no compatibility condition required for the two sides as long as the fibres in the middle region are connected. Namely, to give an embedding of the fibration depicted on the right side of Figure 4 into a fibration that has the same base and whose vanishing cycles satisfy the condition described above, one divides the base into three pieces: a piece on the left that includes the Lefschetz singularity and the broken singularity, a middle piece which is a smooth fibration, and a piece on the right which includes the Lefschetz singularity and the broken singularity. Since the vanishing cycles are as prescribed above, it is easy to construct a fibrewise embedding of the total spaces of the pieces on the left and on the right. Namely, given two simple closed curves intersecting transversely at one point on a fibre F , it is always possible to find a diffeomorphism of F such that those two curves are standardized, in the sense that they sit in the standard way as part of an embedding of a punctured torus to F . Finally in order to give an embedding of the total space of the middle piece, one needs to give a fibrewise embedding of the disc fibration $D^2 \times D^2$ such that, if we consider the base D^2 as $[0, 1]^2$, the embedding is already prescribed above $\{0, 1\} \times [0, 1]$. But now, it is easy to extend this to a fibrewise embedding of $D^2 \times D^2$ by just flowing the fibers above $\{0\} \times [0, 1]$ to fibres above $\{1\} \times [0, 1]$ since the set of embeddings of D^2 to a fibre F is clearly connected provided that F is connected.

Move 3 (Flipping) : This move is originally due to Auroux. The observation was that for a given near-symplectic manifold (X, ω) , if one considers possible broken fibrations adapted to (X, ω) , the rotation number of the image of a given component of the zero-set of ω is not fixed a priori. If one considers a one-parameter family of deformations of broken fibrations, one can possibly get a flip through a real cusp.

However, here we discuss this move in an alternative way to the original approach, using the local modification discussed in Section 2.2. Consider the map $F_s: \mathbb{R} \times \mathbb{R}^3 \rightarrow \mathbb{R}^2$ given by:

$$(t, x, y, z) \rightarrow (t, x^4 - x^2s + xt + y^2 - z^2)$$

Then for $s < 0$, the critical value set consists of a simple curve and F_s is isotopic to the map described on the left side of Figure 5. At $s = 0$, we have a higher order singularity and as before this is where a subtle change in the fibration structure occurs. For $s > 0$, we get a wrinkled map with critical value set, including two cusp singularities, isotopic to the model depicted in the middle part of Figure 5. This map still induces an immersion on the critical point set away from the cusp singularities, however now we have a double point as shown in Figure 5.

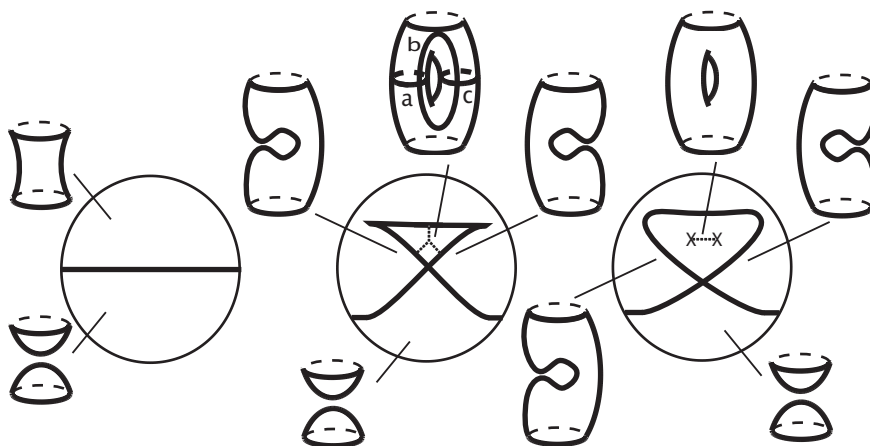


Figure 2-5: Flipping

One can fix a reference fibre in the interior region (the high-genus region) as in the middle portion of Figure 5 so that the vanishing cycles for the three paths drawn are the given loops a , b , c . Indeed, we know from the local model of a cusp singularity that the vanishing cycles corresponding to each branch of a cusp intersect

transversely once. Therefore, the vanishing cycle for the path going up intersects both the vanishing cycle for the lower left path and the vanishing cycle for the lower right path transversely at a point. Furthermore, we know that the two latter vanishing cycles are disjoint since the critical point set in the total space is embedded, and they cannot be homotopic, since otherwise the fibres above the bottom region would have a sphere component. Now, once these intersection properties are understood, it is easy to see that there is a diffeomorphism of the twice punctured torus that sends any configuration of three simple closed curves satisfying the above properties to a , b and c .

On the right side of Figure 5, it follows from monodromy considerations (recall that the monodromy around a Lefschetz singularity is the Dehn twist along the vanishing cycle) as in Section 2.2 that the vanishing cycles for Lefschetz type singularities are as follows: Going along the line segment that connects the two singularities, as one approaches the singularity on the left, the cycle $a + b$ vanishes, and as one approaches the singularity on the right, the cycle $c - b$ vanishes.

Now, we will pass to another kind of deformation which is different in nature from the ones that are described above. Note that for a general smooth map $F: \mathbb{R}^4 \rightarrow \mathbb{R}^2$, the differential $dF_p: \mathbb{R}^4 \rightarrow \mathbb{R}^2$ at a critical point p can have rank either 0 or 1. If the rank is 1, then around p we can find local coordinates such that F is of the form $(t, x, y, z) \rightarrow (t, f(t, x, y, z))$ by the inverse function theorem. Similarly, any perturbation F_s of F around p can be expressed in the form $(t, x, y, z) \rightarrow (t, f_s(t, x, y, z))$. Therefore, the above moves involved the case where the deformation is focused around a critical point p of F such that dF has rank 1. In the case of a wrinkled fibration, these are precisely the points lying in the 1-dimensional part of the critical point set. In fact, any generic deformation around such a critical point is

given by one of the above deformations in some coordinate chart. We will elaborate more on this point in the next section using techniques from singularity theory. Our next move will be deforming F around a point p such that dF_p vanishes. For our purposes, these correspond to deforming a wrinkled fibration around a Lefschetz type singularity.

Move 4 (Wrinkling) : Around a Lefschetz type singularity, we have oriented charts where $F: \mathbb{R}^4 \rightarrow \mathbb{R}^2$ is given by $(t, x, y, z) \rightarrow (t^2 - x^2 + y^2 - z^2, 2tx + 2yz)$, or in complex coordinates $u = t + ix$ and $v = y + iz$, F is given by $(u, v) \rightarrow u^2 + v^2$. Now the simplest non-trivial deformation of such a map is given by the map $F_s: \mathbb{C}^2 \rightarrow \mathbb{C}$ defined by

$$(u, v) \rightarrow u^2 + v^2 + s\text{Re}u$$

or in real coordinates:

$$(t, x, y, z) \rightarrow (t^2 - x^2 + y^2 - z^2 + st, 2tx + 2yz)$$

The stability of this map follows from a standard result in singularity theory, see Morin ([24]). Therefore, the family F_s , for $s \in [0, 1]$, indeed gives us a family of wrinkled fibrations. The critical points of F_s are the solutions of $x^2 + t^2 + \frac{st}{2} = 0, y = z = 0$. This circle can be parametrized by $t = -\frac{s}{4}(1 + \cos \theta), x = \frac{s}{4} \sin \theta$, and the critical value set is given by $\{(-\frac{s^2}{8}(1 + \cos \theta)(2 - \cos \theta), -\frac{s^2}{8}(1 + \cos \theta) \sin \theta) : \theta \in [0, 2\pi]\}$. It is easily checked that this equation defines a curve with 3 cusps. F_0 is the standard map around a Lefschetz type singularity, and F_s for $s > 0$ is a wrinkled fibration with 3 wrinkles as shown in Figure 6. We will refer to the critical value set of this map as triple cuspid.

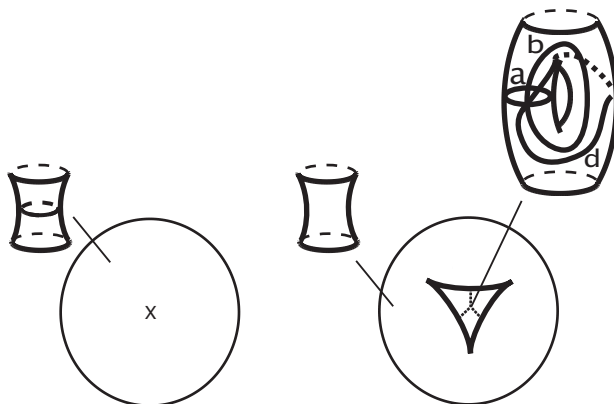


Figure 2-6: Wrinkling

The vanishing cycles are a , b and $d = b + c$, where a, b and d are depicted on the right side of Figure 6. The curves a , b and c , which also appear in the middle picture of Figure 5, are taken to be the standard set of generators for the doubly punctured torus. As shown in Figure 6, we can in fact arrange so that d passes through the intersection point of a and b and intersects a and b transversely at that point.

The importance of this configuration is that all three cycles intersect at a point transversely and there is no path connecting the two boundary components of the doubly punctured torus that does not intersect these three cycles. More precisely, given a configuration of 3 simple closed curves on a doubly punctured torus with this property, there is a diffeomorphism of the doubly punctured torus which brings the set of curves to the curves a , b and d as in Figure 6 (d is a simple closed curve that is homologous to $b + c$ and passes through the intersection point of a and b).

A way to see that the vanishing cycles are as claimed is by considering the fibre above a point w as a double covering of \mathbb{C} branched along 2 or 4 points depending on whether w lies outside of the triple cuspid or in the interior region bounded by the triple cuspid. Specifically, the fibre above w is given by $v^2 = w - u^2 - s\text{Re}u$,

and projecting to the u component gives a double cover of \mathbb{C} branched along $\{u \in \mathbb{C} : u^2 + s\text{Re}u = w\}$. Let $w = w_1 + iw_2$, then in real coordinates one can express the branch locus as:

$$\begin{aligned} t^2 - x^2 + st &= w_1 \\ 2tx &= w_2 \end{aligned}$$

For the rest of the argument, assume for simplicity that $s = 2$. Take a regular value lying in the interior region of the critical values of F_s , such as $w = (w_1, w_2) = (-1/2, 0)$. Connect this to the exterior by the arc of points $(-k/2, 0)$, $k \in [1, 3]$. One can calculate that the branch points are given by either $t = 0$, and $x = \pm\sqrt{k/2}$, or $x = 0$, and $t = -1 \pm \sqrt{4 - 2k}/2$. Note that, when $k < 2$, we have four branch points (fibre is double punctured torus), and when $k > 2$ we have two (fibre is cylinder). The change is the first two branch points corresponding to $t = 0$ more or less stay the same, whereas the branch points corresponding to $x = 0$ come together along a segment and disappear when $k > 2$.

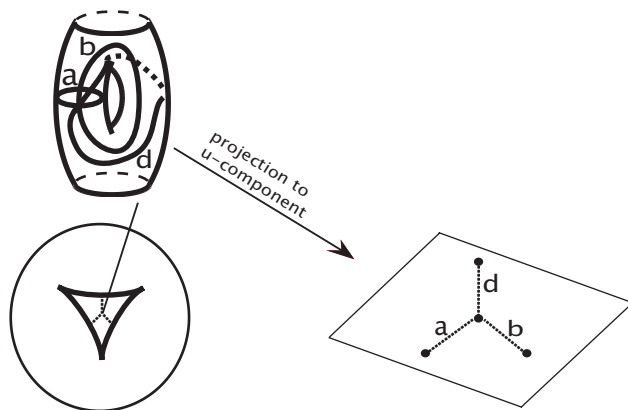


Figure 2-7: The fibre as a double branched cover

To get the other vanishing cycles one has to vary w in other directions. The second

one can be obtained by $w_1 = -1/2$ and $w_2 = 2k$ where k goes from 0 to 1 and the third one can be obtained by $w_1 = -1/2$ and $w_2 = 2k$ where k goes from 0 to -1 . One can then see that depending on k we get 4 branch points if we are in the interior region of the critical values or we have 2 solutions if we are in the exterior. Corresponding to each of the two variations as above, there are two points in the branch locus which come together whereas the other two stay more or less the same. More precisely, one can verify that corresponding to each direction, the four branch locus points collapse either along a , b or d as described in Figure 7.

The preimages of these paths by the branched covering map are precisely the vanishing cycles which were also denoted by a , b and d on the doubly punctured torus (Figure 7). Hence one concludes that the three vanishing cycles intersect transversely at a point. Moreover, it is easy to see by explicit calculation as above that as one approaches a cuspidal point for the fibration F_s , in the branched covering picture three of the four branch points come together. For example, if the vanishing cycles a and b collapse as one approaches a cusp singularity of F_s , then the end points of the paths a and b come together in the base of the branched cover picture. Reversing our viewpoint, as one crosses a cusp singularity from the low-genus side to the high-genus side the topology of the fibres of F_s is modified by a surgery in a neighborhood of a point in the fibre, which is the preimage of one of the two branch points of the double branched covering map. More precisely, the surgery that we mean is removing a tubular disc neighborhood of a point and gluing back in a punctured torus. We will use this important observation in the next paragraph.

Deformation of a wrinkled fibration to a broken fibration

Now, we are ready to prove that the local modification of Section 2.2 can be ob-

tained by a combination of merging, flipping and wrinkling deformations. Therefore, as promised the local modification given in Section 2.2 is also a deformation of wrinkled fibrations. The outcome of this paragraph is the statement that any wrinkled fibration can be deformed to obtain a genuine broken fibration.

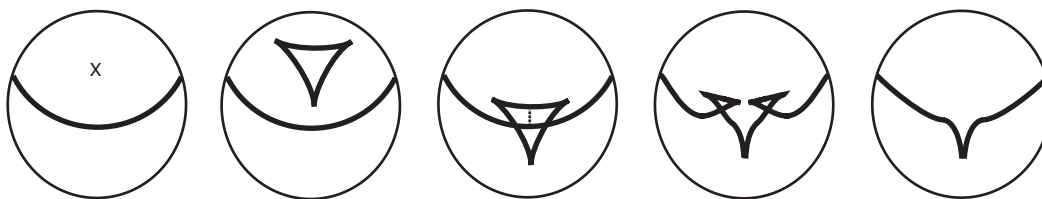


Figure 2-8: Local Deformation

Following Figure 8, first we deform the Lefschetz singularity to a triple wrinkle by applying the wrinkling deformation. Now the key observation here is that we can arrange so that the vanishing cycles corresponding to the bottom cusp of the triple cuspid do not interfere with the vanishing cycle corresponding to the arc we started with. We will explain this in detail below. Therefore, we can isotope the fibration to the third picture in Figure 8. Next, we will verify that one can perform a merging move along the dotted line depicted in the third picture in Figure 8. For this one just needs to verify that the relevant vanishing cycles are in the correct configuration so as to match with the starting point of the local model for the merging move. This will allow us to pass to the fourth picture. Finally, we perform two flipping moves to get to the final result that we wanted.

Let us now describe the missing pieces of the proof in more detail. First, let's see why one can isotope the second fibration to the third fibration in Figure 8. For this, we will need to identify various vanishing cycles for the second fibration and observe indeed that the vanishing cycles corresponding to the bottom cusp do not interfere with

the vanishing cycle corresponding to the arc. For the fibration that we start with, fix a reference fibre at a point p halfway between the Lefschetz singularity and the singular arc. Recall that the fibre is a punctured torus, and without loss of generality we can assume that the vanishing cycle for the Lefschetz singularity is the a curve and moving towards the arc singularity the b curve vanishes, where a and b are drawn on the left side of in Figure 9. Now, let's apply the wrinkling move to the Lefschetz singularity. Consider a line segment from p to a central point q of the triple wrinkle passing through a cusp point (drawn as a dotted line on the right side of Figure 9). As described in the previous section, starting from p if we move along this line segment the fibre above p undergoes a surgery around a neighborhood of a point on the fibre and the genus increases by 1. Now since the wrinkling move only affects a tubular neighborhood of the curve a , after the modification of the Lefschetz singularity by wrinkling move we can choose a reference fibre that is based at the point q which looks like the one drawn in the middle of Figure 9. In particular, the part of the fibre above p outside of the tubular neighborhood of a is canonically identified to the part of the fibre above q outside the doubly punctured torus that appeared after surgery. More importantly, this latter surgery occurs around a neighborhood of a point which can be isotoped (if necessary) to be disjoint from the b curve. Hence one can parallel transport the b curve from the fibre above p to the fibre above q , since the place where the surgery occurs is disjoint from the curve b . In particular, the image of b in the fibre above q is disjoint from the vanishing cycles that correspond to the cusp singularity, which are two simple closed curves on the doubly punctured torus which intersect transversely, we denote them by α and β . Therefore, by applying a diffeomorphism of the doubly punctured torus if necessary the reference fibre above q can be chosen as shown on the right side of Figure 9. Now, it is clear that one can isotope the second fibration to the third fibration in Figure 8, since the vanishing

cycle b is disjoint from α and β .

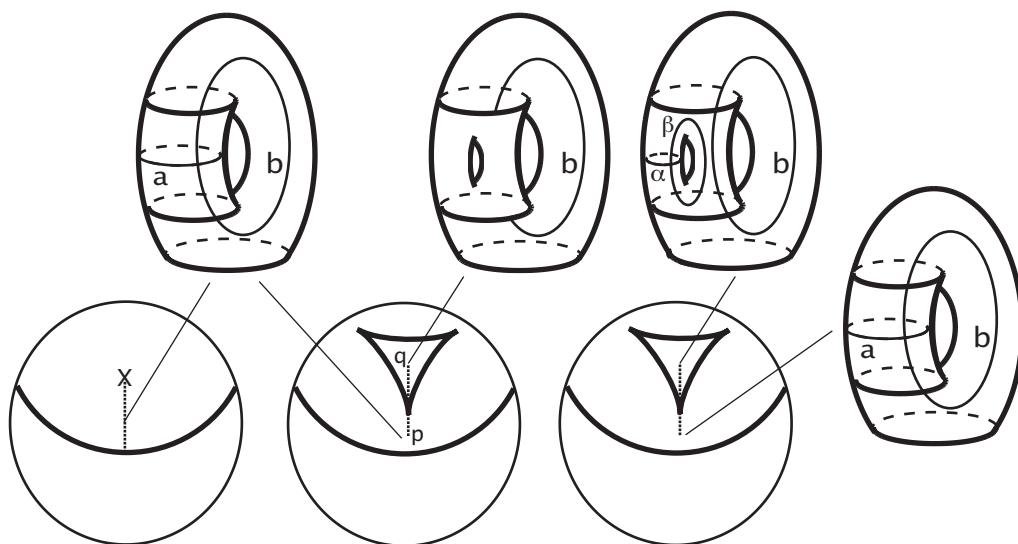


Figure 2-9: Reference fibres

Next, to pass from the third fibration to the fourth fibration in Figure 8, we use a merging move. In order to do that, we need to understand the vanishing cycles above the dotted line segment in the third picture in Figure 8. Choose a reference fibre above a point in the middle of the dotted line segment. As before, we can standardize it so that it looks like the right side of Figure 9. Now, as one goes down the curve b vanishes and as one goes up the vanishing cycle γ has the properties that it lies in the doubly punctured torus, intersects α and β at their intersection point and any path connecting the boundary circles of the doubly punctured torus has to intersect the union of α , β and γ . Therefore, comparing Figure 9 with Figure 6, b has to intersect γ once. Hence we can perform a merging move.

Finally, we apply two flipping moves to the fourth fibration in Figure 8 to pass to the fifth fibration. These are also allowed, since the configuration of α , γ , b and the configuration of β , γ , b match the configuration of a , b , c in Figure 5 of the flipping

move. This completes the proof of the fact that the fibration on the left of Figure 8 is a deformation of the fibration on the right.

2.4 Generic deformations of wrinkled fibrations and $(1, 1)$ –stability

In this section, we prove that the set of moves listed in the Section 2.3 are sufficient to produce any deformation of wrinkled fibrations. More precisely, we prove the following theorem:

Theorem 2.4.1. *Let X be a compact 4–manifold, and let $F_s: X \rightarrow \Sigma$ be a deformation of wrinkled fibrations. Then it is possible to deform F_0 to F_1 by applying to F_0 a sequence of the four moves described in Section 2.3 and isotopies staying within the class of wrinkled fibrations.*

Proof. First, observe that we can get rid of the Lefschetz type singularities of F_0 and F_1 using the wrinkling move. So we can assume that F_0 and F_1 have no Lefschetz type singularities. Also, since Lefschetz type singularities are unstable under small deformations, we can assume that the deformation does not create any new Lefschetz singularity. More precisely, we perturb the deformation by keeping the end points fixed so that we avoid any creation of critical points where dF_s vanishes. This is possible since purely wrinkled fibrations are stable under small perturbation whereas the existence of points where dF_s vanishes is not generic. Therefore, we have reduced to the case where F_s is a wrinkled fibration except for finitely many values of s such that F_s has no Lefschetz singularity for all s . So, we can assume that around a critical point p of F_{s_0} for any $s_0 \in [0, 1]$, we have coordinate charts

so that for $s \in [s_0 - \epsilon, s_0 + \epsilon]$, $F_s: \mathbb{R}^4 \rightarrow \mathbb{R}^2$ is given by $(t, x, y, z) \rightarrow (t, f_s(t, x, y, z))$ and $f_{s_0}(0) = df_{s_0}(0) = 0$. We will next show that generically f_s is given by one of the 3 models described in Section 2.3 corresponding to the moves birth, merging and flipping. For this, we will introduce the notion of $(1, 1)$ -stable unfoldings following Wasserman [43] and give a classification of such maps using the machinery developed in [43], which in turn is based on the celebrated classification of unfoldings by Thom.

Definition 2.4.2. *Let $f: \mathbb{R}^5 \rightarrow \mathbb{R}$ and $g: \mathbb{R}^5 \rightarrow \mathbb{R}$ be map germs with $f(0) = g(0) = 0$. With f we associate a germ $F: \mathbb{R}^5 \rightarrow \mathbb{R}^3$, defined by $F(s, t, x, y, z) = (s, t, f(s, t, x, y, z))$. Similarly we associate a germ $G: \mathbb{R}^5 \rightarrow \mathbb{R}^3$ with g , given by $G(s, t, x, y, z) = (s, t, g(s, t, x, y, z))$. We say that f and g are $(1, 1)$ -equivalent if there are germs at 0, $\Phi \in \text{Diff}(\mathbb{R}^5)$, $\Lambda \in \text{Diff}(\mathbb{R}^3)$ and $\psi \in \text{Diff}(\mathbb{R}^2)$, and $\phi \in \text{Diff}(\mathbb{R})$ fixing the origin such that the following diagram commutes:*

$$\begin{array}{ccccccc} \mathbb{R}^5 & \xrightarrow{F} & \mathbb{R}^3 & \xrightarrow{p} & \mathbb{R}^2 & \xrightarrow{q} & \mathbb{R} \\ \Phi \downarrow & & \Lambda \downarrow & & \psi \downarrow & & \phi \downarrow \\ \mathbb{R}^5 & \xrightarrow{G} & \mathbb{R}^3 & \xrightarrow{p} & \mathbb{R}^2 & \xrightarrow{q} & \mathbb{R} \end{array}$$

where $p: \mathbb{R}^3 \rightarrow \mathbb{R}^2$ is the projection onto the first factor and $q: \mathbb{R}^2 \rightarrow \mathbb{R}$ is the projection onto the first factor.

Note that if a one-parameter family deformation F_s of wrinkled fibrations is represented by $(t, x, y, z) \rightarrow (t, f(s, t, x, y, z))$ in some coordinate charts and g is $(1, 1)$ -equivalent to f , then we can find coordinate charts such that the deformation is represented by $(t, x, y, z) \rightarrow (t, g(s, t, x, y, z))$ in these new coordinate charts. Therefore, in order to complete the proof of theorem 2.4.1, we need a classification theorem of generic functions up to $(1, 1)$ -equivalence, which we state after making precise what

generic means.

Definition 2.4.3. Let $\mathcal{E}(\mathbb{R}^n, \mathbb{R}^p)$ = set of germs at 0 of smooth mappings from $\mathbb{R}^n \rightarrow \mathbb{R}^p$. Let $\mathcal{E}(s, t, x, y, z) = \mathcal{E}(\mathbb{R}^5, \mathbb{R})$, $\mathcal{E}(s, t) = \mathcal{E}(\mathbb{R}^2, \mathbb{R})$, $\mathcal{E}(s) = \mathcal{E}(\mathbb{R}, \mathbb{R})$ such that the labels reflect the parameters that we are using.

Let $f: \mathbb{R}^5 \rightarrow \mathbb{R}$ with $f(0) = 0$ and let $F: \mathbb{R}^5 \rightarrow \mathbb{R}^3$ be given by $F(s, t, x, y, z) = (s, t, f(s, t, x, y, z))$. We say that f is infinitesimally $(1, 1)$ -stable if

$$\mathcal{E}(s, t, x, y, z) = \left\langle \frac{\partial f}{\partial x}, \frac{\partial f}{\partial y}, \frac{\partial f}{\partial z} \right\rangle \mathcal{E}(s, t, x, y, z) + \left\langle \frac{\partial f}{\partial t} \right\rangle \mathcal{E}(s, t) + \left\langle \frac{\partial f}{\partial s} \right\rangle \mathcal{E}(s) + F^* \mathcal{E}(\mathbb{R}^3, \mathbb{R}).$$

One may interpret this condition geometrically as saying roughly that the “tangent space” at f to the $(1, 1)$ -equivalence class of f is maximal, i.e. is equal to the “tangent space” to the unique maximal ideal in $\mathcal{E}(\mathbb{R}^5, \mathbb{R})$ consisting of the set of germs f such that $f(0) = 0$.

We remark here that by Theorem 3.15 in [43] any perturbation of a $(1, 1)$ -stable germ in weak C^∞ -topology can be represented by a $(1, 1)$ -stable germ. Therefore, in this sense, a generic deformation will be $(1, 1)$ -stable.

Theorem 2.4.4. Let $f: \mathbb{R}^5 \rightarrow \mathbb{R}$ be a $(1, 1)$ -stable germ with $f(0) = 0$. Then f is

(1, 1)–equivalent to one of the following functions as germs:

$$\begin{aligned}
 h_0(s, t, x, y, z) &= \pm x^2 \pm y^2 \pm z^2 && \text{Morse singularity} \\
 h_1(s, t, x, y, z) &= x^3 + tx \pm y^2 \pm z^2 && \text{Cusp singularity} \\
 h_2(s, t, x, y, z) &= x^3 + t^2x + sx \pm y^2 \pm z^2 && \text{Birth move} \\
 h_3(s, t, x, y, z) &= x^3 - t^2x + sx \pm y^2 \pm z^2 && \text{Merging move} \\
 h_4(s, t, x, y, z) &= x^4 + x^2s + xt \pm y^2 \pm z^2 && \text{Flipping move}
 \end{aligned}$$

The proof of Theorem 2.4.4 is given in the Appendix A. This completes the proof of Theorem 2.4.1 where the signs in the statement of Theorem 2.4.4 are determined by imposing the condition that the maps become wrinkled fibrations.

2.5 The corresponding deformations on near-symplectic manifolds

Theorem 2.5.1. *Let X be a compact 4–manifold, and let $f: X \setminus P \rightarrow \Sigma$ be a wrinkled pencil. Let Z denote the 1–dimensional part of the critical value set of f . Suppose that there exists a cohomology class $h \in H^2(X)$ such that $h(F) > 0$ for every component F of every fibre of f , then there exist a near-symplectic form ω on X , with zero set Z and such that ω restricts to a symplectic form on the smooth fibres of the fibration. Moreover, ω determines a deformation class of near-symplectic forms canonically associated to f .*

Note that if every component of every fibre of f contains a point in P , then the cohomological assumption holds automatically. We will not give a full proof of this

theorem as the proof in [4] applies here almost verbatim. The only modification required is in part 1 of the proof given in [4], where one constructs a near-symplectic form positive on the fibres which is defined only in a neighborhood of the critical point set. For the wrinkled fibrations, we introduce a new type of singularity on the critical value set, namely the cusp singularity. Therefore one needs to say a word about how to construct a near-symplectic form positive on the fibres for the local model of the cusp singularity. For that, recall the local model for the cusp singularity. To wit, we have oriented charts where the wrinkled fibration is given by:

$$f: (t, x, y, z) \rightarrow (t, x^3 - 3xt + y^2 - z^2)$$

Now, consider the 2-form $\omega = dt \wedge df_t + *(dt \wedge df_t)$, where $f_t(x, y, z) = x^3 - 3xt + y^2 - z^2$ are Morse except at $t = 0$. This form is self-dual by construction. Since f_t is Morse except at $t = 0$, this form is transverse to the 0-section of Λ^+ . The only missing property for ω to be near-symplectic is that it be closed. In fact, in this specific example of f_t that we are considering ω is not closed. The reason that we are considering this specific ω is because it is positive on the fibres by construction. Therefore, we want to modify ω by adding some terms so that it is closed and at the same time preserve the property that it is positive on the fibres. In this section, this will be the general scheme for finding explicit near-symplectic forms on a given fibration. One such modification is as follows:

$$\tilde{\omega} = dt \wedge df_t + *(dt \wedge df_t) - y(3dt \wedge dz + 6xdz \wedge dx)$$

However, in order to control the positivity we need to ensure that the extra terms we added are small when evaluated on a basis of a fibre. Therefore, we multiply that

term with an $\epsilon > 0$, and in order to have a closed form we need to also multiply the $dx \wedge dt + dy \wedge dz$ component of $dt \wedge df_t + *(dt \wedge df_t)$ also by ϵ . In what follows, we will do this modification several times, therefore we introduce a scaling map $R_\epsilon: \Omega_+^2 \rightarrow \Omega_+^2$ given by:

$$\begin{aligned} R_\epsilon(dt \wedge dx + dy \wedge dz) &= \epsilon(dt \wedge dx + dy \wedge dz) \\ R_\epsilon(dt \wedge dy + dz \wedge dx) &= (dt \wedge dy + dz \wedge dx) \\ R_\epsilon(dt \wedge dz + dx \wedge dy) &= (dt \wedge dz + dx \wedge dy) \end{aligned}$$

So finally we have our near-symplectic form given by:

$$\begin{aligned} \omega_\epsilon &= R_\epsilon(dt \wedge df_t + *(dt \wedge df_t)) - \epsilon y(3dt \wedge dz + 6xdz \wedge dx) \\ &= 3\epsilon(x^2 - t)(dt \wedge dx + dy \wedge dz) \\ &\quad + 2ydt \wedge dy + (2y - 6\epsilon xy)dz \wedge dx \\ &\quad - (2z + 3\epsilon y)dt \wedge dz - 2zdx \wedge dy \end{aligned}$$

Now, choose $\epsilon \leq 1/6$. Then one can check easily that ω_ϵ is a near-symplectic form on D^4 and its restriction to smooth fibres of f are symplectic. Thus, we can use ω_ϵ for the local construction in the proof of Theorem 2.5.1.

Theorem 2.5.1 tells us that there is a natural deformation class of near-symplectic forms on each of the local models of wrinkled fibrations. In what follows, we will give explicit models of near-symplectic forms for each of the local model of wrinkled fibrations described in the previous sections. Furthermore, we will provide one-parameter families for the deformations corresponding to the 4 moves given in Section 2.3. These will be near-symplectic cobordisms in the sense of the following definition

given by Perutz [30].

Definition 2.5.2. *A one-parameter family $\{\omega_s\}_{s \in [a,b]}$ of closed 2-forms on X is called a near-symplectic cobordism if, for all $(x, s) \in X \times [a, b]$, either $(\omega_s \wedge \omega_s)(x) > 0$ or, $\omega_s(x) = 0$ and $(\nabla\omega)(x, s)$ has rank 3.*

The strategy will be the same as the construction of the local model around a cusp singularity. We first exhibit a 2-form positive on the fibres which is not necessarily closed. Then we modify it by adding small terms. We will mostly restrict the domain of the wrinkled fibration to D^4 to ensure positivity. Since every deformation is local and the critical value set lies in D^4 , this is not different from the previous considerations.

Deformation 1 (Birth) : The deformation is given by $F_s: D^4 \rightarrow \mathbb{R}^2$:

$$(t, x, y, z) \rightarrow (t, x^3 + 3(t^2 - s)x + y^2 - z^2)$$

Let $f_s = x^3 + 3(t^2 - s)x + y^2 - z^2$. Consider the deformation:

$$\omega_s = R_\epsilon(dt \wedge df_s + *(dt \wedge df_s)) + 6\epsilon y(tdt \wedge dz + xdx \wedge dz) \quad (2.1)$$

This form is closed and if we choose $\epsilon \leq 1/6$, it is near-symplectic on D^4 . Furthermore, an easy calculation shows that ω_s is symplectic on smooth fibres of F_s . Now, here we remark that ω_s is in fact precisely the Luttinger–Simpson model of birth of a circle singularity which was defined in the introduction to this chapter. Therefore, the maps F_s gives a family of wrinkled fibrations adapted to the model of Luttinger–Simpson of near-symplectic cobordism ω_s .

Deformation 2 (Merging) : The deformation is given by $F_s: D^4 \rightarrow \mathbb{R}^2$:

$$(t, x, y, z) \rightarrow (t, x^3 + 3(s - t^2)x + y^2 - z^2)$$

Let $f_s = x^3 + 3(s - t^2)x + y^2 - z^2$. Consider the deformation:

$$\omega_s = R_\epsilon(dt \wedge df_s + *(dt \wedge df_s)) - 6\epsilon y(tdt \wedge dz + xdz \wedge dx) \quad (2.2)$$

As before, this form is closed and for $\epsilon \leq 1/6$, it is near-symplectic on D^4 . This is a variation of the birth model, the zero-set undergoes a surgery by addition of a one handle. Again, this is a near-symplectic cobordism, and the family F_s is adapted to ω_s , i.e., the restriction of ω_s to smooth fibres of F_s is positive.

Deformation 3 (Flipping) : We again follow the same strategy as above. However, in this case we do not need to restrict to D^4 . Namely, consider the deformation for flipping move given by $F_s: \mathbb{R} \times \mathbb{R}^3 \rightarrow \mathbb{R}^2$:

$$(t, x, y, z) \rightarrow (t, x^4 - x^2s + xt + y^2 - z^2)$$

Now, let $f_s = x^4 - x^2s + xt + y^2 - z^2$. Then we calculate:

$$\begin{aligned} dt \wedge df_s + *(dt \wedge df_s) &= (4x^3 - 2xs + t)(dt \wedge dx + dy \wedge dz) \\ &+ 2y(dt \wedge dy + dz \wedge dx) \\ &- 2z(dt \wedge dz + dx \wedge dy) \end{aligned}$$

This form is positive when restricted to the smooth fibres of F_s by design. How-

ever, this form is not closed. Therefore, to make it closed we modify it naively as follows:

$$\begin{aligned}
\omega_s &= (4x^3 - 2xs + t)(dt \wedge dx + dy \wedge dz) \\
&+ (2y - 2z)dt \wedge dy + (12x^2 - 2s + 2)yz \wedge dx \\
&- (2z + y)dt \wedge dz - (12x^2 - 2s + 1)2zdx \wedge dy
\end{aligned} \tag{2.3}$$

Now ω_s is closed and in fact an easy calculation shows that for $s \leq 1/3$, ω_s is still positive when restricted to the smooth fibres of F_s . Furthermore, the zero locus of ω_s is exactly the critical point set of F_s . Therefore, we conclude that ω_s in fact belongs to the canonical class of near-symplectic forms provided by Theorem 2.5.1 for the fibration F_s . Furthermore, the near-symplectic cobordism ω_s for $s \in [-1, 1/3]$ is through near-symplectic forms, that is, for each $s \in [-1, 1/3]$, ω_s is near-symplectic and adapted to F_s in the sense of Theorem 2.5.1. Hence, we conclude that the flipping move does not alter the near-symplectic geometry.

Deformation 4 (Wrinkling) : Recall that the wrinkling move is given by $F_s : \mathbb{R}^4 \rightarrow \mathbb{R}^2$:

$$(t, x, y, z) \rightarrow (t^2 + st - x^2 + y^2 - z^2, 2tx + 2yz)$$

Let $f_s = t^2 + st - x^2 + y^2 - z^2$ and $g = 2tx + 2yz$. Then a natural candidate for an adapted near-symplectic form for F_s is given by $df_s \wedge dg + *(df_s \wedge dg)$ However, as

before,

$$\begin{aligned}
*(df_s \wedge dg) &= ((2t + s)2t + 4x^2)dy \wedge dz + (4y^2 + 4z^2)dt \wedge dx \\
&+ ((2t + s)2z - 4xy)dz \wedge dx + (4xy - 4tz)dt \wedge dy \\
&+ ((2t + s)2y + 4xz)dx \wedge dy - (4xz + 4ty)dt \wedge dz
\end{aligned}$$

is not closed. Therefore we modify it to the following form.

$$\begin{aligned}
\sigma_s &= ((2t + s)2t + 4x^2)dy \wedge dz + (4y^2 + 4z^2)dt \wedge dx \\
&+ 2((2t + s)2z - 4xy)dz \wedge dx + 2(4xy - 4tz - sz)dt \wedge dy
\end{aligned}$$

It is an easy calculation to check that σ_s is closed and positive when restricted to the fibres of F_s . Now, in order to get a near-symplectic form, we restrict to D^4 , so $F_s: D^4 \rightarrow D^2$, and to σ_s we add a large multiple of the pullback of the standard symplectic form on D^2 by F_s . Thus,

$$\omega_s = k(df_s \wedge dg) + \sigma_s \tag{2.4}$$

for k large enough is an adapted near-symplectic form, that is, it vanishes exactly at the critical value set of F_s and restricts positively to smooth fibres of F_s . Observe that, here also we can see a birth of a zero-circle happens as s goes through negative values to positive values. Therefore, it is possible that this form is deformation equivalent through near-symplectic forms to Luttinger–Simpson model.

2.6 Applications

Merging of zero-sets: Here we reprove the Theorem 1.4 in [30] using moves on broken fibrations.

Theorem 2.6.1. *Given a connected near-symplectic manifold (X, ω_0) , with ω_0 having a zero-set with n components, where $n \geq 1$, one can find a near-symplectic cobordism $\omega_{[0,1]}$ such that ω_1 has k components for any given $k \geq 1$. Furthermore, this near-symplectic cobordism is equipped with an adapted wrinkled pencil.*

Our proof will be obtained by applying moves on a broken pencil adapted to the given near-symplectic manifold. However, one can ignore the base points of the pencil since all the modifications will take place away from them. In this way, we obtain a quicker proof as well as our deformation includes a deformation of wrinkled fibrations associated to it.

Proof. Choose an adapted broken pencil for (X, ω_0) which exists by the main construction in [4]. The proof is divided into two parts according to increasing or decreasing the number of components of the zero-set.

First, let's show that we can add a new component. Restrict the given pencil to a smooth D^2 fibration over D^2 , which is isolated from the singularities of the broken pencil and apply the birth move. Deformation 1 above, tells us that this gives us a near-symplectic cobordism $\omega_{[0,1]}$, where ω_1 has one more component in its zero-set.

Second, let's show that if $n > 1$, we can find a near-symplectic cobordism where the number of components decreases by 1. This part will be longer, since we can't directly apply the merging move as the configuration needed for the merging move

is not always possible to achieve. However, we will apply an alternative combination of moves to produce a merging of zero-components in the total space. First, choose two distinct components of the zero-set. Now, connect these components by a path $\alpha: [0, 1] \rightarrow X$ such that the following properties are satisfied.

- $\alpha^{-1}(Z) = \{0, 1\}$ where Z is the zero set of ω_0 .
- $\alpha'(0), \alpha'(1) \in L^+$, where L^+ is the positive eigen-subbundle of NZ as defined in the introduction.
- α is transversal to the fibres of the broken pencil.

Clearly, such paths are in abundance. Indeed, locally near the end points it's easy to build the path using the local models; and everywhere else, being transverse to the fibres is generic. Restrict the pencil to a neighborhood $N = U \cup V \cup W$ of α , where U and W are preimages of a small neighborhood of the image of $\alpha(0)$ and $\alpha(1)$, and V is a tubular neighborhood α . Then we have a picture as depicted on the left of Figure 10, where the fibres depicted lie in U and W . The preimage of the middle region is V , at each fibre this cuts out a disc. Now, we can apply two flipping moves to both sides, and obtain a fibration as depicted in the middle part of Figure 10.

Notice that these flipping moves do not alter the deformation class of the near-symplectic form and hence the isotopy class of the zero-set is unchanged after these moves, only the broken pencil structure has been changed. Finally, given such a configuration, we can apply an inverse merging move to the fibration (See the remark at the end of the description of the merging move in Section 2.3). In the total space this corresponds to merging of the zero-sets and the deformation of the near-symplectic form is given in the form of a near-symplectic cobordism as in Deformation

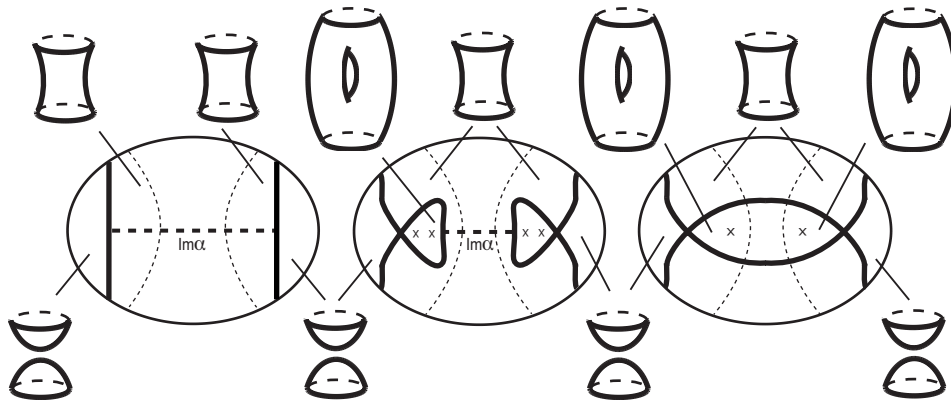


Figure 2-10: Merging of zero-circles along the path α

2, given by the formula 2, except s must be replaced by $-s$, as we apply an inverse merging move.

Broken fibrations with connected fibres: Another application of the techniques discussed in this chapter is based on an idea of Baykur and also appears in [5]. Here we reconstruct that argument for the sake of completeness.

Theorem 2.6.2. *Given a connected near-symplectic manifold (X, ω) , one can always find a broken pencil $f : X \rightarrow S^2$, adapted to ω , the fibres of which are connected.*

Therefore, in order to define Perutz's Lagrangian matching invariant one can always start with a broken fibration with connected fibres. This indeed simplifies some of discussions in [31] and allows us to define Lagrangian matching invariant for a slightly larger number of Spin^c structures.

Proof: For simplicity, we start with the case where the zero-set of ω consists of a single component. Now, observe that, by perturbing ω away from its zero-set, and using the main result in [4], we can ensure that there exists an adapted broken pencil for the perturbed near-symplectic form. Since the perturbation can be taken to be

arbitrarily small, the latter broken pencil will be adapted to ω as well. Without loss of generality we can assume that there are no base points, otherwise we blow-up first, apply the argument below and blow-down in the end.

Either the fibres are connected or suppose the fibres above the northern hemisphere have genera g , and the fibres above the southern hemisphere have genera g_1, g_2 such that $g_1 + g_2 = g$. Since X is connected, this is the only possibility as the fibres above the “high-genus side” have to be connected. Furthermore, we can assume that there are no Lefschetz-type singularities in the “low-genus side” since they can be isotoped to the “high-genus side”. This is simply because starting from a regular fibre in the southern hemisphere adjoining a Lefschetz singularity means adding a 2–handle, and adjoining a broken singularity means adding a 1–handle. But the order of adding these handles can be reversed by an isotopy, therefore one can first add the 1–handle corresponding to the broken singularity, then add the 2–handles corresponding to the Lefschetz-type singularities. Therefore, we can assume that the fibration is trivial above the southern hemisphere. So, the preimage of a neighborhood of the southern hemisphere is given as in Figure 11.

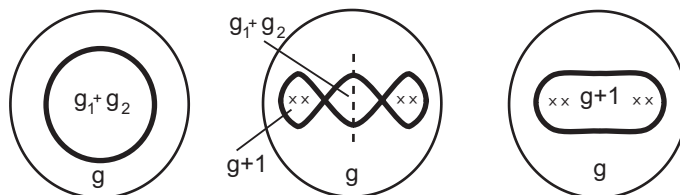


Figure 2-11: Making the fibres connected

Now, we apply two flipping moves to pass to the middle picture in Figure 11. Finally, to obtain the final fibration depicted on the right, we perform an isotopy interchanging the two “legs” of the flips in the middle. This is allowed, since if we consider an arc cutting these “legs” transversely as shown in the middle picture in Figure 11 as a

dotted line, the topology of the fibre changes by first vanishing of a separating cycle (that is, a 2–handle attachment) and then attaching a 1–handle. Again, the order of attachment does not matter, hence by an isotopy one can obtain a broken fibration where the fibres are connected.

When the zero locus of ω consists of more than one circle, these various circles live in disjoint parts of the fibers above the equator of S^2 . We can again push the Lefschetz fibers to the high genus side (northern hemisphere) and ensure that the fibration is trivial above the southern hemisphere. Since the modification explained above is local in the fibre (it only affects a neighborhood of the vanishing cycle for the broken singularity), it can be performed simultaneously on each of the circles. Pictorially this again amounts to the transition shown in Figure 11, but with several circles “stacked” on top of each other in disjoint parts of the fiber.

Removing achiral Lefschetz singularities: In this paragraph, we prove that any achiral Lefschetz singularity can be replaced with a circle of broken singularities and three Lefschetz singularities. Recall that an achiral Lefschetz singularity is modeled in orientation preserving charts by the complex map $(w, z) \rightarrow \bar{w}^2 + z^2$.

Now, given an achiral Lefschetz singularity we can consider the same deformation that was used in the wrinkling move in Section 2.3. Namely, let $F_s : \mathbb{C}^2 \rightarrow \mathbb{C}$ given by:

$$(w, z) \rightarrow \bar{w}^2 + z^2 + s\text{Re}w$$

The map F_s is identical to that considered in Section 2.3 up to the orientation-reversing diffeomorphism $(w, z) \rightarrow (\bar{w}, z)$. Thus its critical values and vanishing cycles are the same as in Section 2.3 up to a reversal of the orientation of the fi-

bre. Namely, when $s > 0$, we observe a birth of a circle of singularities and we get a wrinkled fibration with 3 cusps as on the right side of Figure 6 (except the configuration of the vanishing cycles is reversed). Next, apply the local modification discussed in Section 2.2 to replace each of the three cusps in the base by a smooth arc and a Lefschetz singularity. Thus, we have replaced a neighborhood of an achiral singularity with a genuine broken fibration with a new circle of broken singularities together with three Lefschetz singularities.

We remark that the new singular circle obtained here is an even circle, whereas the new singular circle obtained in the original wrinkling move is an odd circle. (The notions of even and odd circles were defined in the introduction.) The fact that the original wrinkling move yields an odd circle follows from the fact that on a near-symplectic manifold the number of even circles is equal to $1 - b_1 + b_2^+$ modulo 2, as was mentioned in the introduction. A more direct way to see this is as follows: After modifying the cusps as in Section 2.2, we obtain a singular circle of broken singularities and three Lefschetz singularities. Take a small disc including the three Lefschetz singularities but not intersecting the singular circle. Fix a reference fibre above a point on the boundary of this disc such that the curve a vanishes as one approaches the broken singularity. In Figure 7, after modifying the cusps, the reference fibre we are fixing is on the lower left side of the picture. The monodromy around the boundary of this disc is given by the composition of three right handed Dehn twists corresponding to the Lefschetz singularities. Again, from Figure 7 and the calculation of vanishing cycles in Section 2.2, one can conclude that this monodromy is given by $\mu = \tau_{a+d} \circ \tau_{b-d} \circ \tau_{a-b}$. From this, we see that $\mu(a) = -a$, which shows that the circle is an odd circle. Now, in the above perturbation for the achiral Lefschetz singularity case, all the configuration is the same except, the

base picture in Figure 7 is reflected so that the counter-clockwise ordering of a, b, d is changed to a, d, b . Then, one calculates the monodromy to be

$$\mu = \tau_{a+b} \circ \tau_{b+d} \circ \tau_{a-d}$$

which gives $\mu(a) = a$. Hence the singular circle obtained is an even circle.

Corollary 2.6.3. *Let X be an arbitrary closed 4-manifold and let F be a closed surface in X with $F \cdot F = 0$. Then there exists a broken Lefschetz fibration from X to S^2 with embedded singular locus, and having F as a fibre. Furthermore, one can arrange so that the singular set on the base consists of circles parallel to the equator with the genera of the fibres in increasing order from one pole to the other.*

Proof. The existence follows from Gay and Kirby's theorem [10], and the above modification of achiral Lefschetz singularities. Let's prove that this can be done in a certain way so that the singular set on the base consists of circles parallel to the equator. First, note that Gay and Kirby's proof places the round singularities on the tropics of Cancer and Capricorn and the "highest-genus region" is the annular region between the tropics. Now move any Lefschetz or achiral Lefschetz singularities in the southern hemisphere towards the equatorial region (moving across circles towards the higher genus region as in Theorem 2.6.2). Then in the southern hemisphere we are left with only a bunch of parallel circles on the tropic of Capricorn; the corresponding round 1-handles all get attached along disjoint braids (i.e. the circle attachments can be stacked on top of each other or commuted). This is what we need to be able to apply the move on Figure 11 (i.e., on all the circles simultaneously, placing them on top of each other and in different parts of the fibers: first two flipping moves, then an isotopy exactly as in the argument in Theorem 2.6.2). Consequently, we still have circles on the tropic of Capricorn, but oriented in the opposite way (genus increases

towards south pole), and some Lefschetz fibers near the south pole (created by the flips in Figure 11) and the previously given Lefschetz and anti-Lefschetz fibers near the equator. The latter can now be moved towards the north pole by crossing the circles at tropic of Capricorn. Therefore, we can assume that the singular circles are equatorial with all the circles oriented the same way and the “highest-genus region” is over the south pole. Now, we transform one of the achiral singularities to a circle singularity and three Lefschetz singularities. Next, push all the remaining Lefschetz singularities and the achiral singularities (left between the previous circles and the new circle) across the new circle (into the even higher genus region), so the circle is now in equatorial position (parallel to the previous circles). Finally, we repeat this process until there are no more achiral Lefschetz singularities left.

2.7 A summary of moves and further questions

The table below summarizes our set of moves. Only the base parts of the fibrations are drawn. Each move is drawn in pairs, as a move on wrinkled fibrations and as a move on the corresponding broken fibrations obtained by replacing each wrinkle by an arc together with a Lefschetz type singularity as was discussed in Section 2.2. Also the references to the formulas concerning the changes in the naturally associated near-symplectic forms provided by Theorem 2.5.1 are given.

The next important task that we would like to address in the future is to prove that the Lagrangian matching invariant that was described in the introduction is invariant under the set of moves described in this chapter. Of equal importance is the problem of determining the set of equivalence classes of deformations of broken fibrations on a given 4-manifold. The author believes that homotopic broken fibrations should be

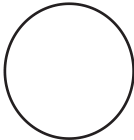
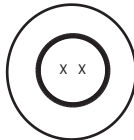
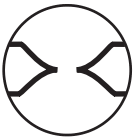
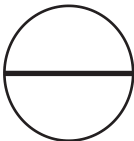
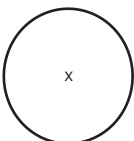
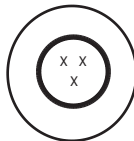
		Wrinkled Fibration	Broken Fibration	Near-Symplectic Form
Birth				Luttinger-Simpson birth model. See eq (1) of Section 5.
Merging				Merging model. See eq (2) of Section 5.
Flipping				No change in the deformation class of near-symplectic form. See eq (3) of Section 5.
Wrinkling				Another birth model. See eq (4) of Section 5.

Figure 2-12: Table of Moves

deformation equivalent. That is, we would like to prove that some sort of h -principle holds for wrinkled fibrations. The main difficulty here is that wrinkled fibrations are constrained to have indefinite Hessian along the critical points.

Chapter 3

Heegaard Floer homology of broken fibrations over the circle

3.1 Introduction

The results that we present in this chapter are formulated in the language of Heegaard Floer homology and interesting by themselves from this perspective. However, the main motivation of our study comes from a different setting, namely that of Lagrangian matching invariants developed by Perutz [31], which are conjecturally isomorphic to Heegaard Floer theoretical invariants. In this chapter, we prove an isomorphism between the 3-manifold invariants of these theories for certain spin^c structures, namely *quilted Floer homology* and *Heegaard Floer homology*. We also outline how the techniques here can be generalized to obtain an identification of 4-manifold invariants and leave the details to a sequel article.

Before giving a review of both of the above mentioned theories, we give the definition

of a broken fibration over S^1 , which will be an important part of the topological setting that we will be working with.

Definition 3.1.1. *A map $f : Y \rightarrow S^1$ from a closed oriented smooth 3-manifold Y to S^1 is called a broken fibration if f is a circle-valued Morse function with all of the critical points having index 1 or 2.*

The terminology is inspired from the terminology of broken Lefschetz fibrations on 4-manifolds which were discussed in Chapter 2. We remark that a 3-manifold admits a broken fibration if and only if $b_1(Y) > 0$, and if it admits one, it admits a broken fibration with connected fibres.

We will mostly restrict ourselves to broken fibrations with connected fibres and we will denote by Σ_{\max} and Σ_{\min} two fibres with maximal and minimal genus. We denote by $\mathcal{S}(Y|\Sigma_{\min})$, the spin^c structures \mathfrak{s} on Y such that $\langle c_1(\mathfrak{s}), [\Sigma_{\min}] \rangle = \chi(\Sigma_{\min})$ (those spin^c structures which satisfy the adjunction *equality* with respect to the fibre with minimal genus).

Definition 3.1.2. *The universal Novikov ring Λ over \mathbb{Z} is the ring of formal power series $\Lambda = \sum_{r \in \mathbb{R}} a_r t^r$ with $a_r \in \mathbb{Z}$ such that $\#\{r | a_r \neq 0, r < N\} < \infty$ for any $N \in \mathbb{R}$.*

The main theorem of this chapter is an isomorphism, for all spin^c structures in $\mathcal{S}(Y|\Sigma_{\min})$, between the quilted Floer homology of a broken fibration $f : Y \rightarrow S^1$ (with coefficients in the universal Novikov ring) and the Heegaard-Floer homology of Y perturbed by a closed 2-form η that pairs positively with the fibers of f :

Theorem 3.1.3. *$QFH(Y, f, \mathfrak{s}; \Lambda) \simeq HF^\pm(Y, \eta, \mathfrak{s})$ for $\mathfrak{s} \in \mathcal{S}(Y|\Sigma_{\min})$.*

When $g(\Sigma_{\min})$ is at least 2 the theorem holds for integral coefficients.

Corollary 3.1.4. *Suppose that $g(\Sigma_{min}) > 1$, then for $\mathfrak{s} \in \mathcal{S}(Y|\Sigma_{min})$ we have*

$$QFH'(Y, f, \mathfrak{s}; \mathbb{Z}) \simeq HF^+(Y, \mathfrak{s})$$

In Section 3.2, we construct a Heegaard diagram associated with a broken fibration and investigate the properties of this diagram. We also give a calculation of perturbed Heegaard Floer homology of fibred 3-manifolds for $\mathfrak{s} \in \mathcal{S}(Y|F)$. In Section 3.3, we give a definition of quilted Floer homology in the language of Heegaard Floer theory and prove that it is isomorphic to the Heegaard Floer homology for the spin^c structures under consideration. In Section 3.4, we relate the group defined in Section 3.3 to the original definition of quilted Floer homology in terms of holomorphic quilts. Here we also prove Floer's excision theorem and discuss the extension of this isomorphism to four-manifold invariants.

We now proceed to review the theories and the notation that are involved in our theorem.

3.1.1 (Perturbed) Heegaard Floer homology

In this section, we review the construction of Heegaard Floer homology, introduced by Ozsváth and Szabó [26]. The usual construction involves certain admissibility conditions, however there is a variant of Heegaard Floer homology where Novikov rings and perturbations by closed 2-forms are introduced in order to make the Heegaard Floer homology group well-defined without any admissibility condition. Our account will be brief since this theory has been well developed in the literature. The reader is encouraged to turn to [13] for a more detailed account of perturbed Hee-

gaard Floer theory. Furthermore, we will mostly find it convenient to work in the set up of Lipshitz's cylindrical reformulation of Heegaard Floer homology [18].

Let $(\Sigma_g, \boldsymbol{\alpha}, \boldsymbol{\beta}, z)$ be a pointed Heegaard diagram of a 3-manifold Y . This gives rise to a pair of Lagrangian tori $\mathbb{T}_\alpha, \mathbb{T}_\beta$ in $\text{Sym}^g(\Sigma_g)$, together with a holomorphic hypersurface $Z = z \times \text{Sym}^{g-1}(\Sigma_g)$. The Heegaard-Floer homology of Y is the Lagrangian Floer homology of these tori, where one uses the orbifold symplectic form pushed down from $\Sigma_g^{\times g}$, though one can also use honest symplectic forms (see [34]). The differential is twisted by keeping track of the intersection number n_z of holomorphic disks contributing to the differential with Z . More precisely, the Heegaard-Floer chain complex $CF^+(Y)$ is freely generated over \mathbb{Z} by $[\mathbf{x}, i]$ where \mathbf{x} is an intersection point of \mathbb{T}_α and \mathbb{T}_β and $i \in \mathbb{Z}_{\geq 0}$, and the differential is given by

$$\partial^+([\mathbf{x}, i]) = \sum_{\mathbf{y}} \sum_{\varphi \in \pi_2(\mathbf{x}, \mathbf{y}), n_z(\varphi) \leq i} \#\widehat{\mathcal{M}}(\varphi)[y, i - n_z(\varphi)]$$

The above definition only makes sense under certain admissibility conditions so that the sum on the right hand side of the differential is finite. In general, one can consider a twisted version of the above chain complex by a closed 2-form in $\Omega^2(Y)$. This is called the *perturbed Heegaard-Floer homology*. The chain complex $CF^+(Y, \eta)$ is freely generated over Λ (see Definition 3.1.2) by $[\mathbf{x}, i]$ where \mathbf{x} is an intersection point and i is a nonnegative integer as before, and the differential is twisted by the area $\int_{[\varphi]} \eta$ of the holomorphic disks that contribute to the differential. More precisely, the differential of the perturbed theory is given by

$$\partial^+([\mathbf{x}, i]) = \sum_{\mathbf{y}} \sum_{\varphi \in \pi_2(\mathbf{x}, \mathbf{y}), n_z(\varphi) \leq i} \#\widehat{\mathcal{M}}(\varphi) t^{\eta(\varphi)} [y, i - n_z(\varphi)]$$

Note that if φ_1, φ_2 are two holomorphic discs that connect an intersection point \mathbf{x} to \mathbf{y} , then their difference is a periodic domain P and we have the equality $\eta(\varphi_1) - \eta(\varphi_2) = \eta([P])$, where the latter only depends on the cohomology class of η . We remark that although the differential depends on the choice of a representative of the class $[\eta]$, the isomorphism class of the homology groups is determined by $\text{Ker}(\eta) \cap H_2(Y; \mathbb{Z})$.

Recall that a 2-form is said to be generic when $\text{Ker}(\eta) \cap H_2(Y; \mathbb{Z}) = \{0\}$. For a generic form coming from an area form on the Heegaard surface, $HF^+(Y, \eta)$ is defined without any admissibility conditions on the Heegaard diagram.

3.1.2 Quilted Floer homology of a 3-manifold

In this section, we review the definition of quilted Floer homology of a 3-manifold Y equipped with a broken fibration $f : Y \rightarrow S^1$. The general theory of holomorphic quilts is under systematic development by Wehrheim and Woodward [44], though the case we consider also appears in the work of Perutz [33]. The relevant part of the theory in the setting of 3-manifolds is obtained from Perutz's construction of Lagrangian matching conditions associated with critical values of broken fibrations, which we now review from [31].

Given a Riemann surface (Σ, j) and an embedded circle $L \subset \Sigma$, denote by Σ_L the surface obtained from Σ by surgery along L , i.e., by removing a tubular neighborhood of L and gluing in a pair of discs. To such data, Perutz associates a distinguished Hamiltonian isotopy-class of Lagrangian correspondences $V_L \subset \text{Sym}^n(\Sigma) \times \text{Sym}^{n-1}(\Sigma_L)$ (where the symmetric products are equipped with Kähler forms in suitable cohomology classes, see [31]). These are described in terms of a symplectic degeneration of

$\text{Sym}^n(\Sigma)$. More precisely, one considers an elementary Lefschetz fibration over D^2 with regular fibre Σ and a unique vanishing cycle L which collapses at the origin. Then one passes to the relative Hilbert scheme, $\text{Hilb}_{D^2}^n(\Sigma)$, of this fibration (the resolution of the singular variety obtained by taking fibre-wise symmetric products). The regular fibres of the induced map from $\text{Hilb}_{D^2}^n(\Sigma)$ are identified with $\text{Sym}^n(\Sigma)$, and the fibre above the origin has a codimension 2 singular locus which can be identified with $\text{Sym}^{n-1}(\Sigma_L)$. V_L then arises as the vanishing cycle of this fibration.

Given a 3-manifold Y and a broken fibration $f : Y \rightarrow S^1$, the *quilted Floer homology* of Y , $QFH(Y, f)$, is a Lagrangian intersection theory graded by spin^c structures on Y . Let p_1, p_2, \dots, p_k be the set of critical values of f . Pick points p_i^\pm in a small neighborhood of each p_i so that the fibre genus increases from p_i^- to p_i^+ . For $\mathfrak{s} \in \text{spin}^c(Y)$, let $\nu : S^1 \setminus \text{crit}(f) \rightarrow \mathbb{Z}_{\geq 0}$ be the locally constant function defined by $\langle c_1(\mathfrak{s}), [F_s] \rangle = 2\nu(s) + \chi(F_s)$, where $F_s = f^{-1}(s)$. Then the construction in the previous paragraph gives Lagrangian correspondences $L_{p_i} \subset \text{Sym}^{\nu(p_i^+)}(F_{p_i^+}) \times \text{Sym}^{\nu(p_i^-)}(F_{p_i^-})$. The quilted Floer homology of Y , $QFH(L_{p_1}, \dots, L_{p_k})$, is then generated by horizontal (with respect to the gradient flow of f) multi-sections of f which match along the Lagrangians L_{p_1}, \dots, L_{p_k} at the critical values of f , and the differential counts rigid holomorphic “quilted cylinders” connecting the generators, [33], [44].

There are various technical difficulties involved in the definition of $QFH(Y, f, s)$ due to bubbling of holomorphic curves. These are addressed by different means depending on the value of $\langle c_1(\mathfrak{s}), [\Sigma_{\max}] \rangle$. The easiest case is the monotone case, that is when $\langle c_1(\mathfrak{s}), [\Sigma_{\max}] \rangle > 0$, where holomorphic bubbles are a priori excluded. However, for $\mathfrak{s} \in \mathcal{S}(Y | \Sigma_{\min})$ we will almost never be in the monotone case. In the strongly negative case, that is when $\langle c_1(\mathfrak{s}), [\Sigma_{\max}] \rangle \leq \chi(\Sigma_{\max})/2$, one can still eliminate bubbles a priori by standard means. For the rest of the cases, bubbles might and will occur in

general, therefore complications arise. The main idea is then to establish a proper combinatorial rule for handling bubbled configurations. One could also try to use the more technical machinery of [20] or [7] in order to tackle this case. Another related issue is showing that quilted Floer homology is an invariant of a three manifold. The isomorphism constructed in this chapter shows this in an indirect way for the spin^c structures under consideration. We will return to this question and various well-definedness questions in [17]. For now we will give an alternative description which we will denote by $QFH'(Y, f, s)$ that suits our purposes and avoids these technical issues, hence is well-defined in all cases; see Section 3.3.1 for the definition, and Section 3.4 and [17] for the equivalence between the two constructions.

In this chapter, we will deal with the spin^c structures $\mathfrak{s} \in \mathcal{S}(Y|\Sigma_{\min})$. In this case, when defined, quilted Floer homology can be interpreted as a variant of the construction of Heegaard Floer homology, because of Theorem 3.4.1 (in Section 3.4) and a version of the main theorem in the work of Wehrheim and Woodward [44]. From now on, we will work with the definition formulated in terms of Heegaard Floer theory as given in Section 3.3.1.

Finally, we remark that in the case when $f : Y \rightarrow S^1$ is a fibration, $QFH(Y, f)$ is given as a fixed point Floer homology theory on the moduli space of vortices and was first introduced by Salamon in [36]. In this case, the spin^c structures $\mathfrak{s} \in \mathcal{S}(Y|\Sigma)$ corresponds to taking the zeroth symmetric product of the fibres. In this case, it is natural to set $QFH(Y, f) = \Lambda$ if \mathfrak{s} is the canonical tangent spin^c structure, and $QFH(Y, f) = 0$ for other $\mathfrak{s} \in \mathcal{S}(Y|\Sigma)$.

3.2 Heegaard diagram for a circle-valued broken fibrations on Y

3.2.1 A standard Heegaard diagram

We start with a 3-manifold Y with $b_1 > 0$. Then Y admits a broken fibration over S^1 . Consider such a Morse function $f : Y \rightarrow S^1$ with the following additional properties :

- $F_{-1} = \Sigma_{\max}$ has the maximal genus $g_{\max} = g$ and $F_1 = \Sigma_{\min}$ has the minimal genus $g_{\min} = k$ among fibres of f .
- The fibres are connected.
- The genera of the fibres are in decreasing order as one travels clockwise and counter-clockwise from -1 to 1 .

A broken fibration with these properties always exists provided $b_1 > 0$. In fact, any broken fibration with connected fibers can be deformed into one with these properties by an isotopy that changes the order of the critical values.

We will now construct a Heegaard diagram for Y adapted to f . Roughly speaking, the Heegaard surface Σ will be obtained by connecting Σ_{\max} and Σ_{\min} by two “tubes” traveling clockwise and counter-clockwise from Σ_{\max} to Σ_{\min} . More precisely, start with a section γ of f over S^1 . Then we can pick a metric for which γ is a gradient flow of f , and since γ is disjoint from the critical points of f , it also avoids the stable/unstable manifolds of the critical points. Now pick two distinct points p and q on Σ_{\max} , connect p to Σ_{\min} by the gradient flow line above the northern semi-circle in the base S^1 which connects -1 to 1 in the clockwise direction and connect q to

Σ_{\min} by the gradient flow line above the southern semi-circle, avoiding the critical points of f in both cases. Denote these flow lines by γ_p and γ_q and their end points in Σ_{\min} by \bar{p} and \bar{q} . Then the Heegaard surface that we are interested in is obtained by removing discs around p, q, \bar{p} and \bar{q} and connecting Σ_{\max} to Σ_{\min} along γ_p and γ_q (see Figure 3-1). We denote the resulting surface by

$$\Sigma = \Sigma_{\max} \cup_{\partial N(\gamma_p) \cup \partial N(\gamma_q)} \Sigma_{\min}$$

where $N(\gamma_p)$ and $N(\gamma_q)$ stands for normal neighborhoods of γ_p and γ_q .

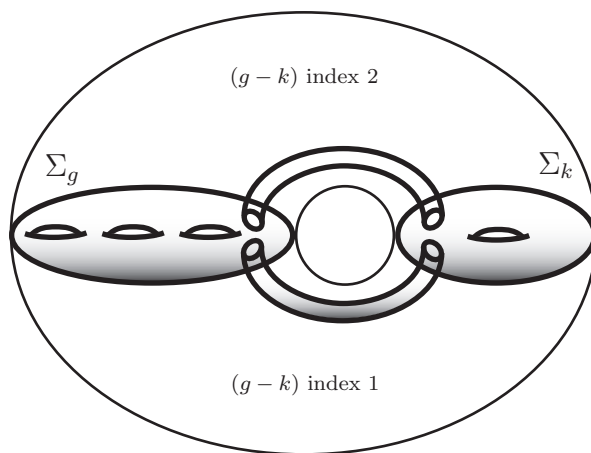


Figure 3-1: Heegaard surface for a broken fibration

Note that $g(\Sigma) = g + k + 1$. Denote the point where γ intersects Σ_{\max} by w and the point where γ intersects Σ_{\min} by z . Next, we will describe α and β curves on Σ in order to get a Heegaard decomposition of Y . First, set α_0 to be $\partial N(\gamma_p) \cap f^{-1}(-i)$ and set β_0 to be $\partial N(\gamma_p) \cap f^{-1}(i)$. The preimage of the northern semi-circle is a cobordism from Σ_{\max} to Σ_{\min} which can be realized by attaching $(g - k)$ 2-handles to $\Sigma_{\max} \times I$, and hence can be described by the data of $g - k$ disjoint attaching circles on Σ_{\max} . These we declare to be $\alpha_1, \dots, \alpha_{g-k}$. Similarly the preimage of the

southern semi-circle is a cobordism from Σ_{\max} to Σ_{\min} , encoded by $g - k$ disjoint attaching circles $\beta_1, \dots, \beta_{g-k}$ on Σ_{\max} . Alternatively, these two sets correspond to the stable and unstable manifolds of the critical points of f . More precisely, orienting the base S^1 in the clockwise direction, $\alpha_1, \dots, \alpha_{g-k}$ are the intersections of the stable manifolds of the critical points above the northern semi-circle with Σ_{\max} , similarly $\beta_1, \dots, \beta_{g-k}$ are the intersections of the unstable manifolds of the critical points above the southern semi-circle with Σ_{\max} . Note that by choosing p and q sufficiently close to w we can ensure that they lie in the same connected component in the complement of $\alpha_1, \dots, \alpha_{g-k}$ and $\beta_1, \dots, \beta_{g-k}$.

Next, we describe the remaining curves, $(\alpha_{g-k+1}, \dots, \alpha_{g+k}, \beta_{g-k+1}, \dots, \beta_{g+k})$. Let F be the part of Σ which consists of Σ_{\max} (except the two discs removed around p and q) together with halves of the connecting tubes up to α_0 and β_0 . Thus F is a genus g surface with 2 boundary components α_0 and β_0 . Also, denote by \bar{F} the complement of $\text{Int}(F)$ in Σ . Thus \bar{F} is a genus k surface with boundary consisting of α_0 and β_0 and $\Sigma = F \cup_{\alpha_0 \cup \beta_0} \bar{F}$. Let us also pick p^+ and q^+ on the boundary of the disks deleted around p and q , and \bar{p}^+ and \bar{q}^+ their images under the gradient flow (so that they lie on the boundary of the discs deleted around \bar{p} and \bar{q}). Now we can find two $2k$ -tuples of ‘‘standard’’ pairwise disjoint arcs in \bar{F} , $(\bar{\xi}_1, \dots, \bar{\xi}_{2k}), (\bar{\eta}_1, \dots, \bar{\eta}_{2k})$ such that $\bar{\xi}_i$ intersect $\bar{\eta}_j$ only if $i = j$, in which case the intersection is transverse at one point. Furthermore, we can arrange that the points z, \bar{p}^+ and \bar{q}^+ lie in the same connected component in the complement of these arcs in \bar{F} . A nice visualization of these curves on \bar{F} can be obtained by considering a representation of \bar{F} by a $4k$ -sided polygon. First, represent a genus k surface by gluing the sides of $4k$ -gon in the way prescribed by the labeling $a_1 b_1 a_1^{-1} b_1^{-1} \dots a_k b_k a_k^{-1} b_k^{-1}$ of the sides starting from a vertex and labeling in the clockwise direction. Now remove a neighborhood

of each vertex of the polygon and a neighborhood of a point in its interior. This now represents a genus k surface with two boundary components. Let us put β_0 at the boundary of the interior puncture and α_0 at the boundary near the vertices then the curves $(\bar{\xi}_{2i-1}, \bar{\xi}_{2i})$ coincide with the portions of the edges labelled (a_i, b_i) left after removing a neighborhood of each vertex and the curves $(\bar{\eta}_{2i-1}, \bar{\eta}_{2i})$ connect the midpoints of $(\bar{\xi}_{2i-1}, \bar{\xi}_{2i})$ radially to β_0 , see Figure 3-2.

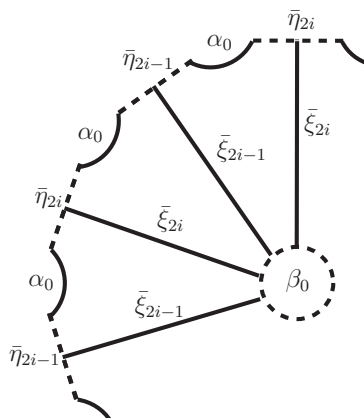


Figure 3-2: The curves $(\bar{\xi}_{2i-1}, \bar{\xi}_{2i})$, $(\bar{\eta}_{2i-1}, \bar{\eta}_{2i})$

Now, using the gradient flow of f we can flow the arcs $(\bar{\xi}_1, \dots, \bar{\xi}_{2k})$ above the northern semi-circle to obtain disjoint arcs (ξ_1, \dots, ξ_{2k}) in F which do not intersect with $\alpha_1, \dots, \alpha_{g-k}$. (Generic choices ensure that the gradient flow does not hit any critical points.) The flow sweeps out discs in Y which bound $(\alpha_{g-k+1}, \dots, \alpha_{g+k}) = (\xi_1 \cup \bar{\xi}_1, \dots, \xi_{2k} \cup \bar{\xi}_{2k})$. Similarly, we define $(\beta_{g-k+1}, \dots, \beta_{g+k})$ by flowing the arcs $(\bar{\eta}_1, \dots, \bar{\eta}_{2k})$ above the southern semi-circle. To complete the Heegaard decomposition of (Y, f) we set the base point to be z which lies in the same region as \bar{p}^+ and \bar{q}^+ on \bar{F} . Therefore, we constructed a Heegaard decomposition of (Y, f) . We will make use of a filtration associated with another base point w which we can ensure to be located in the same region as p^+ and q^+ , this is also the region where the image of z

lands under the gradient flow above the northern and southern semi-circles. Roughly speaking, this point will be used to keep track of the domains passing through the connecting “tubes”.

Note that the Heegaard diagram constructed above might be highly inadmissible. An obvious periodic domain with nonnegative coefficients is given by F , which represents the fibre class. However, the standard winding techniques will give us a Heegaard diagram where F (or its multiples) is the *only* potential periodic domain which might prevent our Heegaard diagram from being admissible (which happens if and only if $k = 1$). In fact, we can achieve this by only changing the diagram in the interior of F , so that the standard configuration of curves on Σ_{\min} is preserved. Furthermore, we will make sure that, in the new Heegaard diagram, the points p^+ and q^+ remain in the same connected component. To get started, fix an arc δ in F , disjoint from all the α and β curves in $\text{Int}(F)$, that connects the two boundary components of F and passes through p^+ and q^+ . We claim that there are $g+k$ simple closed curves $\{\gamma_1, \dots, \gamma_{g+k}\}$ in F such that γ_i do not intersect δ and the algebraic intersection of γ_i with α_j is 1 if $i = j$ and 0 otherwise (Note that we do not require the curves $\gamma_1, \dots, \gamma_{g+k}$ to be disjoint). For that, we will show that the curves $\alpha_1, \dots, \alpha_{g-k}, \xi_1, \dots, \xi_{2k}, \delta$ are linearly independent in $H_1(F, \partial F)$. Then the Poincaré-Lefschetz duality implies the existence of the desired simple closed curves in F which do not intersect δ .

Lemma 3.2.1. *The curves $\alpha_1, \dots, \alpha_{g-k}, \xi_1, \dots, \xi_{2k}, \delta$ are linearly independent in $H_1(F, \partial F)$.*

Proof. It suffices to show that the complement of $\alpha_1, \dots, \alpha_{g-k}, \xi_1, \dots, \xi_{2k}, \delta$ in F is connected. Take any two points a, b in the complement. Now use the gradient flow along the northern semi-circle to obtain \bar{a} and \bar{b} . Also let $\bar{\delta}$ be the image of δ under the flow. Connect \bar{a} and \bar{b} in the complement of $\bar{\xi}_1, \dots, \bar{\xi}_{2k}$ in \bar{F} with a path that is

disjoint from $\bar{\delta}$ (This is easy because of the standard configuration of curves in \bar{F}). Now flow the connecting path back to obtain a path that connects a and b in the complement of $\alpha_1, \dots, \alpha_{g-k}, \xi_1, \dots, \xi_{2k}$. \square

Lemma 3.2.2. *Given a basis of the abelian group of periodic domains in the form F, P_1, \dots, P_n , after winding the α curves sufficiently many times along the curves $\{\gamma_1, \dots, \gamma_{g+k}\}$, we can arrange that any periodic domain in the linear span of P_i has both positive and negative regions on the Heegaard surface. Furthermore, for $\mathfrak{s} \in \mathcal{S}(Y|\Sigma_{min})$, the resulting diagram is weakly admissible if $k > 1$.*

Proof. This follows by winding successively along the curves $\{\gamma_1, \dots, \gamma_{g+k}\}$ in F , first wind along γ_1 all the α curves that intersect γ_1 , then wind the resulting curves around γ_2 , etc. In this way the α curves stay disjoint (each winding is actually a diffeomorphism of F supported near γ_i , and maps disjoint curves/arcs to disjoint curves/arcs). Furthermore, because winding along γ_i is a diffeomorphism of F isotopic to identity, it preserves the property that α_j and α_k have algebraic intersection numbers 1 if $j = k$, 0 otherwise. If we had a periodic domain with a nontrivial boundary along α_i , then after winding sufficiently along γ_i , the multiplicity of some region of the periodic domain with boundary in α_i becomes negative. The argument for that relies on the observation that, since the total boundary of the periodic domain has algebraic intersection number 0 with γ_i , and since all the other α curves have algebraic intersection number 0, while α_i has nonzero algebraic intersection, the boundary of the periodic domain must also include a β curve which has nonzero algebraic intersection number with γ_i . Thus after each winding along γ_i , the domain of the periodic domain which has boundary on α_i has a region where the multiplicity is decreased. Hence after sufficiently many windings, we can ensure that any periodic domain with boundary in one of $\alpha_1, \dots, \alpha_{g+k}$ has at least one negative region.

Furthermore, note that a periodic domain is uniquely determined by the part of its boundary which is spanned by $\{[\alpha_0], \dots, [\alpha_{g+k}]\}$. Therefore, given a basis F, P_1, \dots, P_n , after winding sufficiently many times, we can make sure that each P_i has sufficiently large multiplicities both positive and negative in certain regions of the Heegaard diagram where all other P_j 's have small multiplicities. Thus for a periodic domain to have only positive multiplicities, it must be of the form $mF + m_1P_1 + \dots + m_nP_n$ such that m is much larger than $|m_i|$. Then $\langle c_1(\mathfrak{s}), mF + m_1P_1 + \dots + m_nP_n \rangle = m\langle c_1(\mathfrak{s}), F \rangle + \sum_{i=1}^n m_i\langle c_1(\mathfrak{s}), P_i \rangle$ must be non-zero when $k \neq 1$ since $m\langle c_1(\mathfrak{s}), F \rangle$ dominates the sum and $\langle c_1(\mathfrak{s}), F \rangle = 2 - 2k$ is non-zero. Thus the diagram can be made weakly admissible when $k > 1$. \square

We remark that the configuration of the curves on \bar{F} is left intact. Also, the curve δ in F has not been changed. Therefore, after winding we still have the points p and q lying in the same region of the Heegaard diagram. From now on, we will use the notation $(\Sigma, \alpha_0, \dots, \alpha_{g+k}, \beta_0, \dots, \beta_{g+k}, z, w)$ for this diagram, which is weakly admissible if $k > 1$. We will refer to this kind of diagrams as *almost admissible*. In order to make sense of Heegaard Floer homology groups for our special Heegaard diagram in the case when the lowest genus fibre is a torus (i.e. $k = 1$), we will need to work in the perturbed setting since the periodic domain F prevents the diagram from being weakly admissible. However, because we have an “almost admissible” diagram, it suffices to perturb only in the “direction of the fibre class”.

Lemma 3.2.3. *Given a basis of the abelian group of periodic domains in the form F, P_1, \dots, P_n , we can find an area form A on the Heegaard surface such that $A([F]) > 0$ and $A(\text{span}\{P_1, \dots, P_n\}) = 0$.*

Proof. By the previous lemma, we can arrange that any periodic domain in the linear span of $\{P_1, \dots, P_n\}$ has both positive and negative regions on the Heegaard surface.

The rest of the proof now follows from Farkas' lemma in the theory of convex sets. See [19] Lemma 4.17 – 4.18. \square

Now an area form A on the Heegaard surface gives a real cohomology class $[\eta] \in H^2(Y; \mathbb{R})$ via the bijection between periodic domains and $H_2(Y; \mathbb{Z})$. Namely, set $[\eta](P) = A(P)$. Choosing a representative $\eta \in [A]$ we can consider the perturbed Heegaard Floer homology $HF^+(Y, f, \eta)$. Since F is the only periodic domain which prevents weak admissibility (only in the case $k = 1$) and $\eta([F]) > 0$, we have a well-defined group $HF^+(Y, f, \eta)$ by the following lemma :

Lemma 3.2.4. *Given $\mathbf{x}, \mathbf{y} \in \mathbb{T}_\alpha \cap \mathbb{T}_{\beta, i}, j \in \mathbb{Z}_{\geq 0}$ and $r, s \in \mathbb{R}$ there are only finitely many homology classes $\varphi \in \pi_2(\mathbf{x}, \mathbf{y})$, with $n_z(\varphi) = i - j$ and $\eta(\varphi) = r - s$ which have positive domains.*

Proof. Let φ and ψ be in $\pi_2(\mathbf{x}, \mathbf{y})$, then $\varphi - \psi \in \pi_2(\mathbf{x}, \mathbf{x})$. We can write $\varphi - \psi = mF + m_1P_1 + \dots + m_nP_n + n\Sigma$. Since $n_z(\varphi) = n_z(\psi)$, we have $n = 0$. Also since $\eta(\varphi) = \eta(\psi)$ and $\eta(F) \neq 0$ while $\eta(P_i) = 0$, we conclude that $m = 0$. Finally, since $A(P_i) = 0$, we have $A(\varphi) = A(\psi)$ but then there are only finitely many nonnegative domains which have a fixed area. \square

Now, as explained in the introduction $HF^+(Y, f, \eta)$ is an invariant of $(Y, [\eta])$, in fact it only depends on $\text{Ker}(\eta) \cap H_2(Y; \mathbb{Z})$, hence is independent of the value of $\eta([F])$.

The usual invariance arguments of Heegaard Floer theory, as in [26], imply that $HF^+(Y, f, \eta)$ is independent of the choice of f within its smooth isotopy class. Also note that a geometric way of choosing η is by choosing a section γ of f (a section of f always exists) and letting $[\eta]$ be the Poincaré dual of $[\gamma]$. In that case, we will write $HF^+(Y, f, \gamma)$ for this perturbed Heegaard Floer homology group. In fact, the

choice of the base points w and z as above gives a section of f . Namely, note that we have arranged so that the image of z under the flow above both the northern and the southern semi-circles lies in the same region as w . The union of these two gradient flow lines can therefore be perturbed into a section of f , which we will denote by γ_w . The group $HF^+(Y, f, \gamma_w)$ will be one of the main protagonists in this chapter. The differential of this group can be made more explicit as follows: Choose a basis of the group of periodic domains in the form F, P_1, \dots, P_n such that F is the fibre of f and P_i are periodic domains so that the boundary of P_i does not include α_0 or β_0 (This can be arranged by subtracting a multiple of F). Then if we choose $\eta \in PD[\gamma_w]$ we have $\eta(\text{span}(P_1, \dots, P_m)) = 0$ and $\eta(F) = n_w(F) = 1$. Therefore for any periodic domain P , we have $\eta(P) = n_w(P)$. Thus there exists a function $\lambda : \mathbb{T}_\alpha \cap \mathbb{T}_\beta \rightarrow \mathbb{R}$ such that for any $\varphi \in \pi_2(\mathbf{x}, \mathbf{y})$, we have $\eta(\varphi) - n_w(\varphi) = \lambda(\mathbf{x}) - \lambda(\mathbf{y})$. Hence, we can define the differential for $HF^+(Y, f, \gamma_w)$ as follows:

$$\partial^+([\mathbf{x}, i]) = \sum_{\mathbf{y}} \sum_{\varphi \in \pi_2(\mathbf{x}, \mathbf{y}), n_z(\varphi) \leq i} \# \widehat{\mathcal{M}}(\varphi) t^{n_w(\varphi)}[\mathbf{y}, i - n_z(\varphi)]$$

This yields the same homology groups as the original definition where the differential is weighted by $t^{\eta(\varphi)}$: namely, the two chain complexes are related by rescaling each generator $[\mathbf{x}, i]$ to $t^{\lambda(\mathbf{x})}[\mathbf{x}, i]$. When we consider $HF^+(Y, f, \gamma_w)$, we will always consider the differential above.

3.2.2 Splitting the Heegaard diagram

As explained in the introduction, we will only consider the spin^c structures on Y that satisfy the adjunction equality with respect to Σ_{\min} ; the set of isomorphism classes

of such spin^c structures was denoted by $\mathcal{S}(Y|\Sigma_{\min})$. In this section we observe that for $\mathfrak{s} \in \mathcal{S}(Y|\Sigma_{\min})$, we obtain a nice splitting of the generators of the Heegaard Floer complex into intersections in F and \bar{F} . Furthermore, we prove a key lemma en route to understanding the holomorphic curves contributing to the differential.

Let us denote by I_{left} the intersection of $\alpha_1 \times \dots \times \alpha_{g-k}$ and $\beta_1 \times \dots \times \beta_{g-k}$ in $\text{Sym}^{g-k}(\Sigma)$, and by I_{right} the set of intersection points of $\alpha_0 \times \alpha_{g-k+1} \times \dots \times \alpha_{g+k}$ and $\beta_0 \times \beta_{g-k+1} \times \dots \times \beta_{g+k}$ in $\text{Sym}^{2k+1}(\Sigma)$ such that each intersection point *lies* in \bar{F} . Thus, each element of I_{right} consists of one point from the set of $4k$ intersection points of α_0 with η_1, \dots, η_{2k} , another point from the set of $4k$ intersection points of β_0 with ξ_1, \dots, ξ_{2k} and finally $2k - 1$ points from the set of $2k$ points consisting of the intersections of $\bar{\xi}_i$ with $\bar{\eta}_i$ for $i = 1, \dots, 2l$.

We have $I_{\text{left}} \otimes I_{\text{right}} \subset \mathbb{T}_\alpha \cap \mathbb{T}_\beta$, where $\mathbb{T}_\alpha = \alpha_0 \times \dots \times \alpha_{g+k}$ and $\mathbb{T}_\beta = \beta_0 \times \dots \times \beta_{g+k}$ are the Heegaard tori in $\text{Sym}^{g+k+1}(\Sigma)$. Denote by C_{left} and C_{right} the free Λ -modules generated by I_{left} and I_{right} respectively.

Lemma 3.2.5. *An intersection point $\mathbf{x} \in \mathbb{T}_\alpha \cap \mathbb{T}_\beta$ induces a spin^c structure $\mathfrak{s}_z(\mathbf{x}) \in \mathcal{S}(Y|\Sigma_{\min})$ if and only if $\mathbf{x} \in C_{\text{left}} \otimes C_{\text{right}}$.*

Proof. This follows easily from the following formula from Lemma 4.11 in [18]:

$$\langle c_1(\mathfrak{s}_z(\mathbf{x})), F \rangle = e(F) + 2n_{\mathbf{x}}(F)$$

where $n_{\mathbf{x}}(F)$ is the number of components of the tuple \mathbf{x} which lie in F . Since $\mathfrak{s}_z(\mathbf{x}) \in \mathcal{S}(Y|\Sigma_{\min})$, we have $\langle c_1(\mathfrak{s}_z(\mathbf{x})), F \rangle = \langle c_1(\mathfrak{s}_z(\mathbf{x})), \Sigma_{\min} \rangle = 2 - 2k$. Also $e(F) = -2g$, hence the above formula gives

$$n_{\mathbf{x}}(F) = 1 + g - k$$

which is satisfied if and only if $\mathbf{x} \in C_{\text{left}} \otimes C_{\text{right}}$. □

Next, we prove an important lemma about the behaviour of holomorphic disks on the tubular regions to the left of α_0 and β_0 . This lemma lies at the heart of most of the arguments about the behaviour of holomorphic curves that we are going to consider subsequently. For the purpose of stating the next lemma, let a and b be parallel pushoffs of α_0 and β_0 to the left (into the interior of F). Let us label the connected components of the domains in the cylindrical region between a and α_0 by a_1, \dots, a_{4k} and the cylindrical region between b and β_0 by b_1, \dots, b_{4k} . Choose the labeling so that a_1 and b_1 are in the same region as the arc δ , hence $n_{a_1} = n_{b_1} = n_w$.

Lemma 3.2.6. *Let $\mathbf{x} = \mathbf{x}_{\text{left}} \otimes \mathbf{x}_{\text{right}}$ and $\mathbf{y} = \mathbf{y}_{\text{left}} \otimes \mathbf{y}_{\text{right}}$ be in $C_{\text{left}} \otimes C_{\text{right}}$ and $A \in \pi_2(\mathbf{x}, \mathbf{y})$ and u be a Maslov index 1 holomorphic curve in the homology class A . Assume moreover that the contribution of curves in class A to the differential is non-zero. Then,*

$$n_w(u) = n_{a_1}(u) = \dots = n_{a_{4k}}(u) = n_{b_1}(u) = \dots = n_{b_{4k}}(u)$$

Furthermore, if $n_z(u) = 0$, then the projection to the Heegaard surface induced by u can be arranged to be an unbranched cover around the cylindrical neighborhoods of a and b (In other words, u “converges” to Reeb orbits around a and b upon neck-stretching).

Proof. The proof will be obtained by “stretching the neck” along the curves a and b' , where a is as before a parallel pushoff of α_0 to the left, whereas b' is a parallel pushoff of β_0 to the right (into the interior of \bar{F}), chosen so that the marked point z lies in between β_0 and b' . We could just as well do the stretching along a and b and get the first part of the statement, however it turns out that stretching the neck

around a and b' (and symmetrically a' and b , where a' is similarly a parallel pushoff of α_0 to the right) gives the stronger result stated above.

Suppose that there is an $i \pmod{4k}$ such that $n_{a_i}(u) \neq n_{a_{i+1}}(u)$ (one can argue in the same way for b_i 's). Thus the source S of u has a piece of boundary which maps to the β arc that separates a_i and a_{i+1} . Let β_j be the curve containing that arc. The crucial observation is that the disk u has no corners in $\beta_j \cap F$, since \mathbf{x} and \mathbf{y} have no components in $\beta_j \cap F$.

We now degenerate Σ along the curves a and b' . Specifically, this means that one takes small cylindrical neighborhoods of the curves a and b' , and changes the complex structure in that neighborhood so that the modulus of the cylindrical neighborhoods gets larger and larger. Topologically this degeneration can be understood as follows: After degenerating along a and b' , Σ degenerates into Σ_{\max} and Σ_{\min} and the homology class A splits into A_{left} and A_{right} corresponding to the induced domains on Σ_{\max} and Σ_{\min} from the domain of A on Σ . (The definition of homology classes $\pi_2(\mathbf{x}, \mathbf{y})$ in this degenerated setting is given in Definition 4.8 of [19], it is the homology classes of maps to $\Sigma_{\max} \times [0, 1] \times \mathbb{R}$ (and to $\Sigma_{\min} \times [0, 1] \times \mathbb{R}$) which have strip-like ends converging to \mathbf{x} and \mathbf{y} , and to Reeb chords at points of degeneration).

Next we analyze the holomorphic degeneration of u . Suppose that the moduli space of holomorphic curves representing A is non-empty for all large values of the stretching parameter. Then we conclude by Gromov compactness that there is a subsequence converging to a pair of holomorphic combs of height 1 (in the sense of [19] section 5.3, see proposition 5.20 for the proof of Gromov compactness in this setting) u_0 representing A_{left} and u_1 representing A_{right} (the limiting curves have height 1 because otherwise one of the stages would have index ≤ 0 , contradicting transversality – see Proposition 5.5 of [19]). By assumption, the degeneration of u involves breaking along

a Reeb chord ρ contained in a with one of the ends on $a \cap \beta_j$. Hence some component S_0 of the domain of u_0 has a boundary component Γ , consisting of arc components separated by boundary marked points, such that one of the arcs is mapping to β_j and, at one end of that arc, u_0 has a strip-like end converging to the Reeb chord ρ . Now, since there are no corner points on any of the β -arcs in Σ_{\max} , the marked points on Γ are all labeled by Reeb chords on a (corresponding to arcs connecting intersection points of β curves with a), and any two consecutive punctures on Γ are connected by an arc which is mapped to part of a β arc which lies on the left half of the Heegaard diagram. Thus, in particular there are no arcs in Γ which map to α curves. Now, we can extend u_0 at the punctures on Γ by sending the marked points to the point of Σ_{\max} to which a collapses upon neck-stretching (This is possible since, after collapsing a , $u_0|_{S_0}$ viewed as a map to Σ_{\max} admits a continuous extension at these points. Note that the projection to $[0, 1] \times \mathbb{R}$ also extends continuously at the punctures by the definition of holomorphic combs, see the proof of proposition 5.20 [19] for more details regarding this). Therefore, the image of the boundary component Γ under the projection to $[0, 1] \times \mathbb{R}$ remains bounded and is entirely contained in $0 \times \mathbb{R}$. Moreover, since the projection is holomorphic, the projection of Γ to $0 \times \mathbb{R}$ is a non-increasing function, and hence we conclude that Γ maps to a constant. Now, the maximum principle implies that the entire component S_0 has to be mapped to a constant value in $0 \times \mathbb{R}$. Therefore, S_0 has all of its boundary components mapped to β curves. Furthermore, the image of u_0 restricted to boundary of S_0 does not intersect β_0 because, even after the degeneration, β_0 does not intersect any other β curves; there cannot be a boundary component which is entirely mapped to β_0 , since those type of boundaries are not allowed in the Heegaard Floer differential, and the behaviours of u and u_0 are the same around β_0 as the degeneration takes place outside of a neighborhood of β_0 . Therefore, u_0 maps all of its boundary to β curves

other than β_0 in Σ_{\max} . Thus, u_0 restricted to S_0 gives a homological relation between those β curves. However the β curves other than β_0 remain linearly independent in homology, even after the degeneration (some of them intersect at the degeneration point). Hence, the chain represented by $u_0(S_0)$ has to be a multiple of $[\Sigma_{\max}]$, which contradicts the assumption that $n_{a_i}(u_0|_{S_0}) \neq n_{a_{i+1}}(u_0|_{S_0})$ and thus proves the first part of the lemma.

Furthermore, suppose $n_z = 0$, and after stretching the neck around a , suppose that u is not an unbranched cover around a , which means that u_0 has to have at least one component S_0 which has a boundary marked point where u_0 converges to a Reeb chord around a . The argument above then gives that $u_0(S_0)$ has to be a multiple of $[\Sigma_{\max}]$. However the marked point z lies in one of the domains in between b' and β_0 , hence $n_z(u) = n_z(u_0) = 0$ does not allow u_0 to surject onto Σ_{\max} . Thus we arrive at a contradiction, which gives the second part of the lemma. \square

3.2.3 Calculations for fibred 3-manifolds and C_{right}

Before delving into a general study of Heegaard Floer homology for broken maps, here we will calculate $HF^+(Y, \eta)$ in the case of fibred 3-manifolds. Some of these calculations were done independently by Wu in [45], where perturbed Heegaard Floer homology for $\Sigma_g \times S^1$ is calculated for all spin^c structures. We take the liberty to reconstruct some of the arguments presented there in this section since these calculations will play a role for the calculations we do for general fibred 3-manifolds. Even though we will do calculations in general for any fibred 3-manifold, we will restrict ourselves to spin^c structures in $\mathcal{S}(Y|F)$, which will simplify the calculations. Our conclusion is that $\bigoplus_{s \in \mathcal{S}(Y|F)} HF^+(Y, \eta)$ has rank 1. See also [1] for a different

approach in the case of torus bundles.

For fibred 3-manifolds, we have $g = k$, thus the Heegaard diagram has the curves α_0, β_0 , and the rest of the diagram is constructed from the standard configuration of curves $\bar{\xi}_1, \dots, \bar{\xi}_{2k}, \bar{\eta}_1, \dots, \bar{\eta}_{2k}$ as in Figure 3-2. Also we will see below that, for the spin^c structures in $\mathcal{S}(Y|F)$, the generators of our chain complex are given by the intersection points in C_{right} .

We first discuss the case of torus bundles. It will then be clear that the general case is just a matter of notational complication. Also note that, in the case of torus bundles, we have to use a perturbation η with $\eta([F]) > 0$ as explained in the previous section since our diagram is not weakly admissible. For higher genus fibrations, the diagram is weakly admissible hence our calculation also determines the unperturbed Heegaard Floer homology $HF^+(Y)$. When doing explicit calculations we will always consider the case of $HF^+(Y, f, \gamma_w)$ but clearly all arguments go through for any perturbation with η satisfying $\eta([F]) > 0$, or for the unperturbed case whenever the diagram is weakly admissible.

Figure 3-3 shows the Heegaard diagram for T^3 . Both the left and the right figure are twice punctured tori, and are identified along the two boundaries (the one in the middle and the one formed by the four corners) where the gluing of the left and right figures is made precise by the labels at the four corners. On the right side the standard set of arcs $\bar{\xi}_1, \bar{\xi}_2, \bar{\eta}_1, \bar{\eta}_2$ are depicted; the left side is constructed by taking the images of these arcs under the horizontal flow (which is the identity map for T^3), and winding ξ_1 and ξ_2 along transverse circles so that the diagram becomes almost admissible (Note that the winding process avoids the region where w is placed, as required: first ξ_2 is wound once along a horizontal circle, then ξ_1 is wound twice along a vertical circle). For general torus bundles, the same construction

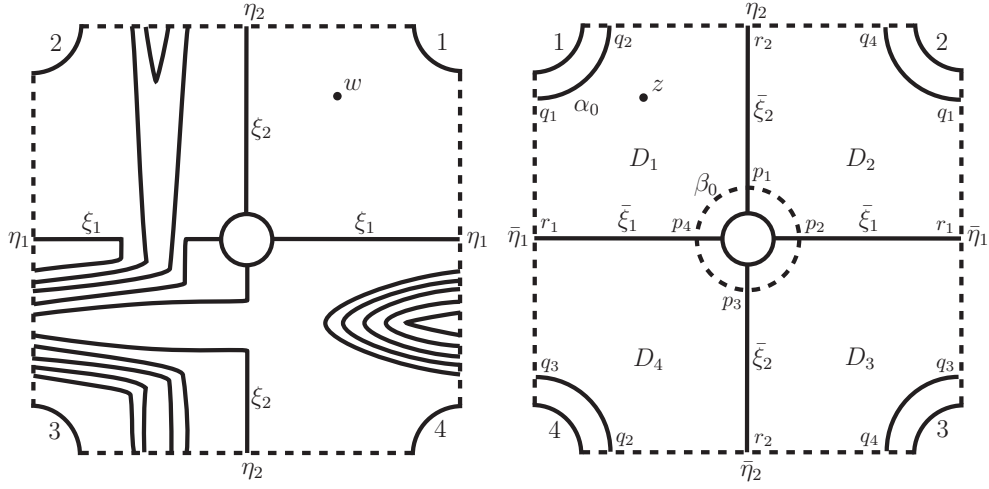


Figure 3-3: Torus bundles

will give a Heegaard diagram, where ξ_1 and ξ_2 are replaced by their images under the monodromy of the torus bundle. The important observation here is that the right side of the diagram is always standard. We will show that all the calculations that we need can be done on the right side of the diagram for the spin^c structures we have in mind. The calculation for T^3 is essentially the same as in [45]. However, we will see that Lemma 3.2.6 plays a crucial role in the calculation for general torus bundles. We first do the calculation for T^3 .

Proposition 3.2.7. $HF^+(T^3, f, \gamma_w, \mathfrak{s}_0) = \Lambda$ where $\mathfrak{s}_0 \in \mathcal{S}(T^3|T^2)$ is the unique torsion spin^c structure on T^3 .

Proof. As in Lemma 3.2.5, $\mathfrak{s}_{\mathbf{x}}(z) \in \mathcal{S}(T^3|T^2)$ if and only if $\mathbf{x} \in C_{\text{right}}$, hence \mathbf{x} can be one of the following tuples of intersections depicted in Figure 3-3:

$$\mathbf{x}_1 = p_1q_2r_1 \quad \mathbf{x}_2 = p_2q_1r_2 \quad \mathbf{x}_3 = p_3q_4r_1 \quad \mathbf{x}_4 = p_4q_3r_2$$

$$\mathbf{y}_1 = p_4q_1r_2 \quad \mathbf{y}_2 = p_1q_4r_1 \quad \mathbf{y}_3 = p_2q_3r_2 \quad \mathbf{y}_4 = p_3q_2r_1$$

Next, we apply the adjunction inequality for the other T^2 components, this implies that the Heegaard Floer groups vanish except for the unique torsion spin^c structure, \mathfrak{s}_0 which has $c_1(\mathfrak{s}_0) = 0$. The two other torus components are realized by periodic domains in Figure 3-3, one of them is the domain P_1 including $D_2 \cup D_3$ and bounded by α_2 and β_1 , the other one is the domain P_2 including $D_3 \cup D_4$ and bounded by α_1 and β_2 . Then the formula $\langle c_1(\mathfrak{s}_z(\mathbf{x})), P_i \rangle = e(P_i) + 2n_{\mathbf{x}}(P_i)$, implies that the only intersection points for which $\mathfrak{s}_z(\mathbf{x}) = \mathfrak{s}_0$ are \mathbf{x}_1 and \mathbf{y}_1 . Furthermore, note that D_1 is a hexagonal region connecting \mathbf{x}_1 to \mathbf{y}_1 , hence it is represented by a holomorphic disk $\varphi_1 \in \pi_2(\mathbf{x}_1, \mathbf{y}_1)$, and the algebraic number of holomorphic disks in the corresponding moduli space of disks in the homology class of φ_1 is given by $\#\widehat{\mathcal{M}}(\varphi_1) = \pm 1$ (See appendix in [35]).

Now, given any other Maslov index 1 homology class $A \in \pi_2(\mathbf{x}_1, \mathbf{y}_1)$, we have $A = D_1 + mF + m_1P_1 + m_2P_2$. In particular, note that $n_z(A) = 1$. Furthermore, if we restrict to those with $n_w = 0$ (that is $m = 0$), since $m_1P_1 + m_2P_2$ has both positive and negative domains by almost admissibility, unless $m_1 = m_2 = 0$ there is no holomorphic representative of A .

We conclude that $\partial^+[\mathbf{x}_1, i] = f(t)[\mathbf{y}_1, i - 1]$, where $f(t) = \pm 1 + O(t)$ is invertible in the Novikov ring. This implies that $[\mathbf{y}_1, i]$ is in the image of ∂^+ . Thus in particular we have $\partial^+[\mathbf{y}_1, i] = 0$ for all i . Finally, there is no Maslov index 1 disk with $n_w = 0$ which connects \mathbf{x}_1 to itself or \mathbf{y}_1 to itself. Thus we conclude that in $CF^+(T^3, f, \gamma_w, \mathfrak{s}_0)$:

$$\partial^+[\mathbf{x}_1, 0] = 0 \quad \partial^+[\mathbf{y}_1, i] = 0$$

$$\partial^+[\mathbf{x}_1, i] = (\pm 1 + O(t))[\mathbf{y}_1, i - 1] \quad \text{for } i > 0$$

Hence the homology is generated by $[\mathbf{x}_1, 0]$, in other words $HF^+(T^3, f, \gamma_w, \mathfrak{s}_0) = \Lambda$

as required. □

From now on, we will simply write \mathbf{x}_1 for $[\mathbf{x}_1, 0]$. The next theorem generalizes this calculation to any torus bundle.

Theorem 3.2.8. *Let (Y, f) be a torus bundle and let \mathfrak{s} be in $\mathcal{S}(Y|T^2)$. Then, $HF^+(Y, f, \gamma_w, \mathfrak{s}) = \Lambda$ if $\mathfrak{s} = \mathfrak{s}_0$ where \mathfrak{s}_0 is the spin^c structure corresponding to vertical tangent bundle and $HF^+(Y, f, \gamma_w, \mathfrak{s}) = 0$ otherwise.*

Proof. The main difficulty for the general torus bundle case that makes the calculation different from the calculation for T^3 is that we cannot a priori eliminate the generators $\mathbf{x}_2, \mathbf{x}_3, \mathbf{x}_4$ and $\mathbf{y}_2, \mathbf{y}_3, \mathbf{y}_4$. In fact, if the first Betti number of the torus bundle is equal to 1, these generators are in the same spin^c class as \mathbf{x}_1 and \mathbf{y}_1 .

Now, the domains D_i are homology classes in $\pi_2(\mathbf{x}_i, \mathbf{y}_i)$, which have holomorphic representatives φ_i with $\#\mathcal{M}(\varphi_i) = \pm 1$. Since any non-trivial periodic domain has to pass through some region to the left of α_0 or β_0 , any other homology class in $\pi_2(\mathbf{x}_i, \mathbf{y}_i)$ which contributes to the differential has to have $n_w \neq 0$ by Lemma 3.2.6. For the same reason, any homology class in $\pi_2(\mathbf{x}_i, \mathbf{y}_j)$ for some $i \neq j$ which contributes to the differential has to have $n_w \neq 0$ since there is no homology class in $\pi_2(\mathbf{x}_i, \mathbf{y}_j)$ that lies in the right side of the diagram (this can be verified either by inspection, or referring to the case of T^3 , where \mathbf{x}_i and \mathbf{y}_j represent different spin^c classes for $i \neq j$). Moreover, the classes in $\pi_2(\mathbf{x}_i, \mathbf{x}_j)$ all have even Maslov index, hence do not contribute to the differential. Therefore, we have

$$\partial^+[\mathbf{x}_1, i] = [\mathbf{y}_1, i - 1] \pmod{t} \text{ for } i > 0$$

$$\partial^+[\mathbf{x}_1, 0] = 0 \pmod{t} \quad \partial^+[\mathbf{x}_2, i] = [\mathbf{y}_2, i] \pmod{t}$$

$$\partial^+[\mathbf{x}_3, i] = [\mathbf{y}_3, i] \pmod{t} \quad \partial^+[\mathbf{x}_4, i] = [\mathbf{y}_4, i] \pmod{t}$$

where the higher order terms do not involve the \mathbf{x}_j 's. As before, because we are working over a Novikov ring of power series, we conclude that $[\mathbf{y}_1, i], [\mathbf{y}_2, i], [\mathbf{y}_3, i]$ and $[\mathbf{y}_4, i]$ are all in the image of ∂^+ . Furthermore, the only possible generator which might be in the kernel of ∂^+ is $[\mathbf{x}_1, 0]$. Finally lemma 3.2.9 below shows that there is no holomorphic disk starting at \mathbf{x}_1 with $n_z = 0$ and $n_w \neq 0$. Hence we have $\partial^+[\mathbf{x}_1, 0] = 0$ and the homology group $\bigoplus_{\mathfrak{s} \in \mathcal{S}(Y|T^2)} HF^+(Y, f, \gamma_w, \mathfrak{s})$ is generated by $[\mathbf{x}_1, 0]$. Furthermore, $\mathfrak{s}_z(\mathbf{x}_1) = \mathfrak{s}_0$ so the theorem is proved. \square

Note also that the adjunction inequality implies that $HF^+(Y, f, \gamma_w, \mathfrak{s})$ vanishes for $\mathfrak{s} \notin \mathcal{S}(Y|T^2)$. Therefore the above calculation is in fact a complete calculation of perturbed Heegaard Floer homology for torus bundles.

The following lemma which we alluded to in the above calculation holds in general (not only in the fibred case). Let Y be any 3-manifold with $b_1 > 0$, and $f : Y \rightarrow S^1$ a broken fibration with connected fibres. Construct the almost admissible Heegaard diagram for f as before and let $\mathbf{x}_1 \in C_{\text{right}}$ be given by the union of the intersection points in $\alpha_0 \cap \beta_2, \alpha_2 \cap \beta_0$, and $\bar{\xi}_i \cap \bar{\eta}_i$ for $i \neq 2$, where the intersection point in $\alpha_0 \cap \beta_2$ and $\alpha_2 \cap \beta_0$ are chosen so that the region containing z includes them as corners. (In the case of the torus bundle this is the generator $[\mathbf{x}_1, 0]$). Note that the generators of C_{right} can always be described from the standard diagram since the right hand side of our Heegaard diagrams is always the same.

Lemma 3.2.9. *Let $\varphi \in \pi_2(\mathbf{x}_{\text{left}} \otimes \mathbf{x}_1, \mathbf{y}_{\text{left}} \otimes \mathbf{y}_{\text{right}})$ be a holomorphic disk in a class that contributes non-trivially to the differential for given $\mathbf{x}_{\text{left}}, \mathbf{y}_{\text{left}}, \mathbf{y}_{\text{right}}$. If $n_z(\varphi) = 0$, then $\mathbf{y}_{\text{right}} = \mathbf{x}_1$ and the domain of φ is contained on the left side of the Heegaard diagram (i.e. it is contained in F).*

Proof. Consider the component of \mathbf{x}_1 which is an intersection point on β_0 , say p_1 . Now, among the four regions which have p_1 as one of their corners, one includes z , namely D_1 , and two of them lie in the left half of the diagram, hence by lemma 3.2.6, they must have the same multiplicity. Denote these regions by L_1 and L_2 , so that L_1 and D_1 share an edge on β_0 . If the component of φ which is asymptotic to p_1 is constant, then p_1 is also part of $\mathbf{y}_{\text{right}}$. Otherwise, since φ has a corner which leaves p_1 and $n_z(\varphi) = 0$, we must have a non-zero multiplicity at L_2 , but since L_1 and L_2 must have the same multiplicity, this implies that p_1 has to be a member in $\mathbf{y}_{\text{right}}$. The same conclusion applies for the point of \mathbf{x}_1 which lies on α_0 . But then there is a unique way to complete these two intersection points to a generator in C_{right} , hence we conclude that $\mathbf{y}_{\text{right}} = \mathbf{x}_1$. Thus φ is in $\pi_2(\mathbf{x}_{\text{left}} \otimes \mathbf{x}_1, \mathbf{y}_{\text{left}} \otimes \mathbf{x}_1)$.

Furthermore, since φ fixes \mathbf{x}_1 , the intersection of the domain of φ with \bar{F} must coincide with the intersection of some periodic domain for $S^1 \times \Sigma_k$ with \bar{F} (since any domain that has no corners on the right side, can be completed to a periodic domain on the Heegaard diagram of $S^1 \times \Sigma_k$ by reflecting). However, it is easy to identify all the periodic domains of $S^1 \times \Sigma_k$ and observe that no non-trivial combination of periodic domains for $S^1 \times \Sigma_k$ (if we leave out F and its multiples), can have the same multiplicity in the regions immediately to the left of α_0 and β_0 . However, by Lemma 3.2.6 this property has to hold. This proves the lemma. \square

Theorem 3.2.10. *Let (Y, f) be a fibre bundle with fibre a genus g surface and let \mathfrak{s} be in $\mathcal{S}(Y|\Sigma_g)$. Then, $HF^+(Y, f, \gamma_w, \mathfrak{s}) = \Lambda$ if $\mathfrak{s} = \mathfrak{s}_0$ where \mathfrak{s}_0 is the spin^c structure corresponding to vertical tangent bundle and $HF^+(Y, f, \gamma_w, \mathfrak{s}) = 0$ otherwise.*

Proof. The proof is essentially the same as the proof of the corresponding theorem for the torus bundles. The only difference is the number of generators which are cancelled out: there are now $8g$ generators $\mathbf{x}_1, \dots, \mathbf{x}_{4g}, \mathbf{y}_1, \dots, \mathbf{y}_{4g}$, and the $4g$ hexagonal regions

of \bar{F} (see Figure 3-2) give $\partial^+[\mathbf{x}_1, i] = [\mathbf{y}_1, i-1] \pmod{t}$ and $\partial^+[\mathbf{x}_j, i] = [\mathbf{y}_j, i] \pmod{t}$ for $j \geq 2$. Arguing as before, the only generator left is again \mathbf{x}_1 which gives $\mathfrak{s}_z(\mathbf{x}_1) = \mathfrak{s}_0$. \square

Note that this gives a new way of obtaining the results of the original calculation of Ozsváth and Szabó in [26] for fibred 3-manifolds.

Corollary 3.2.11. *Let (Y, f) be a fibre bundle with fibre a genus $g > 1$ surface and let \mathfrak{s} be in $\mathcal{S}(Y|\Sigma_g)$. Then, $HF^+(Y, \mathfrak{s}) = \mathbb{Z}$ if $\mathfrak{s} = \mathfrak{s}_0$ where \mathfrak{s}_0 is the spin^c structure corresponding to vertical tangent bundle and $HF^+(Y, \mathfrak{s}) = 0$ otherwise.*

Proof. Since the diagram is weakly admissible, we can let $t = 1$ and the result follows from the previous theorem. \square

In general, let $\partial_{\text{right}}^+$ be the contribution to the Heegaard Floer differential from the holomorphic disks whose domain lies in \bar{F} (i.e. the disks which lie on the right half of our almost admissible Heegaard diagrams), also let $CF_{\text{right}}^+ = C_{\text{right}} \otimes \Lambda[\mathbb{Z}_{\geq 0}]$, the chain complex associated with the right side of the diagram for the purpose of constructing HF^+ theory.

Corollary 3.2.12. *$(CF_{\text{right}}^+, \partial_{\text{right}}^+)$ is a chain complex with rank 1 homology generated by \mathbf{x}_1 .*

Proof. This is only a reformulation of the above results. \square

3.3 The isomorphism

In this section, we prove the main theorem of this chapter. Namely, we prove that the perturbed Heegaard Floer homology group $HF^+(Y, f, \gamma_w)$ is isomorphic to the Floer homology of the chain complex $(C_{\text{left}}, \partial_{\text{left}}; \Lambda)$. Before stating our theorem let

us digress to give a rigorous definition of the latter chain complex.

3.3.1 A variant of Heegaard Floer homology for broken fibrations over the circle

Let Y be a 3-manifold with $b^1 > 0$, and let $f : Y \rightarrow S^1$ be a broken fibration with connected fibres, and satisfying the conditions at the beginning of Section 3.2.1. As before consider the highest genus fibre Σ_g and let $\alpha_1, \dots, \alpha_{g-k}$ and $\beta_1, \dots, \beta_{g-k}$ be tuples of $g - k$ disjoint linearly independent simple closed curves on Σ_g obtained from the attaching circles corresponding to the critical values of f , and let w be a base point that is in the complement of α and β curves. As in Lemma 3.2.2, we can arrange by winding if necessary that there are no periodic domains. We define the Floer homology of such a configuration in a manner similar to the usual Heegaard Floer theory by defining the chain complex to be the Λ -module freely generated by intersection points of $\mathbb{T}_\alpha^{g-k} = \alpha_1 \times \dots \times \alpha_{g-k}$ and $\mathbb{T}_\beta^{g-k} = \beta_1 \times \dots \times \beta_{g-k}$ in $\text{Sym}^{g-k}(\Sigma_g)$, equipped with a differential given as follows:

$$\partial \mathbf{x} = \sum_{\varphi \in \pi_2(\mathbf{x}, \mathbf{y}), \mu(\varphi)=1} \# \widehat{\mathcal{M}}(\varphi) t^{n_w(\varphi)} \mathbf{y}$$

For reasons that will be clarified in Section 3.4, we will denote the homology group that we expect to get from this construction $QFH'(Y, f; \Lambda)$. This stands for *quilted Floer homology* of the broken fibration (Y, f) with coefficients in Λ . There are at least two obvious issues that we need to address in order to make sure that $QFH'(Y, f; \Lambda)$ is well-defined. The first issue is the compactness of the moduli space $\mathcal{M}(\varphi)$. The second issue is proving that $\partial^2 = 0$. The setup here is more delicate than the

usual setup of Heegaard Floer homology due to the fact that $\text{Sym}^{g-k}(\Sigma_g)$ is not a (positively) monotone symplectic manifold when $k > 0$ (it has $\langle c_1, [\Sigma_g] \rangle = 2 - 2k$). Therefore, one expects the existence of configurations with negative Chern number bubbles. However, we will adopt the cylindrical setting of Lipshitz ([18]), whereby one considers pseudo-holomorphic curves in $\Sigma_g \times [0, 1] \times \mathbb{R}$ instead of disks in $\text{Sym}^{g-k}(\Sigma_g)$, and choose our almost complex structures from a sufficiently general class. Namely, one chooses a translation-invariant almost-complex structure J on $\Sigma_g \times [0, 1] \times \mathbb{R}$ such that J preserves a 2-plane distribution ξ on $\Sigma_g \times [0, 1]$ which is tangent to Σ_g near $(\alpha \cup \beta) \times [0, 1]$ and near $\Sigma_g \times \partial[0, 1]$ (see [18], axiom J5'). Now we can show that transversality can be achieved for holomorphic curves in the homology class of the fibre of the projection $\Sigma_g \times [0, 1] \times \mathbb{R} \rightarrow [0, 1] \times \mathbb{R}$. However the expected dimension of these curves is negative, hence bubbling at interior points can be ruled out a priori (see [18] Lemma 8.2). Furthermore, since we assumed that all the fibres are connected, the $(g-k)$ -tuples of curves are linearly independent in homology; this implies that any boundary bubble lifts to a spherical class in $\pi_2(\text{Sym}^{g-k}(\Sigma_g))$. By choosing almost complex structures in a specific way as in [18] Lemma 8.2, we can also avoid disk bubbles. Thus the compactness of $\mathcal{M}(\varphi)$ is ensured.

The drawback of this approach is that it does not correspond in a straightforward way to the original setting in $(\text{Sym}^{g-k}\Sigma_g, \mathbb{T}_\alpha^{g-k}, \mathbb{T}_\beta^{g-k})$ since such general almost complex structures prevent the fibres of the projection to $[0, 1] \times \mathbb{R}$ from being complex. In this case, in order to be able work in $\text{Sym}^{g-k}(\Sigma_g)$ one needs to establish a proper combinatorial rule for handling bubbled configurations (for example by applying the general machinery of virtual fundamental cycles [20]). It is reasonable to expect that one would then get the same differential as above, but the argument would be technically very involved. However, there is an exception to this, namely when we

are in the strongly negative case, that is when $g < 2k$. We show in Section 3.4 that in this case we can indeed use integrable complex structures of the form $\text{Sym}^{g-k}(j_s)$ for a path j_s of complex structures on Σ and still avoid bubbling by making use of the Abel-Jacobi map.

The proof of $\partial^2 = 0$ for $QFH'(Y, f; \Lambda)$ will be part of the proof of the isomorphism that we will construct between $QFH'(Y, f; \Lambda)$ and $HF^+(Y, f, \gamma_w)$. Namely, this follows from an identification between the Maslov index 1 moduli spaces in both theories. Furthermore, we will also see in this section that $QFH'(Y, f; \Lambda)$ is an invariant of $(Y, [f])$, that is it only depends on the homotopy class of f and, when defined over \mathbb{Z} , it will be an invariant of Y .

As usual in Floer homology theories, the groups $QFH'(Y, f; \Lambda)$ are graded by equivalence classes of spin^c structures. Given an intersection point in $\mathbf{x} \in \mathbb{T}_\alpha^{g-k} \cap \mathbb{T}_\beta^{g-k}$ one gets a spin^c structure $\mathfrak{s}(\mathbf{x}) \in \mathcal{S}(Y|\Sigma_{\min})$, as in Heegaard Floer theory, except we do not need to consider any additional base point since the intersection point \mathbf{x} gives a matching of index 1 and 2 critical points of f , which in turn determines a spin^c structure by taking the gradient vector field of f outside of tubular neighborhoods of these matching flow lines and extending it in a non-vanishing way to the tubular neighborhoods. We remark that in our setup of Heegaard diagram for (Y, f) , we have the equality $\mathfrak{s}(\mathbf{x}_{\text{left}}) = \mathfrak{s}_z(\mathbf{x}_{\text{left}} \otimes \mathbf{x}_1)$ (where \mathbf{x}_1 is as in Lemma 3.2.9).

Remark: Note that if we restrict to the case where we only count $n_w = 0$ curves and forget the data encoded in the α and β that do not come from the critical values of f , we obtain Juhász's sutured Floer homology groups associated with the diagram $(F, \alpha_1, \dots, \alpha_{g-k}, \beta_1, \dots, \beta_{g-k})$ (see [14]). We will return to this below.

3.3.2 Isomorphism between $QFH'(Y, f; \Lambda)$ and $HF^+(Y, f, \gamma_w)$

We now proceed to prove an isomorphism between $QFH'(Y, f; \Lambda)$ and $HF^+(Y, f, \gamma_w)$. As a first step, we make use of the calculations of the previous section. Let $CF_{\text{left}}^+ = C_{\text{left}} \otimes \Lambda[\mathbb{Z}_{\geq 0}]$ and $CF_{\text{right}}^+ = C_{\text{right}} \otimes \Lambda[\mathbb{Z}_{\geq 0}]$, using the splitting of generators of $HF^+(Y, f, \gamma_w)$ as discussed in Section 3.2.2, so that we have $CF^+(Y, f, \gamma_w) = CF_{\text{left}}^+ \otimes CF_{\text{right}}^+$. We denote by ∂_F and $\partial_{\bar{F}} = \mathbb{1} \otimes \partial_{\text{right}}$ the contributions to the Heegaard Floer differential from holomorphic curves whose domains lie in F and \bar{F} respectively. Furthermore, we denote by $\partial_{\text{left}} \otimes \mathbb{1}$, the contribution of those holomorphic curves whose domain lies in F and which act by identity on C_{right} with respect to the splitting $C_{\text{left}} \otimes C_{\text{right}}$. (since the boundary of F includes points of intersections occurring in C_{right} , this is a priori more restrictive than ∂_F). Lemma 3.2.9 implies that $\partial_{\text{left}} \otimes \mathbb{1}$ is a differential on $C_{\text{left}} \otimes \mathbf{x}_1$. The next proposition says that the homology of this differential is isomorphic to $HF^+(Y, f, \gamma_w)$.

Proposition 3.3.1. $HF^+(Y, f, \gamma_w, \mathfrak{s}) \simeq H(C_{\text{left}} \otimes \mathbf{x}_1, \partial_{\text{left}} \otimes \mathbb{1}, \gamma_w, \mathfrak{s})$ for $\mathfrak{s} \in \mathcal{S}(Y | \Sigma_{\min})$.

Proof. Both homology groups are filtered by n_w . Therefore, there are spectral sequences converging to both sides induced by the n_w filtration. Furthermore, we claim that there is a chain map:

$$F : C_{\text{left}} \otimes \mathbf{x}_1 \rightarrow CF_{\text{left}}^+ \otimes CF_{\text{right}}^+$$

given by

$$F(\mathbf{x}_{\text{left}} \otimes \mathbf{x}_1) = [\mathbf{x}_{\text{left}} \otimes \mathbf{x}_1, 0]$$

which induces an isomorphism of E^1 -pages of the spectral sequences associated with both chain complexes. The fact that F is a chain map, is a consequence of Lemma

3.2.9. More precisely, Lemma 3.2.9 gives that if a holomorphic map contributing to the differential originates at $[\mathbf{x}_{\text{left}} \otimes \mathbf{x}_1, 0]$ then it has to converge to a generator of the form $[\mathbf{y}_{\text{left}} \otimes \mathbf{x}_1, 0]$, and the domain of the map has to lie on the left half of the Heegaard diagram; these are exactly the contributions to the differential captured by $\partial_{\text{left}} \otimes \mathbb{1}$.

Furthermore, showing that F induces an isomorphism on the E^1 -pages of the spectral sequences on both sides amounts to checking that

$$F' : (C_{\text{left}} \otimes \mathbf{x}_1, \partial_{\text{left}}^0 \otimes \mathbb{1}) \rightarrow (CF_{\text{left}}^+ \otimes CF_{\text{right}}^+, \partial_{\text{left}}^0 \otimes \mathbb{1} + \mathbb{1} \otimes \partial_{\text{right}})$$

is an isomorphism in homology, where $\partial_{\text{left}}^0 \otimes \mathbb{1}$ denotes those holomorphic maps contributing to the differential ∂_F with $n_w = 0$ (Here we have used Lemma 3.2.6 to identify $n_w = 0$ part of ∂^+ with $\partial_{\text{left}}^0 \otimes \mathbb{1} + \mathbb{1} \otimes \partial_{\text{right}}$). The injectivity of F' in homology follows from the fact that, by Corollary 3.2.12 (see also the proof of Theorem 3.2.10), \mathbf{x}_1 does not lie in the image of ∂_{right} . Thus, we only need to check that F' is surjective in homology. Suppose that $\mathbf{a}_1 \mathbf{x}_1 + \dots + \mathbf{a}_{4k} \mathbf{x}_{4k} + \mathbf{b}_1 \mathbf{y}_1 + \dots + \mathbf{b}_{4k} \mathbf{y}_{4k} \in CF_{\text{left}}^+ \otimes CF_{\text{right}}^+$ is in the kernel of $\partial_{\text{left}}^0 \otimes \mathbb{1} + \mathbb{1} \otimes \partial_{\text{right}}$, where we have chosen the notation so that \mathbf{a}_i and \mathbf{b}_i are elements in $CF_{\text{left}}^+ = C_{\text{left}} \otimes \Lambda[\mathbb{Z}_{\geq 0}]$, and \mathbf{x}_i and \mathbf{y}_i are the generators of C_{right} as in Theorem 3.2.10. Now, because this element is in the kernel of $\partial_{\text{left}}^0 \otimes \mathbb{1} + \mathbb{1} \otimes \partial_{\text{right}}$, we have

$$\begin{aligned} \partial_{\text{left}}^0 \mathbf{a}_1 &= 0 & \text{and} & & U \mathbf{a}_1 + \partial_{\text{left}}^0 \mathbf{b}_1 &= 0 \\ \partial_{\text{left}}^0 \mathbf{a}_i &= 0 & \text{and} & & \mathbf{a}_i + \partial_{\text{left}}^0 \mathbf{b}_i &= 0 \quad \text{for } i \neq 1 \end{aligned}$$

where $U : CF_{\text{left}}^+ \rightarrow CF_{\text{left}}^+$ is the usual map in Heegaard Floer theory which maps

$[\mathbf{a}, i] \rightarrow [\mathbf{a}, i - 1]$. It appears in the above equation because the disk D_1 connecting \mathbf{x}_1 to \mathbf{y}_1 intersects the base point z with multiplicity 1. (Here we also chose an orientation system so that $\partial_{\text{right}}\mathbf{x}_i = \mathbf{y}_i$, one can also do the same calculation if $\partial_{\text{right}}\mathbf{x}_i = -\mathbf{y}_i$.)

Now, observe that the above equations give

$$(\partial_{\text{left}}^0 \otimes \mathbf{1} + \mathbf{1} \otimes \partial_{\text{right}})(\mathbf{b}_i\mathbf{x}_i) = -\mathbf{a}_i\mathbf{x}_i + \mathbf{b}_i\mathbf{y}_i \quad \text{for } i \neq 1$$

This gives us that $2\mathbf{b}_i\mathbf{y}_i$ is in the kernel, which in turn, implies that $\partial_{\text{left}}^0\mathbf{b}_i = 0$ (This holds unless we work over a field of characteristic 2, see below for that case). Thus, $\mathbf{a}_i = 0$ and $\mathbf{b}_i\mathbf{y}_i$ is in the image of $\partial_{\text{left}}^0 \otimes 1 + 1 \otimes \partial_{\text{right}}$ (In characteristic 2, we directly conclude that $\mathbf{a}_i\mathbf{x}_i + \mathbf{b}_i\mathbf{y}_i$ is in the image). Therefore, in either case we can ignore all the terms other than $\mathbf{a}_1\mathbf{x}_1 + \mathbf{b}_1\mathbf{y}_1$. Furthermore, note that

$$(\partial_{\text{left}}^0 \otimes 1 + 1 \otimes \partial_{\text{right}})(U^{-1}\mathbf{b}_1\mathbf{x}_1) = U^{-1}\partial_{\text{left}}^0\mathbf{b}_1\mathbf{x}_1 + \mathbf{b}_1\mathbf{y}_1 = -\mathbf{a}_1\mathbf{x}_1 + \mathbf{b}_1\mathbf{y}_1$$

Thus, we conclude that $2\mathbf{b}_1\mathbf{y}_1$ is in the kernel, which implies that $\partial_{\text{left}}^0\mathbf{b}_1 = 0$ hence, $U\mathbf{a}_1 = 0$ and $(\partial_{\text{left}}^0 \otimes 1 + 1 \otimes \partial_{\text{right}})(U^{-1}\mathbf{b}_1\mathbf{x}_1) = \mathbf{b}_1\mathbf{y}_1$ hence we can ignore the term $\mathbf{b}_1\mathbf{y}_1$ and the fact that $U\mathbf{a}_1 = 0$ implies that $\mathbf{a}_1\mathbf{x}_1$ is in the image of F as desired.

This concludes the proof of Proposition 3.3.1 since a chain map that induces an isomorphism of E^1 -pages induces an isomorphism at all pages of the spectral sequences (see e.g. Theorem 3.5 of [23]), in particular the E^∞ -pages are the groups that we have written in the statement of Proposition 3.3.1. \square

An immediate corollary that follows from the proof of Proposition 3.3.1 is that the U -action on $HF^+(Y, f, \gamma_w, \mathfrak{s})$ is trivial for $\mathfrak{s} \in \mathcal{S}(Y|\Sigma_{\min})$. In fact, we have a splitting of

the long exact sequence induced by the U -action, which implies the following relation with the hat-version of Heegaard Floer homology where the differential counts the holomorphic curves with $n_z = 0$ (see [26]).

Corollary 3.3.2. *For $\mathfrak{s} \in \mathcal{S}(Y|\Sigma_{min})$,*

$$\widehat{HF}(Y, f, \gamma_w, \mathfrak{s}) \simeq HF^+(Y, f, \gamma_w, \mathfrak{s}) \oplus HF^+(Y, f, \gamma_w, \mathfrak{s})[1] \quad \square$$

Note that in the case that $g(\Sigma_{min}) = k > 1$, there is no perturbation required thus the above equality holds for the homology groups with integer coefficients. In particular, this implies that $HF^+(Y, \mathfrak{s})$ is algorithmically computable for $\mathfrak{s} \in \mathcal{S}(Y|\Sigma_{min})$ since in [38] an algorithm for computing $\widehat{HF}(Y, \mathfrak{s})$ was given.

Finally, we are ready to state and prove our main result. Over the course of the proof of the following theorem, we will see why the variant of Heegaard Floer homology that we denoted by $QFH'(Y, f, \mathfrak{s}; \Lambda)$ is well-defined. More precisely, we will see that the differential that we defined for $QFH'(Y, f, \mathfrak{s}; \Lambda)$ squares to zero.

Theorem 3.3.3. *$HF^+(Y, f, \gamma_w, \mathfrak{s}) \simeq QFH'(Y, f, \mathfrak{s}; \Lambda)$ for $\mathfrak{s} \in \mathcal{S}(Y|\Sigma_{min})$.*

Proof. Because of Proposition 3.3.1, it suffices to prove that

$$H(C_{\text{left}} \otimes \mathbf{x}_1, \partial_{\text{left}} \otimes \mathbb{1}, \gamma_w, \mathfrak{s}) \simeq H(C_{\text{left}}, \partial, \mathfrak{s})$$

where the latter group is what we previously called $QFH(Y, f, s)$. Clearly, we have a one-to-one correspondence between the generators. Next, we will show that there is an isomorphism of chain complexes. In fact, we will show that the signed counts of Maslov index 1 holomorphic curves in $\pi_2(\mathbf{x}_{\text{left}} \otimes \mathbf{x}_1, \mathbf{y}_{\text{left}} \otimes \mathbf{x}_1)$ which contribute to $\partial_{\text{left}} \otimes 1$ and Maslov index 1 holomorphic curves in $\pi_2(\mathbf{x}_{\text{left}}, \mathbf{y}_{\text{left}})$ that contribute to the differential ∂ are equal. First observe that for curves which stay away from

the necks at α_0 and β_0 , which are precisely those with $n_w = 0$, this one to one correspondence is clear. (These are the curves that contribute to the differential $\partial_{\text{left}}^0 \otimes 1$ in Proposition 3.3.1).

Next, we discuss the curves which have $n_w \neq 0$. The correspondence in this case will be obtained by stretching the necks along a and b , which are respectively parallel pushoffs of α_0 and β_0 to the left of the Heegaard diagram (into the region F).

Let us first describe the holomorphic curves that contribute to $\partial_{\text{left}} \otimes \mathbb{1}$ with $n_w \neq 0$ more precisely. Remember that by definition $\partial_{\text{left}} \otimes \mathbb{1}$ counts those holomorphic curves whose domain lies in F , hence they have $n_z = 0$. Now, recall that Lemma 3.2.6 says that the projection to the Heegaard surface is an unbranched cover around the necks a and b . Let $A \in \pi_2(\mathbf{x}_{\text{left}} \otimes \mathbf{x}_1, \mathbf{y}_{\text{left}} \otimes \mathbf{x}_1)$ be a Maslov index 1 homology class which is contributing to $\partial_{\text{left}} \otimes \mathbb{1}$. By degenerating the almost complex structure around a and b on Σ , we get two homology classes $A_{\text{left}} \in \pi_2(\mathbf{x}_{\text{left}}, \mathbf{y}_{\text{left}})$ and $A_{\text{right}} \in \pi_2(\mathbf{x}_1, \mathbf{x}_1)$. The domain of A_{left} lies on Σ_{max} and it determines a homology class for the type of holomorphic curves contributing to the differential ∂ . The domain of A_{right} has two components A_{right}^a and A_{right}^b , both supported in disks which are the domains between α_0 and a , with a collapsed to a point, and between β_0 and b with b collapsed to a point. We claim that the Maslov index of A_{left} is equal to 1, and the Maslov indices of each of the components in A_{right} are equal to $2n_w$. Since the degeneration is along Reeb orbits, we have the formula

$$\text{ind}(A) = \text{ind}(A_{\text{left}}) + \text{ind}(A_{\text{right}}^a) + \text{ind}(A_{\text{right}}^b) - 2(N_a + N_b)$$

where N_a and N_b are the numbers of connected components of the unramified covering in the necks at a and b (clearly $N_a, N_b \in [1, n_w]$). Therefore, it suffices to see that

$\text{ind}(A_{\text{right}}^a) = \text{ind}(A_{\text{right}}^b) = 2n_w$. This follows from the usual formula $\text{ind}(A_{\text{right}}^a) = \langle c_1(\mathfrak{s}), A_{\text{right}}^a \rangle = e(A_{\text{right}}^a) + 2n_{\mathbf{x}}(A_{\text{right}}^a) = 2n_w$ (since the homology class A_{right}^a is n_w times the disk with boundary on α_0 , $e(A_{\text{right}}^a) = n_w$ and $n_{\mathbf{x}}(A_{\text{right}}^a) = n_w/2$); similarly for A_{right}^b . We deduce that $\text{ind}(A_{\text{left}}) = 1 + 2(N_a + N_b) - 4n_w$, which implies that $\text{ind}(A_{\text{left}}) = 1$ and the coverings in the cylindrical necks near a and b are both trivial (in other terms, after neck-stretching we have n_w distinct cylinders passing through each neck).

Furthermore, we have the evaluation maps :

$$\begin{aligned} ev_{\text{left}}^a & : \mathcal{M}(A_{\text{left}}) \rightarrow \text{Sym}^{n_w}(\mathbb{D}) \\ ev_{\text{right}}^a & : \mathcal{M}(A_{\text{right}}^a) \rightarrow \text{Sym}^{n_w}(\mathbb{D}) \\ ev_{\text{left}}^b & : \mathcal{M}(A_{\text{left}}) \rightarrow \text{Sym}^{n_w}(\mathbb{D}) \\ ev_{\text{right}}^b & : \mathcal{M}(A_{\text{right}}^b) \rightarrow \text{Sym}^{n_w}(\mathbb{D}) \end{aligned}$$

given by taking the preimages of the degeneration points of a and b and projecting to $\mathbb{D} = [0, 1] \times \mathbb{R}$. We claim that the moduli space $\mathcal{M}(A)$ can be identified with the fibre product of moduli spaces $\mathcal{M}(A_{\text{left}}) \times_B \mathcal{M}(A_{\text{right}})$, where $B = \text{Sym}^{n_w}(\mathbb{D}) \times \text{Sym}^{n_w}(\mathbb{D})$ and the fibre product is taken with respect to the above evaluation maps. This is a consequence of a gluing theorem (see [28] Theorem 5.1 for the proof in a very closely related situation and [6] for a discussion of gluing in a general context).

Finally, we will prove that $(ev_{\text{right}}^a, ev_{\text{right}}^b) : \mathcal{M}(A_{\text{right}}^a) \times \mathcal{M}(A_{\text{right}}^b) \rightarrow \text{Sym}^{n_w}(\mathbb{D}) \times \text{Sym}^{n_w}(\mathbb{D})$ has degree 1. This implies that, for the purpose of counting pseudoholomorphic curves, the fibre product of moduli spaces $\mathcal{M}(A_{\text{left}}) \times_B \mathcal{M}(A_{\text{right}})$ can be identified with $\mathcal{M}(A_{\text{left}})$. Therefore, we can identify the moduli spaces $\mathcal{M}(A)$ and

$\mathcal{M}(A_{\text{left}})$, as required.

To see that the evaluation maps have degree 1, we argue as follows: First, we represent the domain of the strips in $\mathcal{M}(A_{\text{right}}^a)$ by the upper half of the unit disk so that the upper half circle maps to α_0 and the interval $[-1, 1]$ maps to the β curve. Also, represent the target disk by the unit disk, so that α_0 corresponds to the unit circle and the β arc is represented by the real positive axis, furthermore the degeneration point of a as used to define the map ev_{right}^a is mapped to the origin in this representation. Thus, the moduli space $\mathcal{M}(A_{\text{right}}^a)$ consists of holomorphic maps from the upper half disk to the unit disk and ev_{right}^a records the positions of the n_w zeroes of these maps. Now, any holomorphic map from the upper half disk to the unit disk can be reflected ($u(1/\bar{z}) := 1/\overline{u(z)}$) to get a holomorphic map from the upper half-plane to \mathbb{P}^1 , mapping the real axis to the real positive axis. This can then be further reflected about the real axis to get holomorphic maps from \mathbb{P}^1 to \mathbb{P}^1 which are hence rational fractions of degree $2n_w$, with real coefficients (forced by the invariance under conjugation) and with equivariance under $z \rightarrow 1/\bar{z}$. Now, such holomorphic maps are classified by their zeroes (the poles are the reflections of the zeroes). In our case, there are $2n_w$ zeroes and none of these are real, so they are n_w pairs of complex conjugate points. Finally, we note that ev_{right}^a maps any such holomorphic map to the positions of its n_w zeroes which lie inside the upper half-disk. Therefore, $ev_{\text{right}}^a : \mathcal{M}(A_{\text{right}}^a) \rightarrow \text{Sym}^{n_w}(\mathbb{D})$ is in fact a diffeomorphism. In particular, it has degree 1. \square

Note that when the minimal genus fibre has genus greater than 1, there is no perturbation required since the diagrams that we consider are weakly admissible in that case. Hence, we get the above isomorphism for the homology groups with integer coefficients.

Corollary 3.3.4. *Suppose that $g(\Sigma_{min}) = k > 1$, then for $\mathfrak{s} \in \mathcal{S}(Y|\Sigma_{min})$ we have*

$$QFH'(Y, f, \mathfrak{s}; \mathbb{Z}) \simeq HF^+(Y, \mathfrak{s}).$$

Proof. This follows from the above result by letting $t = 1$. □

In some cases, the quilted Floer homology groups can be calculated easily, the following special case is an example of this. Given two simple closed curves α and β on a surface of genus greater than 1, let $\iota(\alpha, \beta)$ denote the geometric intersection number of α and β , i.e. the number of transverse intersections of their geodesic representatives for a hyperbolic metric.

Corollary 3.3.5. *Suppose that f has only two critical points, and let $\alpha, \beta \subset \Sigma_{max}$ be the vanishing cycles for these critical points. Then $\bigoplus_{\mathfrak{s} \in (\mathcal{S}|\Sigma_{min})} HF^+(Y, f, \gamma_w, \mathfrak{s})$ is free of rank $\iota(\alpha, \beta)$.*

Proof. When f has only two critical points, $QFH'(Y, f)$ reduces to the Lagrangian Floer homology of the simple closed curves α and β on the surface Σ_{max} . This is easily calculated by representing the free homotopy classes of simple closed curves α and β by geodesics, which ensures that there are no non-constant holomorphic discs contributing to the differential. In fact, any holomorphic disk would lift to a holomorphic disk in the universal cover \mathbf{H}^2 , which would contradict the fact that there is a unique geodesic between any two points in \mathbf{H}^2 . Therefore, the quilted Floer homology is freely generated by the number of intersection points of geodesic representatives of α and β . □

We remark that if $\iota(\alpha, \beta) = 1$, then the critical values can be cancelled. Thus for non-fibred manifolds which admit a broken fibration with only 2 critical points the rank of quilted Floer homology is greater than 1.

3.3.3 An application to sutured Floer homology

The following definition of a sutured 3-manifold can be easily seen to be equivalent to the standard definition (see Juhász [14]). A connected balanced sutured manifold is a compact oriented 3-manifold with boundary Y such that Y can be equipped with a broken fibration $f : Y \rightarrow [0, 1]$ whose fibers are surfaces with non-empty boundary and $f^{-1}(0)$ and $f^{-1}(1)$ are homeomorphic surfaces such that each connected component has exactly one boundary component (balanced condition). We can always arrange that $f^{-1}(1/2) = \Sigma_{\max}$ is the highest genus fibre which is connected and as one travels from $1/2$ to 0 one attaches two handles along $\beta_1, \dots, \beta_{g-k}$ and as one travels from $1/2$ to 1 one attaches two handles along $\alpha_1, \dots, \alpha_{g-k}$ which are realized as vanishing cycles of f on Σ_{\max} . The balanced condition translates to the condition that the set of α curves and respectively the set of β curves are linearly independent in $H_1(\Sigma_{\max})$. The sutures $s(\gamma)$ of Y correspond to the boundary components of $\partial\Sigma_{\max}$ and the annular neighborhoods $A(\gamma)$ of Y are obtained from $s(\gamma)$ by flowing using the gradient flow of f along $[0, 1]$ with respect to a metric such that the gradient vector field of f preserves the boundary of Y .

In [14], Juhász constructs a variant of Heegaard Floer homology for sutured 3-manifolds. This is simply, the Lagrangian Floer homology group $HF(\text{Sym}^{g-k}(\Sigma_{\max}), \alpha_1 \times \dots \times \alpha_{g-k}, \beta_1 \times \dots \times \beta_{g-k})$ where the projections of the holomorphic curves contributing to the differential on Σ_{\max} are required to stay away from the boundary of Σ_{\max} .

In [15], Kronheimer and Mrowka construct an invariant of sutured manifolds using monopole (resp. instanton) Floer homology, by constructing a closed 3-manifold Y_n and setting the sutured Floer homology of Y by defining it to be the monopole

(resp. instanton) Floer homology of Y_n . The construction of (Y_n, f_n) is by first gluing $T \times [0, 1]$ where T is an oriented connected genus $n \geq 1$ surface with non-empty boundary, so that $\partial T \times [0, 1]$ is glued to the union of annuli $A(\gamma)$, and then identifying the fibres over 0 and 1 by choosing a homeomorphism between them. Note that the balanced condition implies that f_n has connected fibres. In the monopole (resp. instanton) setting, Kronheimer and Mrowka define the sutured monopole (resp. instanton) Floer homology of Y to be $\bigoplus_{\mathfrak{s} \in \mathcal{S}(Y|\Sigma_{\min})} HM(Y_n, \mathfrak{s})$ and prove that this is an invariant of the sutured manifold Y (in particular, it is also independent of the genus n of T and the homeomorphism chosen in identifying fibres over 0 and 1). It was raised in [15] as a question, whether one can recover Juhász's definition of sutured Floer homology from the construction given above applied in the setting of Heegaard Floer homology. In the next theorem, we give an affirmative answer to this.

Theorem 3.3.6. *For $n \geq 1$,*

$$SFH(Y, f) \simeq \bigoplus_{\mathfrak{s} \in \mathcal{S}(Y_n, \Sigma_{\min})} HF^+(Y_n, \mathfrak{s})$$

Note that this theorem in particular implies that the group on the right hand side is independent of n and the chosen surface homeomorphism in the construction of Y_n . As usual, in the case that the lowest genus fibre of f_1 has genus 1, one needs to use coefficients in Λ .

Proof. Theorem 3.3.3 applied to (Y_n, f_n) yields that $\bigoplus_{\mathfrak{s} \in \mathcal{S}(Y_n, \Sigma_{\min})} HF^+(Y_n, \mathfrak{s}) = QFH'(Y_n, f_n)$. Therefore, the proof will follow once we establish that $SFH(Y, f) \simeq QFH'(Y_n, f_n)$. This in turn relies on a simple observation about the Heegaard diagrams used in the definition of these groups, namely let us denote the maximal genus

fibre of f by Σ , and the maximal genus fibre of f_n by $\Sigma \cup T$. Now, if an admissible sutured Heegaard diagram of (Y, f) is given by $(\Sigma, \alpha_1, \dots, \alpha_{g-k}, \beta_1, \dots, \beta_{g-k})$, then the Heegaard diagram for calculating $QFH'(Y_n, f_n)$ is given by $(\Sigma \cup T, \alpha_1, \dots, \alpha_{g-k}, \beta_1, \dots, \beta_{g-k})$. Note that there is no α or β curve entering T . Thus, the proof will be complete once we prove that holomorphic curves contributing to the differential of $QFH'(Y_n, f_n)$ do not enter to the region including T . Note that because of the admissibility condition of the sutured Heegaard diagram of (Y, f) we can use an almost complex structure which is vertical in a neighborhood of $\Sigma \times [0, 1] \times \mathbb{R}$ so that the holomorphic curves contributing to the differential of sutured Floer homology appear as holomorphic curves contributing to the differential of $QFH'(Y_n, f_n)$. On the other hand, we use a non-vertical almost complex structures as in Section 3.3.1, along $T \times [0, 1] \times \mathbb{R}$ away from the boundary of T . Now, let $u : (S, \partial S) \rightarrow (\Sigma \cup T) \times [0, 1] \times \mathbb{R}$ be a holomorphic map contributing to the differential of $QFH'(Y_n, f_n)$. We would like to show that the image of the projection of u to the Heegaard surface does not hit T . This follows from a degeneration argument. Namely, suppose that the image of the projection of u does hit T , then we can degenerate along Reeb orbits corresponding to the attaching region of T to Σ , this would on one side give a holomorphic map $\tilde{u} : \tilde{S} \rightarrow \tilde{T} \times [0, 1] \times \mathbb{R}$ where \tilde{T} is the closed surface obtained by shrinking each boundary component of T to a point and \tilde{S} is a part of the domain of the degenerated map. The index formula (see for example [18]) gives that the expected dimension of the moduli space of such maps is a positive multiple of $\chi(\tilde{T})$, which is less than or equal to zero since T has genus at least 1. Furthermore, our choice of almost complex structures ensure transversality for such holomorphic maps, which yields the desired contradiction (note that in the case that T has genus 1, we still obtain a contradiction since we get a negative dimension for the transversely cut moduli space after quotienting by the \mathbb{R} action). \square

3.4 Isomorphism between $QFH(Y, f; \Lambda)$ and $QFH'(Y, f; \Lambda)$

In this section, we relate $QFH'(Y, f)$ defined as a variant of Heegaard Floer homology as in Section 3.3.1 with the original definition in terms of holomorphic quilts given in the introduction, which we called $QFH(Y, f)$. The arguments given here are complete except in the statement of the main theorem (see Theorem 3.4.3) we make an assumption about the non-existence of figure-eight bubbles. This is a new kind of bubbling that arises in the study of holomorphic quilts when the width of a strip is shrunk to zero (see [44] for more background on this). Under suitable strong negativity assumptions, when $g < 2k$, we argue that figure-eight bubbles do not arise by assuming a removal of singularities result. The assumption $g < 2k$ is required in order to avoid disk and sphere bubbles so that the group $QFH(Y, f; \Lambda)$ is well defined. The new input here is that this condition is also sufficient to discard figure-eight bubbles. However, a removal of singularities theorem for figure-eight bubbles is missing at the time of this writing. It appears likely that this is actually not an issue in the setting we consider; we hope to return to this at a later time. Until then when discussing our results we make our arguments under the assumption that the figure-eight bubbles do not arise.

Finally, we remark that all the theorems are stated for Floer homology groups over the universal Novikov ring Λ , but as before, in the case where the lowest genus fibre has genus greater than 1, one can use integer coefficients.

3.4.1 Heegaard tori as composition of Lagrangian correspondences

Recall that given a broken fibration $f : Y \rightarrow S^1$ with connected fibres, the quilted Floer homology of Y is defined as the Floer homology of the Lagrangian correspondences $L_{\alpha_1}, \dots, L_{\alpha_{g-k}}$ and $L_{\beta_1}, \dots, L_{\beta_{g-k}}$ associated with the critical values of f , where as before we let the vanishing cycles for the critical values along the northern semi-circle be $\alpha_1, \dots, \alpha_{g-k}$ and those along the southern semi-circle be $\beta_1, \dots, \beta_{g-k}$. Let us call the Floer homology of these Lagrangian correspondences $HF(\mathbb{L}_\alpha, \mathbb{L}_\beta)$. Note that the construction of these Lagrangians involves a choice of almost complex structure j on the fibres of f .

Recall that given two Lagrangian correspondences, $L_1 \subset X \times Y$ and $L_2 \subset Y \times Z$ such that $L_1 \times L_2$ is transverse to the diagonal in Y , the composition $L_1 \circ L_2$ is a Lagrangian correspondence in $X \times Z$ given by the union of tuples (x, z) such that there exists a $y \in Y$ with the property that $(x, y) \in L_1$ and $(y, z) \in L_2$.

Now, for the class of almost complex structures j that are sufficiently stretched along the vanishing cycles of f near its critical points, we have the following important technical lemma about these correspondences which was conjectured by Perutz in [31]:

Lemma 3.4.1. *For $g > k$, $L_{\alpha_1} \circ \dots \circ L_{\alpha_{g-k}}$ and $L_{\beta_1} \circ \dots \circ L_{\beta_{g-k}}$ are respectively Hamiltonian isotopic to $\alpha_1 \times \dots \times \alpha_{g-k}$ and $\beta_1 \times \dots \times \beta_{g-k}$ in $\text{Sym}^{g-k}(\Sigma)$ equipped with a Kähler form ω which lies in the cohomology class $\eta + \lambda\theta$ with $\lambda > 0$. \square*

Here the classes η and θ are cohomology classes which generate the subspace of cohomology classes which are invariant under the action of the mapping class group . η is the Poincaré dual of the divisor $\{pt\} \times \text{Sym}^{g-k-1}(\Sigma)$ and θ corresponds to

the intersection form on $H^2(\Sigma, \mathbb{R})$ via the Abel-Jacobi map, more precisely it is the pullback by the Abel-Jacobi map of the theta divisor on the Jacobian.

This lemma is proved in appendix B. The proof is obtained by carrying out the construction of Lagrangian correspondences as a family of degenerations. As the required technical set-up is rather different we leave the proof to appendix B.

Recall that when defining $QFH'(Y, f, \Lambda)$ as a variant of Heegaard Floer homology we have used Lipshitz's cylindrical reformulation, by setting up the theory in $\Sigma_{\max} \times [0, 1] \times \mathbb{R}$. This was convenient because of the bubbling issues that may occur in the negatively monotone manifold $\text{Sym}^{g-k}(\Sigma_{\max})$. However, in the strongly negative case, when $g < 2k$, where bubbling can be ruled out for a generic path J_s of almost complex structures on $\text{Sym}^{g-k}(\Sigma_{\max})$ on the grounds that the moduli space of bubbles in this case has negative virtual dimension. In fact, the proof of the lemma below shows that in this case, one can also use a path of integrable complex structures as in the case of the usual Heegaard Floer homology to make sense of this group. Thus, the Floer homology groups can be formulated as a Lagrangian intersection theory in $\text{Sym}^{g-k}(\Sigma_{\max})$.

Lemma 3.4.2. *Suppose that Y admits a broken fibration with $g < 2k$. Then for $\mathfrak{s} \in \mathcal{S}(Y|\Sigma_{\min})$,*

$$QFH'(Y, f, \mathfrak{s}; \Lambda) \simeq HF(\text{Sym}^{g-k}(\Sigma_{\max}); \alpha_1 \times \dots \times \alpha_{g-k}, \beta_1 \times \dots \times \beta_{g-k}, \mathfrak{s}; \Lambda)$$

Proof. We first argue that for a generic path of almost complex structures $\{j_s\}$ on Σ_{\max} the induced integrable complex structures $\text{Sym}^{g-k}(j_s)$ achieve transversality for the holomorphic disks mapping to $\text{Sym}^{g-k}(\Sigma_{\max})$ which contribute to the differential and furthermore for these complex structures no bubbling can occur because of the

strong negativity assumption $g < 2k$. The fact that these complex structures achieve transversality is standard and follows exactly as in the case of the usual Heegaard Floer homology set-up, see for example Proposition A.5 of [18]. To avoid bubbling, we make use of the Abel-Jacobi map:

$$\text{AJ} : \text{Sym}^{g-k}(\Sigma_{\max}) \rightarrow \text{Jac}(\Sigma_{\max})$$

The assumption $g < 2k$ ensures that the Abel-Jacobi map is injective for j chosen outside of a subset of complex codimension at least 1 (so that for a generic path j_s it's injective for all s). A generic choice of j_s therefore ensures that there cannot be any non-constant holomorphic spheres mapping to $\text{Sym}^{g-k}(\Sigma_{\max})$. One can also rule out disk bubbles in the same way: since the inclusions of $\alpha_1 \times \dots \times \alpha_{g-k}$ and $\beta_1 \times \dots \times \beta_{g-k}$ to $\text{Sym}^{g-k}(\Sigma_{\max})$ are injective at the level of fundamental groups and since the Abel-Jacobi map is injective and induces an isomorphism on the first homology when $g < 2k$, the image of a holomorphic disc by the Abel-Jacobi map represents a trivial relative homology class, therefore it is trivial. Hence, there cannot be any non-constant holomorphic disk bubbles.

Now, applying the reformulation of Lipshitz, as in [18], allows us to translate the Lagrangian Floer homology in $\text{Sym}^{g-k}(\Sigma_{\max})$ “tautologically” to the cylindrical set-up in $\Sigma_{\max} \times [0, 1] \times \mathbb{R}$ (see appendix A in [18]). \square

Finally, we are ready state our theorem that establishes the isomorphism between quilted Floer homology groups arising from Lagrangian correspondences with Heegaard Floer homology.

Theorem 3.4.3. *Suppose that Y admits a broken fibration with $g < 2k$ and furthermore assume that the widths of holomorphic quilts can be shrunk to zero without*

hitting any figure eight bubbles. Then for $\mathfrak{s} \in \mathcal{S}(Y|\Sigma_{min})$,

$$HF^+(Y, f, \gamma_w, \mathfrak{s}) \simeq QFH'(Y, f; \mathfrak{s}, \Lambda) \simeq QFH(Y, f; \mathfrak{s}, \Lambda)$$

Proof. The proof will be obtained by putting together the results obtained so far together with Wehrheim-Woodward's Theorem 5.0.3 in [44] which allows one to compose Lagrangian correspondences without changing the Floer homology groups. More precisely, Theorem 3.3.3 and Lemma 3.4.2 give us that $HF^+(Y, f, \gamma_w, \mathfrak{s}) \simeq QFH'(Y, f; \mathfrak{s}, \Lambda) \simeq HF(\text{Sym}^{g-k}(\Sigma_{max}); \alpha_1 \times \dots \times \alpha_{g-k}, \beta_1 \times \dots \times \beta_{g-k}; \Lambda)$. Now, Lemma 3.4.1 expresses the Lagrangians $\alpha_1 \times \dots \times \alpha_{g-k}$ and $\beta_1 \times \dots \times \beta_{g-k}$ as transverse and embedded compositions of the Lagrangians L_{α_i} and L_{β_j} . Therefore, we are in a position to apply Wehrheim-Woodward theorem (for the statement of this theorem in the case we are using here, namely when the differential is perturbed by the intersection number with n_w see also Theorem 6.4 in [22]), which says that by shrinking the width of the strips which are part of the holomorphic quilts contributing to the differential one can obtain an isomorphism between the Floer homology of the Lagrangians $\alpha_1 \times \dots \times \alpha_{g-k}, \beta_1 \times \dots \times \beta_{g-k}$ and the quilted Floer homology of the Lagrangian correspondences $L_{\alpha_1}, \dots, L_{\alpha_{g-k}}$ and $L_{\beta_1}, \dots, L_{\beta_{g-k}}$. This completes the proof. \square

Recall from [44] that a figure-eight bubble is given by a triple of holomorphic maps:

$$v_0 : \mathbb{R} \times (-\infty, -1] \rightarrow A, \quad v_1 : \mathbb{R} \times [-1, 1] \rightarrow B, \quad v_2 : \mathbb{R} \times [1, \infty) \rightarrow C$$

such that

$$(v_0(\tau, -1), v_1(\tau, -1)) \in L_{AB}, \quad (v_1(\tau, 1), v_2(\tau, 1)) \in L_{BC}$$

where A, B and C are symplectic manifolds, and $L_{AB} \subset A \times B$ and $L_{BC} \subset B \times C$ are Lagrangian correspondences. This is called a figure-eight bubble since, after compactifying the domain to $\mathbb{C}P^1 = S^2$, when viewed from $z = \infty$ the lines $\text{Im}(z) = \pm 1$ appear as a figure eight. It is conjectured in [44] that the maps (v_0, v_1, v_2) can be extended continuously to S^2 by a point $(v_0(\infty), v_1(\infty), v_2(\infty))$ that lies in both $L_{AB} \times C$ and $A \times L_{BC}$. In the next lemma, we show that if we assume this removal of singularities at $z = \infty$ for finite energy figure-eight bubbles, then figure-eight bubbles can be avoided in the proof of the previous theorem. We use the removal of singularity assumption in order to define the homotopy class of a figure-eight bubble which we then show to be trivial in the case $g < 2k$.

Lemma 3.4.4. *Assuming the removal of singularities at $z = \infty$ for figure-eight bubbles and $g < 2k$, the widths of the strips occurring in the differential of $QFH(Y, f; \Lambda)$ can be shrunk to zero without hitting any figure-eight bubbles, i.e., the assumption about non-occurrence of figure-eight bubbles can be removed in Theorem 3.4.3.*

Proof. We first explain how to associate a homotopy class with a figure-eight bubble. Consider the figure-eight bubble as two polar caps and an equatorial region, mapping to manifolds A, B, C (B is where the strip near the equator maps) - with seams mapping to the correspondences L_{AB} and L_{BC} in $A \times B$ and in $B \times C$. The image of the equator is a loop γ inside B .

Let l_1 be the loop obtained by reflecting the equator along the “north” seam: it’s a loop inside the northern polar region, bounding some disc D_1 . Similarly, let l_2 be the loop obtained by reflecting the equator along the “south” seam, i.e. a loop inside the southern polar region, bounding some disc D_2 . All these loops and the equator touch each other at the point at infinity where the seams come together.

Now we can deform the maps in the polar regions so that they are constant over D_1

and D_2 : namely, let (a, b, c) in $A \times B \times C$ be the value of the map at the point at infinity where everything attaches together (This is the precise moment where we assume that there is a removal of singularity theorem for the figure-eight bubbles). Then after a homotopy we can assume that every point of D_1 maps to a , and every point of D_2 maps to c . After we do this, cut the domain along the equator, and look first at the north hemisphere. We have on one hand a strip in B , and on the other hand a disc in A , but the disc is constant north of l_1 , so we can cut it to a strip in A . Then we can reflect, and get a strip in $A \times B$, with one boundary (the seam) on the given Lagrangian correspondence L_{AB} , and the other boundary (the equator and the reflected loop l_1) mapping to $\{a\} \times \gamma$. Similarly from the southern hemisphere we get a strip in $B \times C$, with one boundary mapping on the given Lagrangian correspondence L_{BC} , and the other boundary mapping to $\gamma \times \{c\}$. Now take the strip in $A \times B$, and make it into a map to $A \times B \times C$ just by taking the constant function c in the last factor: so we get a strip with boundaries in $L_{AB} \times \{c\}$ and $\{a\} \times \gamma \times \{c\}$. Take the strip in $B \times C$ and similarly add in the constant map to a in A to get a strip with boundaries in $\{a\} \times L_{BC}$ and $\{a\} \times \gamma \times \{c\}$. Now we can glue these two together and get a strip in $A \times B \times C$ with boundaries in $L_{AB} \times \{c\}$ and $\{a\} \times L_{BC}$. So there is a relative homology class associated with it.

We next argue that in the case $g < 2k$, this homology class has to be trivial for any figure-eight bubble that might arise from shrinking the width of the strips that are considered in the definition of $QFH(Y, f, \mathfrak{s}; \Lambda)$ in the above theorem; this implies that figure-eight bubbles would be just constant maps, i.e. no such bubbling occurs. Namely, suppose $A = \text{Sym}^n(\Sigma)$, $B = \text{Sym}^{n-1}(\Sigma_L)$ and $C = \{pt\}$, where L is an α curve or a β curve. (Recall that Σ_L is obtained from Σ by collapsing L to a point and taking the normalisation). This case is sufficient for our purposes as, when we shrink

the widths of holomorphic strips that arise in quilted Floer homology, we can always do successive shrinking in an order such that one of the seam conditions involves the zeroth symmetric of the lowest genus fibre which is just a point. In our case we have $n \leq g - k$ which is assumed to be less than k , and the genus of Σ is $k + n$ which is greater than $2n$. As in Lemma 3.4.2, these conditions guarantee that the Abel-Jacobi maps from A and B to corresponding Picard tori are injective. Furthermore, the Abel-Jacobi map is holomorphic when it is viewed as a map from the relative Hilbert scheme to the relative Picard fibration. Therefore, a figure-eight bubble for the symmetric products gives rise to a figure-eight bubble for the Picard tori, with seam conditions given by taking the images of L_{AB} and L_{BC} by the Abel-Jacobi map. Let us denote by A' and B' be the Picard tori $T^{2(k+n)}(\Sigma)$, $T^{2(k+n-1)}(\Sigma_L)$, and $C' = \{pt\}$ so that the Abel-Jacobi map sends A, B to A', B' , and let $L_{A'B'}$ and $L_{B'C'}$ be the images of the Lagrangian correspondence L_{AB} and L_{BC} by the Abel-Jacobi map. Now, in the previous paragraph, we have seen that homotopically a figure-eight bubble can be regarded as a loop based at the constant path at (a, b, c) in the path space $\Omega(\{a\} \times L_{BC}, L_{AB} \times \{c\})$, i.e., the set of paths $\omega : [0, 1] \rightarrow A \times B \times C$ such that $\omega(0) \in \{a\} \times L_{BC}$ and $\omega(1) \in L_{AB} \times \{c\}$. Thus the homotopy class of a figure-eight bubble is an element in $\pi_1(\Omega(\{a\} \times L_{BC}, L_{AB} \times \{c\}))$. Now note that, the evaluation maps $(ev_0, ev_1) : \Omega(\{a\} \times L_{BC}, L_{AB} \times \{c\}) \rightarrow (\{a\} \times L_{BC}) \times (L_{AB} \times \{c\})$ give rise to a Serre fibration with fibre space homotopy equivalent to the loop space $\Omega(A \times B \times C)$:

$$\begin{array}{ccc} \Omega(A \times B \times C) & \longrightarrow & \Omega(\{a\} \times L_{BC}, L_{AB} \times \{c\}) \\ & & \downarrow \\ & & (\{a\} \times L_{BC}) \times (L_{AB} \times \{c\}) \end{array}$$

A similar argument applies to A' , B' and C' with the seam conditions $L_{A'B'}$ and $L_{B'C'}$. Therefore, we get the following homotopy exact sequences which are connected by the Abel-Jacobi maps:

$$\begin{array}{ccccc}
\pi_1(\Omega(\{a\} \times L_{BC}, L_{AB} \times \{c\})) & \longrightarrow & \pi_1(L_{BC}) \times \pi_1(L_{AB}) & \longrightarrow & \pi_1(A \times B \times C) \\
& & \downarrow (aj)_* & & \downarrow \\
0 \longrightarrow \pi_1(\Omega(\{a'\} \times L_{B'C'}, L_{A'B'} \times \{c'\})) & \longrightarrow & \pi_1(L_{B'C'}) \times \pi_1(L_{A'B'}) & &
\end{array}$$

Now, we would like to show that the image of a figure-eight bubble by the Abel-Jacobi map is contractible. Thus, we would like to show that the vertical map denoted by $(aj)_*$ is zero. In fact, when $n > 2$ one can show that $\pi_1(\Omega(\{a'\} \times L_{B'C'}, L_{A'B'} \times \{c'\}))$ is zero, but in order to also cover the case $n = 2$, we need to do a little bit of diagram chasing. First observe that the rightmost vertical arrow is an isomorphism since $L_{A'B'} = AJ(L_{AB})$, $L_{B'C'} = AJ(L_{BC})$ and the Abel-Jacobi map is injective. Also note that $\pi_2(A' \times B' \times C') = 0$ since A' and B' are tori and $C' = \{pt\}$. Therefore, it suffices to show that the map $\pi_1(L_{BC}) \times \pi_1(L_{AB}) \rightarrow \pi_1(A \times B \times C)$ is injective. Perutz shows in [31] Lemma 3.18 that the inclusion of a Lagrangian correspondences is injective at the level of fundamental groups. This is done by calculating the maps $\pi_1(L_{AB}) \rightarrow \pi_1(A \times B)$ and $\pi_1(L_{BC}) \rightarrow \pi_1(B \times C)$. In the case at hand topologically we have $A = \text{Sym}^n(\Sigma)$, $B = \text{Sym}^{n-1}(\Sigma_L)$, L_{AB} is a trivial circle bundle over $\text{Sym}^{n-1}(\Sigma_L)$ so has fundamental group $\mathbb{Z} \times H_1(\Sigma_L)$ when $n > 2$ and $\mathbb{Z} \times \pi_1(\Sigma_L)$ when $n = 2$, where the fibre of the circle bundle generates the \mathbb{Z} component. This maps to $\pi_1(A \times B) = H_1(\Sigma) \times H_1(\Sigma_L)$ when $n > 2$ and $\pi_1(A \times B) = H_1(\Sigma) \times \pi_1(\Sigma_L)$ when $n = 2$, where the fibre class is mapped to L and the restriction to $H_1(\Sigma_L)$ sends a class $[\gamma]$ to $([\gamma], [\gamma])$ in $H_1(\Sigma) \times H_1(\Sigma_L)$, where the first component of this map is given by making sure γ doesn't pass through the region

of normalization and hence can be identified with a loop in Σ via parallel transport. Furthermore, $C = \{pt\}$ and L_{BC} is a product torus $L_1 \times \dots \times L_{n-1}$, such that when viewed as loops on Σ , L, L_1, \dots, L_{n-1} are linearly independent in $H_1(\Sigma)$.

Thus, the map $\pi_1(L_{BC}) \times \pi_1(L_{AB}) \rightarrow \pi_1(A \times B \times C)$ is given by:

$$\begin{aligned} \mathbb{Z} \times H_1(\Sigma_L) \times \mathbb{Z}^{n-1} &\rightarrow H_1(\Sigma) \times H_1(\Sigma_L) \\ (m, \gamma, r_1, \dots, r_{n-1}) &\rightarrow (mL + \gamma, \gamma + r_1L_1 + \dots + r_{n-1}L_{n-1}) \end{aligned}$$

for $n > 2$. The formula is similar in the case $n = 2$ if one replaces $H_1(\Sigma_L)$ by $\pi_1(\Sigma_L)$. This map is clearly injective since the lift of γ to Σ and L are independent in $H_1(\Sigma)$. Therefore, the map $(aj)_*$ is zero, and the image of a figure-eight bubble by the Abel-Jacobi map has to be contractible, which implies that it cannot carry any symplectic energy, thus it cannot have any holomorphic representative unless it is a constant map. Since the Abel-Jacobi map is holomorphic, this completes the proof of the non-occurrence of figure-eight bubbles. \square

3.4.2 Floer's excision theorem

Here we describe a proof of Floer's excision theorem for quilted Floer homology. In light of the theorem in the previous section this gives a new and more straightforward proof of Floer's excision theorem for Heegaard Floer homology. In this section, we will denote by $QFH(Y, f; \Lambda)$, the quilted Floer homology of (Y, f) thought as the Floer homology group, $HF(\mathbb{L}_\alpha, \mathbb{L}_\beta; \mathfrak{s}, \Lambda)$, using Theorem 3.4.3.

In order to prepare the set-up, consider two broken fibrations $f_1 : Y_1 \rightarrow S^1$ and $f_2 : Y_2 \rightarrow S^1$. Let g_1 and g_2 be the genera of the maximal genus fibres of f_1 and f_2

and k be the genus of the minimal genus fibres of f_1 and f_2 which we assume to be equal. Let us denote by Σ_i a fixed minimal genus fibre of f_i . Now cut each Y_i along Σ_i , to obtain manifolds Y'_i with boundary $\Sigma_i \cup (-\Sigma_i)$. Choose a diffeomorphism $\phi : \Sigma_1 \rightarrow \Sigma_2$ and form a new closed 3-manifold Y by gluing Σ_1 to $-\Sigma_2$ and $-\Sigma_1$ to Σ_2 using ϕ . Y comes equipped with a broken fibration f induced by f_1 and f_2 . Furthermore, given spin^c structures $\mathfrak{s}_1 \in \mathcal{S}(Y_1|\Sigma_1)$ and $\mathfrak{s}_2 \in \mathcal{S}(Y_2|\Sigma_2)$, one gets an induced spin^c structure $\mathfrak{s} = \mathfrak{s}_1 \# \mathfrak{s}_2 \in \mathcal{S}(Y|\Sigma_{\min})$. Floer's excision theorem in this context is as follows :

Theorem 3.4.5. *Suppose that $g_1 + g_2 < 3k$, then for $\mathfrak{s} \in \mathcal{S}(Y|\Sigma_{\min})$ we have a split short exact sequence of graded groups*

$$\begin{aligned} \bigoplus_{\{\mathfrak{s}_1, \mathfrak{s}_2 | \mathfrak{s}_1 \# \mathfrak{s}_2 = \mathfrak{s}\}} QFH(Y_1, f_1, \mathfrak{s}_1; \Lambda) \otimes QFH(Y_2, f_2, \mathfrak{s}_2; \Lambda) &\rightarrow QFH(Y, f, \mathfrak{s}; \Lambda) \\ \rightarrow \bigoplus_{\{\mathfrak{s}_1, \mathfrak{s}_2 | \mathfrak{s}_1 \# \mathfrak{s}_2 = \mathfrak{s}\}} \text{Tor} (QFH(Y_1, f_1, \mathfrak{s}_1; \Lambda), QFH(Y_2, f_2, \mathfrak{s}_2; \Lambda)) & \end{aligned}$$

Proof. The proof of this theorem in the setting of $QFH(Y, f; \Lambda)$ follows from the definition of quilted Floer homology in a straightforward way. The crucial observation is that for the spin^c structures in consideration, the function $\nu : S^1 \setminus \text{crit}(f) \rightarrow \mathbb{Z}_{\geq 0}$ defined by $\langle c_1(\mathfrak{s}), F_s \rangle = 2\nu(s) + \chi(F_s)$ is zero for the fibres Σ_1 , Σ_2 and Σ_{\min} , hence the cutting and gluing operations take place where the holomorphic quilts contributing to differentials live in a zeroth symmetric product and so are constant in those regions. Therefore, there is an isomorphism of the tensor product of chain complexes associated with (Y_1, f_1) and (Y_2, f_2) with the chain complex associated with (Y, f) , thus the theorem follows. \square

One issue that we are not addressing here is the fact that, as constructed, f does

not satisfy the conditions stated at the beginning of Section 3.2.1 on the ordering of index 1 and 2 critical values. However the results of [17] imply that perturbing f to achieve these conditions would not affect $QFH(Y, f, \mathfrak{s})$.

We remark that the excision theorem for quilted Floer homology allows us to apply the constructions developed by Kronheimer and Mrowka in [15] in the context of quilted Floer homology. In particular, one can define knot invariants in this way.

3.4.3 4–manifold invariants

We first recall the definition of broken Lefschetz fibrations on smooth 4-manifolds.

Definition 3.4.6. *A broken fibration on a closed 4–manifold X is a smooth map to a closed surface with singular set $A \cup B$, where A is a finite set of singularities of Lefschetz type near which a local model in oriented charts is the complex map $(w, z) \rightarrow w^2 + z^2$, and B is a 1-dimensional submanifold along which the fibration is locally modelled by the real map $(t, x, y, z) \rightarrow (t, x^2 + y^2 - z^2)$, B corresponding to $t = 0$.*

It was proven in chapter 2 that every closed oriented smooth 4–manifold admits an *equatorial* broken Lefschetz fibration to S^2 (see also [2] where the authors give a new proof of this result using Kirby calculus). Equatorial here means that the 1–dimensional part of the critical value set is a set of embedded parallel circles on S^2 . Lagrangian matching invariants of a 4–manifold as defined by Perutz in [31] are obtained by counting quilted holomorphic sections of a broken fibration associated with the 4–manifold. These invariants, which are conjecturally equal to Seiberg-Witten invariants, have a TQFT-like structure where the three manifold invariants

are the quilted Floer homology groups that we have discussed in this chapter. Similarly, Heegaard Floer homology is the three manifold part of a TQFT-like structure, which underlies the construction of Ozvath-Szabo 4-manifold invariants [29].

By cutting a broken fibration along a family of circles that are transverse to the equatorial circles of critical values, one can obtain a cobordism decomposition of the 4-manifold, such that each cobordism is an elementary cobordism, namely it is a cobordism obtained by either a one or two handle attachment. Therefore, because of Theorem 3.4.3, in order to equate the above mentioned four-manifold invariants for the spin^c structures which satisfy the adjunction equality with respect to the minimal genus fibre of the broken fibration, one needs to check only that the cobordism maps for one and two handle attachments in both theories coincide. This will be in turn obtained by extending the techniques developed in this chapter to cobordism maps. We plan to investigate this latter claim in a sequel to this chapter. This will in particular prove that for the spin^c structures considered, the Lagrangian matching invariants are independent of the broken fibration that is chosen on the 4-manifold.

Appendix A

Classification of $(1, 1)$ -stable unfoldings

Throughout, we denote by $\mathcal{E}(n)$ the set of germs at $0 \in \mathbb{R}^n$ of smooth mappings from \mathbb{R}^n to \mathbb{R} , and $\mathfrak{m}(n)$ is the unique maximal ideal of $\mathcal{E}(n)$ consisting of those germs f such that $f(0) = 0$.

Definition A.0.1. *Let $\eta \in \mathfrak{m}(n)$. An r -dimensional unfolding of η is a germ $f \in \mathcal{E}(n+r)$ such that $f|_{\mathbb{R}^n} = \eta$.*

For the next definition, recall the definition of $(1, 1)$ -equivalence of unfoldings was given in Definition 2.4.2.

Definition A.0.2. *Let $f \in \mathfrak{m}(n+d+2)$ and let $g \in \mathfrak{m}(n+2)$. We say f $(1, 1)$ -reduces to g if there is a non-degenerate quadratic form Q on \mathbb{R}^d such that f is $(1, 1)$ -equivalent to the germ $g' \in \mathfrak{m}(n+d+2)$ given by $g'(s, t, x, y) = g(s, t, x) + Q(y)$ for $s \in \mathbb{R}, t \in \mathbb{R}, x \in \mathbb{R}^n, y \in \mathbb{R}^d$.*

We will give a classification $(1, 1)$ -stable unfoldings up to $(1, 1)$ -equivalence based

on the algorithm described in [43]. We shall make direct use of the lemmas and theorems in [43] without restating them here.

Theorem A.0.3. *Let $f \in \mathfrak{m}(n+2)$ be a $(1,1)$ -stable unfolding of $\eta \in \mathfrak{m}(n)^2$. Then either f has Morse singularity at 0, or f $(1,1)$ -reduces to a unique one of the following unfoldings h_i of germs v_i :*

v_i	h_i
$v_0(x) = x^3$	$h_0(s, t, x) = x^3 + tx$
$v_1(x) = x^3$	$h_1(s, t, x) = x^3 + t^2x + sx$
$v_2(x) = x^3$	$h_2(s, t, x) = x^3 - t^2x + sx$
$v_3(x) = x^4$	$h_3(s, t, x) = x^4 + sx^2 + tx$

We follow the same method as Wasserman's classification of $(3,1)$ -stable unfoldings in [43]. In particular, the following special case of Theorem 4.11 from [43] plays a crucial role in the classification. We say that $f \in \mathfrak{m}(n+2)$ is 2-stable if

$$\mathcal{E}(u, x) = \left\langle \frac{\partial f}{\partial x} \right\rangle \mathcal{E}(u, x) + \left\langle \frac{\partial f}{\partial u} \right\rangle \mathcal{E}(u) + F^* \mathcal{E}(\mathbb{R}^3)$$

where $F(u, x) = (u, f(u, x))$ for $u \in \mathbb{R}^2, x \in \mathbb{R}^n$. This notion is very similar to $(1,1)$ -stability which was given in Definition 2.4.3. The difference is that here we do not distinguish the variables s and t . In particular, $(1,1)$ -stability implies 2-stability.

Theorem A.0.4. *Let $g \in \mathfrak{m}(n+2)$ be a $(1,1)$ -stable unfolding of $\eta \in \mathfrak{m}(n)$, and suppose that $f \in \mathfrak{m}(n+2)$ is a 2-stable unfolding of η . Then there exists a polynomial germ $p \in \mathfrak{m}(\mathbb{R})$ of degree at most 2 such that g is $(1,1)$ -equivalent to either $f(s +$*

$p(t), t, x$ or $f(t, s + p(t), x)$.

Proof of Theorem A.0.3: If f is $(1, 1)$ -stable, then f is 2-stable and hence f has a simple singularity or f reduces (in the sense of Definition 2.24 of [43]) to a unique one of the unfoldings g_i in Thom's list of seven elementary catastrophes (see Theorem 2.20 of [43]). If the latter case occurs, then η reduces to a unique one of the germs μ_i in Thom's list. By Lemma 4.18 of [43], if η reduces to μ_i then f $(1, 1)$ -reduces to a two-dimensional unfolding h of μ_i which by Lemma 4.17 of [43] must be $(1, 1)$ -stable. Moreover, Lemma 4.19 together with Lemma 4.20 in [43] implies that the set of $(1, 1)$ -stable unfoldings of μ_i to which f $(1, 1)$ -reduces is exactly the $(1, 1)$ -equivalence class of h . Hence to complete the proof we need only to show that for each germ μ_i in Thom's list, the list of Theorem A.0.3 gives exactly the classification of $(1, 1)$ -stable unfoldings of μ_i up to $(1, 1)$ -equivalence.

First, consider the case of $\mu_1(x) = x^3$. By Theorem A.0.4, a $(1, 1)$ -stable unfolding f up to $(1, 1)$ -equivalence of $\mu_1(x) = x^3$ is either $x^3 + tx$ or of the form $x^3 + (s + at^2 + bt)x$ where $a, b \in \mathbb{R}$. The former case is h_0 , so we concentrate on the latter case.

Corollary 4.13 of [43] gives the $(1, 1)$ -stable condition for f as :

$$\mathcal{E}(t, x) = \left\langle \frac{\partial f_0}{\partial x} \right\rangle \mathcal{E}(t, x) + \left\langle \frac{\partial f_0}{\partial t} \right\rangle \mathcal{E}(t) + \mathbb{R} \left\langle \frac{\partial f}{\partial s} \Big|_{\{s=0\}} \right\rangle + \langle 1, f_0 \rangle \mathcal{E}(t) + \mathbf{m}(t)^2 \mathcal{E}(t, x) + \mathbf{m}(t, x)^4$$

where $f_0 = f|_{\{s=0\}}$. Thus, f is $(1, 1)$ -stable if and only if

$$\begin{aligned} \mathcal{E}(t, x) &= \langle 3x^2 + (at^2 + bt) \rangle \mathcal{E}(t, x) + \langle 2atx + bx \rangle \mathcal{E}(t) + \mathbb{R} \langle x \rangle + \langle 1, x^3 + (at^2 + bt)x \rangle \mathcal{E}(t) \\ &+ \mathbf{m}(t)^2 \mathcal{E}(t, x) + \mathbf{m}(t, x)^4. \end{aligned}$$

An easy calculation then reveals that f is $(1, 1)$ -stable if and only if a or b is nonzero.

Suppose $b \neq 0$, then we change coordinates by setting $t' = s + at^2 + bt$, $s' = s$ and get f is $(1, 1)$ -equivalent to h_0 . On the other hand, if $b = 0$, then by scaling t , we obtain that f is $(1, 1)$ -equivalent to either h_1 or h_2 . Furthermore, it is clear that none of h_0 , h_1 and h_2 are $(1, 1)$ -equivalent.

Now consider the case of $\mu_2(x) = x^4$. By Theorem A.0.4, a $(1, 1)$ -stable unfolding f up to $(1, 1)$ -equivalence of $\mu_2(x) = x^4$ is either $x^4 + (s + at^2 + bt)x^2 + tx$ or $x^4 + tx^2 + (s + at^2 + bt)x$, where $a, b \in \mathbb{R}$. In order to determine for which values of a and b these maps are $(1, 1)$ -stable, we again apply the criteria given by Corollary 4.13 of [43]. Suppose first f is given by $x^4 + (s + at^2 + bt)x^2 + tx$. Then f is $(1, 1)$ -stable if and only if

$$\begin{aligned} \mathcal{E}(t, x) &= \langle 4x^3 + 2at^2x + 2btx + t \rangle \mathcal{E}(t, x) + \langle 2atx^2 + bx^2 + x \rangle \mathcal{E}(t) + \mathbb{R}\langle x^2 \rangle \\ &+ \langle 1, x^4 + (at^2 + bt)x^2 + tx \rangle \mathcal{E}(t) + \mathfrak{m}(t)^2 \mathcal{E}(t, x) + \mathfrak{m}(t, x)^4. \end{aligned}$$

It turns out that in this case f is $(1, 1)$ -stable for all values of a and b . By Lemma 4.9 of [43] stably homotopic $(1, 1)$ -stable germs are $(1, 1)$ -equivalent. Therefore we can set $a = b = 0$ and conclude that f is $(1, 1)$ -equivalent to $h_3 = x^4 + sx^2 + tx$.

Finally, suppose that f is given by $x^4 + tx^2 + (s + at^2 + bt)x$. Then Corollary 4.13 of [43] yields that f is $(1, 1)$ -stable if and only if

$$\begin{aligned} \mathcal{E}(t, x) &= \langle 4x^3 + 2tx + at^2 + bt \rangle \mathcal{E}(t, x) + \langle x^2 + 2atx + bx \rangle \mathcal{E}(t) + \mathbb{R}\langle x \rangle \\ &+ \langle 1, x^4 + tx^2 + (at^2 + bt)x \rangle \mathcal{E}(t) + \mathfrak{m}(t)^2 \mathcal{E}(t, x) + \mathfrak{m}(t, x)^4. \end{aligned}$$

It is then an easy calculation to conclude that f is $(1, 1)$ -stable if and only if b is nonzero. Next, we again apply Lemma 4.9 of [43] to set $a = 0$, and conclude that f

is $(1, 1)$ -equivalent to $x^4 + tx^2 + (s + bt)x$. Now, we change coordinates by setting $t' = s + bt, s' = -s/b$. Then f becomes $x^4 + (s' + t'/b)x^2 + t'x$. So we are back to the previous case, hence we conclude that f is $(1, 1)$ -equivalent to h_3 , as desired.

Appendix B

Heegaard tori as compositions of Lagrangian correspondences

Given a Riemann surface (Σ, j) and an embedded circle $L \subset \Sigma$, denote by Σ_L , the surface obtained by considering an elementary degeneration of Σ associated with the Lefschetz fibration with vanishing cycle L over D^2 and taking the normalization of the singular fibre. Alternatively, Σ_L is the surface obtained after surgery along L , which is given by removing a tubular neighborhood of L and gluing in a pair of discs. We also choose an almost complex structure \bar{j} on Σ_L which agrees with j outside a neighborhood of L . Note that this is a canonical construction, namely the moduli of choices that are involved is a contractible space. To such data, Perutz associates a Lagrangian correspondence $V_L \subset \text{Sym}^n(\Sigma) \times \text{Sym}^{n-1}(\Sigma_L)$ for a symplectic form of the shape $-\omega \oplus \omega_L$ where ω and ω_L are Kähler forms in certain cohomology classes to be specified below (see [31]). This is described in terms of a symplectic degeneration of $\text{Sym}^n(\Sigma)$. More precisely, one considers an elementary Lefschetz fibration over D^2

with regular fibre diffeomorphic to Σ and a unique vanishing cycle L which collapses at the origin to a nodal curve Σ_0 . Here we fix complex isomorphisms between the fibre above 1 and (Σ, L, j) , and between the normalization of the fibre above 0 and (Σ_L, \bar{j}) . Then one passes to the relative Hilbert scheme, $\text{Hilb}_{D^2}^n(\Sigma)$, of this fibration (a resolution of the singular variety obtained by taking fibre-wise symmetric products). The regular fibres of the induced map from $\text{Hilb}_{D^2}^n(\Sigma)$ to D^2 are diffeomorphic (non-canonically) to $\text{Sym}^n(\Sigma)$ and we identify the fibre above 1 with $\text{Sym}^n(\Sigma)$. The fibre above the origin, $\text{Hilb}^n(\Sigma_0)$ is singular along a codimension 2 subset which we identify with $(\text{Sym}^{n-1}(\Sigma_L))$. V_L then arises from the vanishing cycle of this fibration. More precisely, let $\rho : \text{Sym}^n(\Sigma) \rightarrow \text{Hilb}^n(\Sigma_0)$ be the parallel transport map along $[0, 1]$ induced by a global closed fibre-wise symplectic form Ω on $\text{Hilb}_{D^2}^n(\Sigma)$ whose restrictions to $\text{Sym}^n(\Sigma)$ and $\text{Sym}^{n-1}(\Sigma_L)$ are in the same cohomology classes as ω and ω_L . Then one sets $V_\Omega = \{(x, \rho(x)) \mid \rho(x) \in \text{Sym}^{n-1}(\Sigma_L)\}$ and $V_L = (\phi \times \bar{\phi})(V_\Omega)$, where $(\phi, \bar{\phi})$ is a symplectomorphism of $\text{Sym}^n(\Sigma) \times \text{Sym}^{n-1}(\Sigma_L)$ which sends the symplectic forms obtained by restriction of Ω to $\text{Sym}^n(\Sigma)$ and $\text{Sym}^{n-1}(\Sigma_L)$ to the symplectic forms ω and ω_L (this symplectomorphism is produced using Moser's lemma with a specific class of Moser primitives that makes the flux of the resulting Lagrangian isotopy zero, which is possible by Lemma 2.12 in [31]). Perutz proves in [31] that the Hamiltonian isotopy class of V_L is independent of the choice of Ω (see Theorem A in [31]).

Consider now a Riemann surface (Σ, j) with two *disjoint* embedded circles $L_1, L_2 \subset \Sigma$. Applying the above construction to L_1 , we obtain a Lagrangian correspondence

$$V_{L_1} \subset (\text{Sym}^n(\Sigma) \times \text{Sym}^{n-1}(\Sigma_{L_1}), -\omega \oplus \omega_1)$$

Since L_2 is disjoint from L_1 , we have an embedded circle in Σ_{L_1} , still denoted by L_2 ,

which is the image of L_2 after surgery along L_1 . Now, applying the above construction to $L_2 \subset \Sigma_{L_1}$ under the assumption that $n \geq 2$, we get

$$\bar{V}_{L_2} \subset (\text{Sym}^{n-1}(\Sigma_{L_1}) \times \text{Sym}^{n-2}(\Sigma_{L_1 L_2}), -\omega_1 \oplus \omega_{12})$$

where $\Sigma_{L_1 L_2}$ is the result of surgery along L_1 and L_2 .

It is then natural to consider the composition of Lagrangian correspondences :

$$V_{L_1} \circ \bar{V}_{L_2} \subset \text{Sym}^n(\Sigma) \times \text{Sym}^{n-2}(\Sigma_{L_1 L_2})$$

Recall that as a point set this is given by $(x, y) \in V_{L_1} \circ \bar{V}_{L_2}$ if and only if there exists a $z \in \text{Sym}^{n-1}(\Sigma_{L_1})$ such that $(x, z) \in V_{L_1}$ and $(z, y) \in \bar{V}_{L_2}$. $V_{L_1} \circ \bar{V}_{L_2}$ can be more geometrically described as the image of the projection to $\text{Sym}^n(\Sigma) \times \text{Sym}^{n-2}(\Sigma_{L_1 L_2})$ of the intersection $(V_{L_1} \times \bar{V}_{L_2}) \cap \Delta$ in $\text{Sym}^n(\Sigma) \times \text{Sym}^{n-1}(\Sigma_{L_1}) \times \text{Sym}^{n-1}(\Sigma_{L_1}) \times \text{Sym}^{n-2}(\Sigma_{L_1 L_2})$ where $\Delta = \{(x, y, z, t) | y = z\}$

To see that $V_{L_1} \circ \bar{V}_{L_2}$ is a Lagrangian submanifold of $\text{Sym}^n(\Sigma) \times \text{Sym}^{n-2}(\Sigma_{L_1 L_2})$ we need to check the following properties :

- (transverse) $(V_{L_1} \times \bar{V}_{L_2}) \bar{\cap} \Delta$
- (embedded) Given $(x, y) \in V_{L_1} \circ \bar{V}_{L_2}$ there exists a unique $z \in \text{Sym}^{n-1}(\Sigma_{L_1})$ such that $(x, z) \in V_{L_1}$ and $(z, y) \in \bar{V}_{L_2}$.

Lemma B.0.1. *The composition $V_{L_1} \circ \bar{V}_{L_2}$ is transverse and embedded. In particular, $V_{L_1} \circ \bar{V}_{L_2}$ is a Lagrangian submanifold.*

Proof. To see that the composition is transverse, let x, y, z such that $(x, y) \in V_{L_1}$ and $(y, z) \in \bar{V}_{L_2}$. Observe that $d(pr_2)(T_{(x,y)}V_{L_1}) = T_y \text{Sym}^{n-1}(\Sigma_{L_1})$, where $pr_2 :$

$\text{Sym}^n(\Sigma) \times \text{Sym}^{n-1}(\Sigma_{L_1}) \rightarrow \text{Sym}^{n-1}(\Sigma_{L_1})$ (because the parallel transport map from V_{L_1} to $\text{Sym}^{n-1}(\Sigma_{L_1})$ is onto, in fact V_{L_1} is a circle bundle over $\text{Sym}^{n-1}(\Sigma_{L_1})$, see Theorem A [31]). Therefore, $T_{(x,y)}V_{L_1} + T_{(x,y,y,z)}\Delta$ already spans the tangent space of $\text{Sym}^n(\Sigma) \times \text{Sym}^{n-1}(\Sigma_{L_1}) \times \text{Sym}^{n-1}(\Sigma_{L_1}) \times \text{Sym}^{n-2}(\Sigma_{L_1L_2})$ at (x, y, y, z) . Hence the composition is transverse as required. Suppose now that $(x, y) \in V_{L_1}$ then $(x, y) = (x, \rho(x))$, where $\rho : \text{Sym}^n(\Sigma) \rightarrow \text{Hilb}^n(\Sigma_0)$ is the parallel transport map (here Σ_0 is the nodal curve obtained by collapsing L_1 to a point). Therefore, y is determined by x hence the composition is embedded. \square

Perutz proves that the Hamiltonian isotopy class of V_L is independent of the choice of Ω in $\text{Hilb}_{D^2}^n(\Sigma)$, we will need the same type of statement for $V_{L_1} \circ \bar{V}_{L_2}$. The following general lemma will be useful.

Lemma B.0.2. *Suppose $L, L' \subset A \times B$ and $N, N' \subset B \times C$ are Lagrangian correspondences such that L and L' are Hamiltonian isotopic via a product isotopy (ϕ^t, ψ^t) on $A \times B$, and N and N' are Hamiltonian isotopic via a product isotopy (ψ^t, ρ^t) . If the compositions $L \circ N$ and $L' \circ N'$ are transverse and embedded, then $L \circ N$ and $L' \circ N'$ are Hamiltonian isotopic via (ϕ^t, ρ^t) .*

Proof. The crucial point here is the fact, the components of the Hamiltonian isotopies on the manifold B are the same, namely ψ^t . This ensures in a straightforward way that the composition of $(\phi^t, \psi^t)(L)$ and $(\psi^t, \rho^t)(N)$ is transverse and embedded. \square

Lemma B.0.3. *The construction of $V_{L_1} \circ \bar{V}_{L_2}$ in $\text{Sym}^n(\Sigma) \times \text{Sym}^{n-2}(\Sigma_{L_1L_2})$ is independent of the choices of global closed fibre-wise symplectic forms $\Omega \in \text{Hilb}_{D^2}^n(\Sigma)$ and $\Omega_1 \in \text{Hilb}_{D^2}^{n-1}(\Sigma_{L_1})$ up to Hamiltonian isotopy.*

Proof. Suppose Ω^s and Ω_1^s are closed fibrewise symplectic forms staying in the same cohomology classes for $s \in [0, 1]$. Perutz proves that $V_{L_1}^s$ and $\bar{V}_{L_2}^s$ stay in the same

Hamiltonian isotopy class. However, this does not imply immediately that $V_{L_1}^s \circ \bar{V}_{L_2}^s$ are in the same Hamiltonian isotopy class as $V_{L_1}^0 \circ \bar{V}_{L_2}^0$. Now, the first observation is that the Hamiltonian isotopies that Perutz constructs are in product form, namely he proves in Section 3.5 of [31] that there exists Hamiltonian diffeomorphisms (ϕ^s, ψ^s) of $\text{Sym}^n(\Sigma) \times \text{Sym}^{n-1}(\Sigma_{L_1})$ which sends V_{L_1} to $V_{L_1}^s$, furthermore it follows from the proof of Theorem A in [31] that ψ^s can be chosen to be arbitrary Hamiltonian diffeomorphism of $\text{Sym}^{n-1}(\Sigma_{L_1})$. Namely, the existence of the Hamiltonian isotopy (ϕ^s, ψ^s) is due to a vanishing of a flux class as described in Lemma 2.8 of [31], and the vanishing of the flux enables one to extend a chosen isotopy $V_{L_1}^s$ to an ambient isotopy by modifying the chosen isotopy using vector fields that are tangent to the isotropic distribution on $V_{L_1}^s$, hence this does not modify the isotopy on $\text{Sym}^{n-1}(\Sigma_{L_1})$ (see Lemma 2.10 and Proposition 2.11 in [31]). We also have a Hamiltonian diffeomorphism (μ^s, η^s) of $\text{Sym}^{n-1}(\Sigma_{L_1}) \times \text{Sym}^{n-2}(\Sigma_{L_1 L_2})$ which sends V_{L_2} to $V_{L_2}^s$. If we choose $\psi^s = \mu^s$, we are in a situation where we can apply Lemma B.0.2. The result then follows. \square

Note that Lemma B.0.3 has an obvious generalization to compositions of k Lagrangians and the proof is the same.

Now we reverse the order of L_1 and L_2 , and apply the same construction we obtain another Lagrangian correspondence for the same symplectic manifold :

$$V_{L_2} \circ \bar{V}_{L_1} \subset (\text{Sym}^n(\Sigma) \times \text{Sym}^{n-2}(\Sigma_{L_1 L_2}), -\omega \oplus \omega_{12})$$

Note that implicitly, we pick a symplectic form ω_2 on $\text{Sym}^{n-1}(\Sigma_{L_2})$ in order to construct the correspondences V_{L_2} and \bar{V}_{L_1} .

Perutz proves that $V_{L_1} \circ \bar{V}_{L_2}$ and $V_{L_2} \circ \bar{V}_{L_1}$ are smoothly isotopic and conjectures

that in fact they should be Hamiltonian isotopic. This is the content of the following theorem. Recall that the classes η and θ are cohomology classes in $H^2(\text{Sym}^n(\Sigma))$ which generate the subspace of cohomology classes which are invariant under the action of the mapping class group. η is the Poincaré dual of the divisor $\{pt\} \times \text{Sym}^{n-1}(\Sigma)$ and θ corresponds to the intersection form on $H^2(\Sigma, \mathbb{R})$ via the Abel-Jacobi map, more precisely it is the pullback by the Abel-Jacobi map of the theta divisor on the Jacobian.

In general, we work with Kähler forms $(\omega, \omega_1, \omega_2, \omega_{12})$ which lie in cohomology classes $(s\eta_\Sigma + t\theta_\Sigma, s\eta_{\Sigma_{L_1}} + t\theta_{\Sigma_{L_1}}, s\eta_{\Sigma_{L_2}} + t\theta_{\Sigma_{L_2}}, s\eta_{\Sigma_{L_1L_2}} + t\theta_{\Sigma_{L_1L_2}})$ for $s, t > 0$.

When we deal with product tori, we will need to restrict to a more special class of Kähler forms. Given an almost complex structure j on Σ , and n disjoint embedded curves L_1, \dots, L_n on Σ , we will call a symplectic form ω on $\text{Sym}^n(\Sigma)$ taming $\text{Sym}^n(j)$ *nearly symmetric* if there exists an area form α on Σ compatible with j such that:

- ω agrees with $\pi_*(\alpha^{\times n})$ on a neighborhood of the $L_1 \times \dots \times L_n$, where $\pi : \Sigma^{\times n} \rightarrow \text{Sym}^n(\Sigma)$ is the projection map.
- ω represents the class $\eta + \lambda\theta$ for $\lambda > 0$ sufficiently small real number.

In Proposition 1.1 of [34] Perutz constructs nearly symmetric Kähler forms on $\text{Sym}^n(\Sigma)$ using smoothing theory for currents.

Theorem B.0.4. $V_{L_1} \circ \bar{V}_{L_2}$ and $V_{L_2} \circ \bar{V}_{L_1}$ are Hamiltonian isotopic in $\text{Sym}^n(\Sigma) \times \text{Sym}^{n-2}(\Sigma_{L_1L_2})$ for $-\omega \oplus \omega_{12}$, where ω and ω_{12} are Kähler forms lying in cohomology classes $([\omega], [\omega_{12}]) = (s\eta_\Sigma + t\theta_\Sigma, s\eta_{\Sigma_{L_1L_2}} + t\theta_{\Sigma_{L_1L_2}})$ for $s, t > 0$.

Furthermore, for $n = 2$, if ω is nearly symmetric for a complex structure j on Σ which is sufficiently stretched along L_1 and L_2 , then $V_{L_1} \circ \bar{V}_{L_2}$ and $V_{L_2} \circ \bar{V}_{L_1}$ are

Hamiltonian isotopic to $L_1 \times L_2$ in $(Sym^2(\Sigma), \omega)$.

The proof will be obtained by generalizing the construction of Lagrangian correspondences and their related properties worked out by Perutz in [31] to families of such. Therefore, we will find it convenient to use the machinery developed in [31]. In order to have a self-contained exposition, we will borrow the statements of some of the lemmas in [31], however for proofs of these lemmas we refer the reader to [31]. The statement of the theorem has an obvious generalization to composition of k Lagrangians. The proof we give below easily adapts to that case. At the end of each step, we indicate the necessary adjustments, and at the end of the proof we state the result for k compositions as a corollary.

Proof. Step 1: We first construct a holomorphic singular fibration $f : X \rightarrow D^2 \times D^2$ with the following properties :

- X is a complex manifold and the fibres of f above $(s, t) \in D^2 \times D^2$ for $s, t \neq 0$ are complex submanifolds homeomorphic to Σ .
- For $t \neq 0$, restricting the fibration to $D^2 \times \{t\}$ in the base, we get a Lefschetz fibration with vanishing cycle L_1 , similarly for $s \neq 0$, restricting the fibration to $\{s\} \times D^2$ in the base, we get a Lefschetz fibration with vanishing cycle L_2 . (Here we fix a complex isomorphism from Σ to the fibre above $(1, 1)$ and the vanishing cycles are the images of L_1 and L_2 on Σ under this identification.)
- The fibre above the origin is a complex submanifold, which is a nodal curve with two nodal singularities obtained from Σ by collapsing both L_1 and L_2 .

Consider first the map $q : \mathbb{C}^2 \rightarrow \mathbb{C}$ given by $(a, b) \rightarrow a^2 + b^2$, and let

$$U = \{x \in \mathbb{C}^2 : |q(x)| \leq 1, \|x\|^4 - |q(x)|^2 \leq c\}$$

Let $Z = \{x \in \mathbb{C}^2 : |q(x)| \leq 1, \|x\|^4 - |q(x)|^2 = 0\}$. Then $q : U \setminus Z \rightarrow D^2$ is a holomorphic submersion whose fibres are pairs of holomorphic annuli. Next construct the map $\tilde{q} : (pr_1^*U) \sqcup (pr_2^*U) \rightarrow D^2 \times D^2$ by pulling back q using the projections $D^2 \times D^2 \rightarrow D^2$ and taking the disjoint union of fibres.

Now, to construct $f : X \rightarrow D^2 \times D^2$, we will glue the fibration $\tilde{q} : (U \times D^2) \sqcup (D^2 \times U) \rightarrow D^2 \times D^2$ to the trivial fibration $(\Sigma \setminus (A_1 \sqcup A_2)) \times D^2 \times D^2$, where A_1 and A_2 are annular neighborhoods of L_1 and L_2 . In order to do this gluing in a way that the resulting manifold X has an integrable complex structure, we now study the fibration on U more explicitly. Namely, let $x = (z_1, z_2)$, then $\|x\|^4 - |q(x)|^2 = 4(\text{Im}(z_1 \bar{z}_2))^2$. Hence $U = \{(z_1, z_2) \in \mathbb{C}^2 : |q| \leq 1, |\text{Im}(z_1 \bar{z}_2)| \leq \sqrt{c}/2\}$. Thus, $U = U^+ \sqcup Z \sqcup U^-$, where $U^+ = U \cap \{|z_1 + iz_2| > |z_1 - iz_2|\}$, $U^- = U \cap \{|z_1 + iz_2| < |z_1 - iz_2|\}$ and $Z = U \cap \{|z_1 + iz_2| = |z_1 - iz_2|\}$. Note that the set Z coincides with the zero set of $\|x\|^4 - |q(x)|^2$ in U . Now, the fibres of U^+ and U^- are annuli (of varying moduli). Consider now U^+ (same discussion applies to U^-) and the holomorphic map $U^+ \rightarrow D^2 \times \mathbb{C}^*$ given by $(z_1, z_2) \rightarrow (z_1^2 + z_2^2, z_1 + iz_2) = (q, w)$. This is a biholomorphism onto $\{|q| < |w|^2 \leq \sqrt{c} + \sqrt{c + |q|^2}\}$. Therefore, if we choose $c \geq 1$ (this may require stretching j on Σ slightly along L_1 and L_2 so that we can still fix a complex isomorphism between Σ and the fibre of f above $(1, 1)$) then U^+ has a holomorphic subbundle, which is identified with $\{(q, w) : 1 < |w|^2 \leq 2\sqrt{c}\}$. Now, to glue $U^+ \times D^2$ to the corresponding end of $(\Sigma \setminus (A_1 \sqcup A_2)) \times D^2 \times D^2$, identify the end of $\Sigma \setminus (A_1 \sqcup A_2)$ with an annulus of inner radius ρ , with $1 < \rho^2 < 2\sqrt{c}$ and glue the product of this annulus with $D^2 \times D^2$ to the holomorphic subbundle of $U^+ \times D^2$ along the region $\{(q, w) : \rho^2 \leq |w|^2 \leq 2\sqrt{c}\} \times D^2$.

Doing this gluing at each end the construction of $f : X \rightarrow D^2 \times D^2$ can be completed. Note that the choice of the gluing parameters ρ at each end is from a contractible

set. Furthermore, X comes equipped with an integrable complex structure for which f is holomorphic and the required properties above are satisfied.

In order to cover the case of k compositions, one constructs a fibration over $D^2 \times \dots \times D^2$ (k times) by pulling back k disjoint copies of U as above and doing exactly the same gluing operation along the boundary components of each U .

Step 2: We now pass to the relative Hilbert scheme of n points for the map $f : X \rightarrow D^2 \times D^2$. This replaces each fibre of f , by the Hilbert scheme of n points on that fibre. Therefore we get, $F : \text{Hilb}_{D^2 \times D^2}^n(X) \rightarrow D^2 \times D^2$, where the fibres above (s, t) are $\text{Hilb}^n(X_{s,t})$, $X_{s,t}$ being the fibre of the map f above (s, t) .

One way to define the relative Hilbert scheme of a family of curves is to define it as the pull back of the “universal” family over the moduli space of curves. These are smooth projective varieties relative to the base. For details of this construction we refer the reader to [31]. Here, we list the properties of $F : \text{Hilb}_{D^2 \times D^2}^n(X) \rightarrow D^2 \times D^2$.

- The total space $\text{Hilb}_{D^2 \times D^2}^n(X)$ is a smooth Kähler manifold where the complex structure J is induced by the complex structure on X .
- $\text{Hilb}^n(X_{s,t}) = \text{Sym}^n(X_{s,t})$ for $s \neq 0$ and $t \neq 0$.
- The critical value set of F above $(0, t)$ for $t \neq 0$ is $\text{Sym}^{n-1}(\Sigma_{L_1})$, and the critical value set of F above $(s, 0)$ for $s \neq 0$ is $\text{Sym}^{n-1}(\Sigma_{L_2})$.

All of these properties follow easily from the case of a relative Hilbert scheme of n points for a D^2 -family of curves, which has been worked out by Perutz in [31], so we do not reproduce the proofs here (the same reasoning applies in the case where one considers fibrations over $D^2 \times \dots \times D^2$). Nevertheless, let us briefly indicate the proof of the fact that the total space is smooth. In fact, note that we can cover

$\text{Hilb}_{D^2 \times D^2}^n(X)$, by open sets of the form $\text{Hilb}_{D^2 \times D^2}^{k_1}(U_1) \times_{D^2 \times D^2} \text{Hilb}_{D^2 \times D^2}^{k_2}(U_2) \times_{D^2 \times D^2} \text{Hilb}_{D^2 \times D^2}^{n-k_1-k_2}(\Sigma \setminus (A_1 \cup A_2))$, where U_1 and U_2 are respectively the components of the domain of \tilde{q} corresponding to L_1 and L_2 . (This was used above to construct the fibration f), and A_1, A_2 are slightly smaller annular regions in U_1 and U_2 respectively. More precisely, we have:

$$\text{Hilb}_{D^2 \times D^2}^n(X) = \bigcup_{0 \leq k_1, k_2 \leq n} \text{Hilb}_{D^2 \times D^2}^{k_1}(U_1) \times_{D^2 \times D^2} \text{Hilb}_{D^2 \times D^2}^{k_2}(U_2) \times_{D^2 \times D^2} \text{Hilb}_{D^2 \times D^2}^{n-k_1-k_2}(\Sigma \setminus (A_1 \cup A_2))$$

Now, each piece appearing above are open smooth pieces, namely they are biholomorphic to either $D^2 \times \text{Hilb}_{D^2}^*(q : U \rightarrow D^2)$ or $D^2 \times D^2 \times \text{Sym}^*(\Sigma \setminus (A_1 \cup A_2))$. Furthermore, we know from [31] that each of these are smooth, and the fibered product in this case is nothing but $\text{Hilb}_{D^2}^{k_1}(U_1) \times \text{Hilb}_{D^2}^{k_2}(U_2) \times \text{Sym}^{n-k_1-k_2}(\Sigma \setminus (A_1 \cup A_2))$.

One more property of $F : \text{Hilb}_{D^2 \times D^2}^n(X) \rightarrow D^2 \times D^2$ concerning the critical value set of F above which follows from the description above is as follows:

- Let S denote the fibre of f above the origin (a curve with two nodal singularities obtained by collapsing L_1 and L_2 to singular points). Then the singular locus of $\text{Hilb}^n(S)$ can be naturally identified to $\text{Hilb}^{n-1}(\Sigma_{L_1,0}) \cup_{\text{Sym}^{n-2}(\Sigma_{L_1 L_2})} \text{Hilb}^{n-1}(\Sigma_{L_2,0})$, where $\Sigma_{L_i,0}$ stands for the nodal curve obtained by collapsing L_1 and L_2 to a point and normalizing only along L_i .

We will write $K = \text{Sym}^{n-2}(\Sigma_{L_1 L_2})$ for the corresponding singular locus in the critical value set of F . Furthermore, let $F_{s,t} \subset \text{Hilb}_{D^2 \times D^2}^n(X)$ denote the fibres of F and let $C_t \subset F_{0,t}$, $D_s \subset F_{s,0}$ denote the fibre-wise critical point sets of F for s and t non-zero. We then set $C_0 = \text{Hilb}^{n-1}(\Sigma_{L_1,0})$ and $D_0 = \text{Hilb}^{n-1}(\Sigma_{L_2,0})$ using the above identification of the singular locus above the origin. We will also make identifications

of $C_1 = \text{Sym}^{n-1}(\Sigma_{L_1})$ and $D_1 = \text{Sym}^{n-1}(\Sigma_{L_2})$.

Now, let $\Omega \in \Omega^2(\text{Hilb}_{D^2 \times D^2}^n(X))$ be a fibre-wise non-degenerate Kähler form in the cohomology class $s\eta_{D^2 \times D^2} + t\theta_{D^2 \times D^2}$. The existence of such a form is the content of Lemma 3.12 in [31]. For large n , one uses the fact that $\text{Hilb}_{D^2 \times D^2}^n(X)$ is the total space of a projective bundle over the relative Picard bundle. (the projective variety fibering over $D^2 \times D^2$ such that each fibre parametrizes torsion-free sheaves of rank 1 and degree n over $X_{s,t}$. See Section 3.3 in [31]). For smaller n , this follows from descending induction (see also Step 7 below for a construction in the nearly symmetric case).

For such an Ω , note that at the cohomological level one has

$$[\Omega|_{\text{Sym}^n(\Sigma)}] = [\omega] \ , \ [\Omega|_{\text{Sym}^{n-1}(\Sigma_{L_1})}] = [\omega_1] \ , \ [\Omega|_{\text{Sym}^{n-1}(\Sigma_{L_2})}] = [\omega_2] \ , \ [\Omega|_{\text{Sym}^{n-2}(\Sigma_{L_1 L_2})}] = [\omega_{12}]$$

Here $\text{Sym}^n(\Sigma)$ is identified with the regular fibre of $F_{1,1}$, $\text{Sym}^{n-1}(\Sigma_{L_1})$ is identified with C_1 , $\text{Sym}^{n-1}(\Sigma_{L_2})$ is identified with D_1 and $\text{Sym}^{n-2}(\Sigma_{L_1 L_2})$ is as before identified with the corresponding stratum K of the singular set above the origin.

- $(C = \bigcup C_t \rightarrow D^2, \Omega|_C, J|_C)$ and $(D = \bigcup D_s \rightarrow D^2, \Omega|_D, J|_D)$ are symplectic Morse-Bott fibrations.

This again follows from the open cover of $\text{Hilb}_{D^2 \times D^2}^n(X)$ of the form $\text{Hilb}_{D^2}^{k_1}(U_1) \times \text{Hilb}_{D^2}^{k_2}(U_2) \times \text{Hilb}^{n-k_1-k_2}(\Sigma \setminus (A_1 \cup A_2))$, as considered above which allows us to reduce to the case of a relative Hilbert scheme of n -points for D^2 -family of curves and that was worked out by Perutz (see Proposition 3.6 in [31]).

Step 3: Next, using Ω we will define parallel transport maps.

Let $\alpha, \beta : [0, 1] \rightarrow D^2 \times D^2$ be the paths defined by

$$\alpha(\tau) = \begin{cases} (1 - 2\tau, 1) & \text{if } \tau \leq \frac{1}{2} \\ (0, 2 - 2\tau) & \text{if } \tau \geq \frac{1}{2} \end{cases}, \quad \beta(\tau) = \begin{cases} (1, 1 - 2\tau) & \text{if } \tau \leq \frac{1}{2} \\ (2 - 2\tau, 0) & \text{if } \tau \geq \frac{1}{2} \end{cases}$$

Now, outside of the critical point set of F , one constructs the parallel transport as usual by considering the horizontal distribution given by the symplectic complement of the vertical bundle with respect to Ω . Namely, let

$$\text{Hor} = \{v : \Omega(v, w) = 0 \text{ for all } w \in TF_{s,t}\}$$

Identify C_1 with $\text{Sym}^{n-1}(\Sigma_{L_1})$ and D_1 with $\text{Sym}^{n-1}(\Sigma_{L_2})$. Along the paths $\alpha, \beta : [0, \frac{1}{2}] \rightarrow D^2 \times D^2$, the set of points that flow from $\text{Sym}^n(\Sigma)$ to $\text{Sym}^{n-1}(\Sigma_{L_1})$ and $\text{Sym}^{n-1}(\Sigma_{L_2})$ defines the Lagrangian correspondences $V_{L_1}^\Omega \subset \text{Sym}^n(\Sigma) \times \text{Sym}^{n-1}(\Sigma_{L_1})$ and $V_{L_2}^\Omega \subset \text{Sym}^n(\Sigma) \times \text{Sym}^{n-1}(\Sigma_{L_2})$.

Let $F|_C : C \rightarrow D^2$ be the symplectic Morse-Bott fibration with fibre C_t . By definition, the Lagrangian correspondence $\bar{V}_{L_2}^\Omega$ is defined by using the connection

$$\text{Hor}_C = \{v \in TC : \Omega|_C(v, w) = 0 \text{ for all } w \in TC_t\}$$

Similarly, let $F|_D : D \rightarrow D^2$ be symplectic Morse-Bott fibration with fibre D_s . Then again by definition the connection

$$\text{Hor}_D = \{v \in TD : \Omega|_D(v, w) = 0 \text{ for all } w \in TD_t\}$$

defines the Lagrangian correspondence $\bar{V}_{L_1}^\Omega$.

In what follows, we will prove that $V_{L_1}^\Omega \circ \bar{V}_{L_2}^\Omega$ is Hamiltonian isotopic to $V_{L_2}^\Omega \circ \bar{V}_{L_1}^\Omega$ for the symplectic form $-\Omega|_{\text{Sym}^n(\Sigma)} \oplus \Omega|_{\text{Sym}^{n-2}(\Sigma_{L_1 L_2})}$. Here we pause to explain why this implies the statement of Theorem B.0.4.

Let us denote $\omega^t = t\Omega|_{\text{Sym}^n(\Sigma)} + (1-t)\omega$. Similarly define ω_1^t , ω_2^t and ω_{12}^t . By Moser's lemma, these induce symplectomorphisms ϕ^t , ϕ_1^t , ϕ_2^t , ϕ_{12}^t . Then, as explained in the proof of Lemma B.0.3 by Theorem A of [31] we have:

$$\begin{aligned} (\phi^1, \phi_1^1)(V_{L_1}) &\simeq V_{L_1}^\Omega \\ (\phi_1^1, \phi_{12}^1)(\bar{V}_{L_2}) &\simeq \bar{V}_{L_2}^\Omega \\ (\phi^1, \phi_2^1)(V_{L_2}) &\simeq V_{L_2}^\Omega \\ (\phi_2^1, \phi_{12}^1)(\bar{V}_{L_1}) &\simeq \bar{V}_{L_1}^\Omega \end{aligned}$$

where \simeq denotes Hamiltonian isotopic. Furthermore, as in Lemma B.0.3, these Hamiltonian isotopies can be arranged so that

$$\begin{aligned} (\phi^1, \phi_{12}^1)(V_{L_1} \circ \bar{V}_{L_2}) &\simeq V_{L_1}^\Omega \circ \bar{V}_{L_2}^\Omega \\ (\phi^1, \phi_{12}^1)(V_{L_2} \circ \bar{V}_{L_1}) &\simeq V_{L_2}^\Omega \circ \bar{V}_{L_1}^\Omega \end{aligned}$$

Therefore, a Hamiltonian isotopy between $V_{L_1}^\Omega \circ \bar{V}_{L_2}^\Omega$ and $V_{L_2}^\Omega \circ \bar{V}_{L_1}^\Omega$ yields a Hamiltonian isotopy between $V_{L_1} \circ \bar{V}_{L_2}$ and $V_{L_2} \circ \bar{V}_{L_1}$.

Now, we return to proving that $V_{L_1}^\Omega \circ \bar{V}_{L_2}^\Omega$ is Hamiltonian isotopic to $V_{L_2}^\Omega \circ \bar{V}_{L_1}^\Omega$. We will drop Ω from the notation, and simply refer to these Lagrangian correspondences by $V_{L_1} \circ \bar{V}_{L_2}$ and $V_{L_2} \circ \bar{V}_{L_1}$. Furthermore, we will write $\Omega|_{\text{Sym}^n(\Sigma)} = \omega$, $\Omega|_{\text{Sym}^{n-1}(\Sigma_{L_1})} = \omega_1$, $\Omega|_{\text{Sym}^{n-1}(\Sigma_{L_2})} = \omega_2$, $\Omega|_{\text{Sym}^{n-2}(\Sigma_{L_1 L_2})} = \omega_{12}$.

To be careful, we have to note that a priori there is no reason why Hor , Hor_C and Hor_D would match up nicely so that one could just homotope the paths α and β to get Hamiltonian isotopies between $V_{L_1} \circ \bar{V}_{L_2}$ and $V_{L_2} \circ \bar{V}_{L_1}$. To ensure that, we will modify the Kähler form Ω to a “good form” in a neighborhood of the origin, generalizing the construction in Proposition 2.17 of [31].

Digression: Morse-Bott tubular neighborhoods and associated symplectic forms

In this digression, we recall some of the necessary aspects of the theory of symplectic Morse-Bott fibrations and apply them to our setting. Our approach is to lay out only the essentials in order to complete the proof of Theorem B.0.4, thus the interested reader is invited to turn to [31] for a more comprehensive exposition of the tools used here.

First, let us describe the local behaviour of the fibration F in a neighborhood of the origin in terms of the normal bundles of $K = \text{Sym}^{n-2}(\Sigma_{L_1 L_2})$ (the codimension 2 part of the singular locus of F above the origin). Recall that $F|_C : C \rightarrow D^2$ and $F|_D : D \rightarrow D^2$ are Morse-Bott fibrations with singular locus equal to K . Let $p_C : N_C \rightarrow K$ and $p_D : N_D \rightarrow K$ denote the normal bundles of K in C and D . Note that these are complex bundles where the complex structures J^{N_C} and J^{N_D} are obtained by linearizing the restriction complex structures $J|_C$ and $J|_D$ where J is the complex structure on $\text{Hilb}_{D^2 \times D^2}^n(X)$. By the holomorphic Morse-Bott lemma one can find a Morse-Bott tubular neighborhood of K in C (resp. D). More precisely, this is a tubular neighborhood embedding $\iota : DN_C \rightarrow C$ from a disc bundle neighborhood of K in N_C such that when restricted to a fibre over a point $x \in K$, $\iota_x : DN_{C,x} \rightarrow C$ is $(J^{N_C}, J|_C)$ -holomorphic and $\iota_x^* \Omega_C$ is a Kähler form, and the fibration p_C (resp. p_D) is represented by its Hessian on each fibre in this tubular neighborhood. (The existence

of Morse-Bott tubular neighborhoods is proved in Lemma 2.4 of [31]). Therefore, in order to study the Kähler structure in a neighborhood of K , one can “linearize” the problem by studying N_C and N_D . These have natural non-degenerate complex quadratic forms, namely the Hessian of $F|_C$ and $F|_D$, hence the structure groups are reduced to $O(2, \mathbb{C})$ (the group of complex isometries with respect to the quadratic forms). Furthermore, the normal bundle N_C has a distinguished totally real subbundle $\{v \in N_C : (D^2F)_{p_C(v)}(v, v) = |v|^2\}$, where $|\cdot|$ denotes the Hermitian metric induced by restriction to fibres of the pull-back Kähler form $\iota^*\Omega$, so the structure group further reduces to the compact subgroup $SO(2)$ (The same statement is true for N_D). Therefore, we can write $N_C = P_C \times_{SO(2)} \mathbb{C}^2$ and $N_D = P_D \times_{SO(2)} \mathbb{C}^2$, where P_C and P_D are principal $SO(2)$ -bundles (orthonormal frame bundles).

Recall that the linear action of $SO(2)$ on \mathbb{C}^2 is Hamiltonian with moment map given by $\mu : \mathbb{C}^2 \rightarrow \mathfrak{so}(2)^*$, $\mu(x) = (\xi \rightarrow \frac{1}{2}(x, \xi x))$. Note that $\mu^{-1}(0) = 0$.

Now choose connection 1-forms $\alpha_C \in \Omega^1(P_C, \mathfrak{so}(2))$ and $\alpha_D \in \Omega^1(P_D, \mathfrak{so}(2))$. These induce associated symplectic forms on tubular neighborhoods corresponding to N_C and N_D given by

$$\Omega_C := p_C^* \omega_{12} + d\langle \mu, \alpha_C \rangle + \omega_{\mathbb{C}^2}, \quad \Omega_D := p_D^* \omega_{12} + d\langle \mu, \alpha_D \rangle + \omega_{\mathbb{C}^2}$$

Recall that we have $\omega_{12} = \Omega|_K$. Now, let $p : N = N_C \oplus N_D \rightarrow K$ be the normal bundle of K in $\text{Hilb}_{D^2 \times D^2}^n(X)$. The above description of N_C and N_D yields $N = (P_C \times P_D) \times_{SO(2) \times SO(2)} \mathbb{C}^4$. Now consider the following associated symplectic form on the tubular neighborhood of K corresponding to N :

$$\Omega_N := p^* \omega_{12} + \kappa(d\langle \mu, \alpha_C \rangle + d\langle \mu, \alpha_D \rangle + \omega_{\mathbb{C}^4})$$

where $\kappa > 0$ is some small real number, which is determined by the following proposition. We are now ready to state the next proposition which will allow us to replace Ω by Ω_N in N . This is a slight generalization of the proposition 2.17 in [31]. For the sake of exposition, here we give a sketch of the proof following closely the proof contained in proposition 2.17. (Note that in the case of composition of k Lagrangians, one would have the deepest singular stratum over the fibre above $(0, \dots, 0)$ identified with $K = \text{Sym}^{n-k}(\Sigma_{L_1 \dots L_k})$ and the normal neighborhood of K would be given as a direct sum of k Morse-Bott tubular neighborhoods. One would then construct associated symplectic forms on this neighborhood as above, and the proof of the below proposition goes through just as well in that case).

Proposition B.0.5. *Let $(F : \text{Hilb}_{D^2 \times D^2}^n(X) \rightarrow D^2 \times D^2, \Omega, J)$ be the relative Hilbert scheme associated to (Σ, L_1, L_2, j) . There is a family of forms $\{\Omega_r\}_{r \in [0,1]}$ such that $\Omega_0 = \Omega$ and $\Omega_1|_N = \Omega_N$ in a neighborhood of K . Furthermore,*

- Ω_r is tamed by J for all r .
- There exist one-forms α_r such that $\frac{d\Omega_r}{dr} = d\alpha_r$ with $\alpha_r|_{\text{Hilb}_{D^2 \times D^2}^n(X) \setminus N} = 0$ and $\alpha_r|_K = 0$.

Proof. First, one proves that one can deform Ω in a Morse-Bott tubular neighborhood of K so that it becomes invariant under unitary gauge transformations in the sense that along K one can arrange that, $\Omega|_{T^{\text{vert}}N} = \kappa\omega_{\mathbb{C}^4}$ where $\kappa > 0$ is a fixed small constant (which we can take arbitrarily small). This is the content of Lemma B.0.6 below, where we set $S = (P_C \times P_D) \times_{SO(2) \times SO(2)} \mathbb{R}^4$ and $g = D^2F$; we refer to Lemma 2.18 in [31] for a proof. (In fact, by adapting the proof of lemma B.0.6 to our case we can arrange that Ω becomes invariant under $SO(2) \times SO(2)$ -gauge transformations only, this would mean $\Omega|_{T^{\text{vert}}N} = s\omega_{\mathbb{C}^2} \oplus t\omega_{\mathbb{C}^2}$ where $s, t > 0$ but we do not need this here.)

Now, fixing the connection 1-forms α_C and α_D , introduce the form $\Omega_N = p^*\omega_{12} + \kappa(d\langle\mu, \alpha_C\rangle + d\langle\mu, \alpha_D\rangle + \omega_{\mathbb{C}^4})$ defined on N and is gauge invariant. Furthermore, note that $[\Omega|_N] = [\Omega_N]$ at the level of cohomology when restricted to N , hence $\Omega|_N = \Omega_N + d\gamma$ for some 1-form γ on N . Note that $d\gamma$ vanishes along K since Ω and Ω_N have been arranged to agree along K by applying Lemma B.0.6 in the previous paragraph. Thus we can arrange for γ to vanish to order 2 along K . This also implies that Ω_N tames J in a neighborhood of K .

Now, let $\chi_\delta : N \rightarrow \mathbb{R}$ be cutoff functions such that for $\delta > 0$, $\chi_\delta(\nu) = \chi(\frac{|\nu|}{\delta})$, where $|\cdot|$ is the norm defined by the Hessian of F on N and $\chi : \mathbb{R}_{\geq 0} \rightarrow \mathbb{R}$ is identically 0 on $[0, 1]$ and 1 on $[2, \infty)$. Since Ω_N and $\Omega_N + d\gamma = \Omega|_N$ tame J in a neighborhood of K (by choosing δ small we can assume that it contains the 2δ -neighborhood of K), by convexity, we conclude that $\Omega_N + \chi_\delta d\gamma$ tames J . Now consider the forms $\Omega_N + d(\chi_\delta \gamma)$. These differ from $\Omega_N + \chi_\delta d\gamma$ by $d\chi_\delta \wedge \gamma$. Choosing δ small, we can make $d\chi_\delta \wedge \gamma$ small within the 2δ -neighborhood of K . Thus we can assure that $\Omega_N + d(\chi_\delta \gamma)$ tames J . Therefore the required family can be obtained by taking the convex combination $\Omega_r = (1 - r)\Omega + r(\Omega_N + d(\chi_\delta \gamma))$. The required properties are now obvious. \square

Lemma B.0.6. (*Perutz [31], see also Seidel [39]*) *Let K be a compact manifold, $S \rightarrow K$ be a real vector bundle with Euclidean metric g , and J an almost complex structure on the total space of $S \otimes \mathbb{C}$ acting by scalar multiplication by i on the fibres of $S_x \otimes \mathbb{C}$. Furthermore, suppose that K is an almost complex submanifold. Let Ω be a symplectic form on the disc-subbundle $U = \{v \in S \otimes \mathbb{C} : g_{\mathbb{C}}(v, v) < R\} \subset S \otimes \mathbb{C}$, compatible with J (where $g_{\mathbb{C}}$ is the hermitian extension of g). Then there is a deformation $\{\Omega_s\}_{s \in [0,1]}$ of Ω through symplectic forms taming J such that $\Omega_s|_K = \Omega|_K$ and Ω_s agrees with Ω near ∂U , $\Omega_0 = \Omega$, and Ω_1 is invariant under unitary gauge*

transformations along K . □

Continuation of the proof of Theorem B.0.4:

Step4: Next, based on Proposition B.0.5 we can assume that Ω is equal to Ω_N in a neighborhood of K . More precisely, Proposition B.0.5 gives the existence of a Ω which is equal to Ω_N in a neighborhood of K and Lemma B.0.3 implies that the constructions of the Lagrangian correspondences $V_{L_1} \circ \bar{V}_{L_2}$ and $V_{L_2} \circ \bar{V}_{L_1}$ do not depend on the choice of Ω up to Hamiltonian isotopy. (One could also say this without invoking Lemma B.0.3, since the conditions on α_r in Proposition B.0.5 imply that the deformation Ω_r induces a Hamiltonian isotopy $V_{L_1}^r \circ \bar{V}_{L_2}^r$).

Now, we argue that we can reduce to the case $\Omega = \Omega_N$. We will put all the constructions in a sufficiently small neighborhood of K in order to work with the good form Ω_N . This will allow us to show that with respect to Ω_N , $V_{L_1} \circ V_{L_2} = V_{L_2} \circ V_{L_1}$ exactly as point sets and this will conclude the proof of B.0.4.

Let $\lambda > 0$ a small real number and identify the fibre above (λ, λ) with $\text{Sym}^n(\Sigma)$ using the parallel transport with respect to Ω along the diagonal path from (λ, λ) to $(1, 1)$ and the identification of $\text{Sym}^n(\Sigma)$ with the fibre above $(1, 1)$. Similarly identify the fibre above $(\lambda, 0)$ with $\text{Sym}^{n-1}(\Sigma_{L_1})$ using the parallel transport along the path from $(\lambda, 0)$ to $(1, 0)$. Now, construct $V_{L_1}^\lambda \circ \bar{V}_{L_2}^\lambda$ using the parallel transport maps from (λ, λ) to $(\lambda, 0)$ to $(0, 0)$. Similarly, one constructs $V_{L_2}^\lambda \circ \bar{V}_{L_1}^\lambda$. Now, as in Lemma B.0.3 and the discussion at the end of Step 3, constructing a Hamiltonian isotopy between $V_{L_1}^\lambda \circ \bar{V}_{L_2}^\lambda$ and $V_{L_2}^\lambda \circ \bar{V}_{L_1}^\lambda$ guarantees the existence of a Hamiltonian isotopy between $V_{L_1} \circ \bar{V}_{L_2}$ and $V_{L_2} \circ \bar{V}_{L_1}$. Therefore, from now on we will assume that we are in a sufficiently small neighborhood of K and we will use the good form $\Omega_N = p^*\omega_{12} + \kappa(d\langle\mu, \alpha_C\rangle + d\langle\mu, \alpha_D\rangle + \omega_{\mathbb{C}^4})$. The proof will be completed once we

prove that $V_{L_1} \circ \bar{V}_{L_2} = V_{L_2} \circ \bar{V}_{L_1}$ (point-wise equality) with respect to Ω_N for λ sufficiently small.

Note that the tangent space of N_C (resp. N_D and $N = N_C \oplus N_D$) has two horizontal-vertical decompositions. The original decomposition we had comes from the fibration $F|_C : C \rightarrow D^2$ and the Kähler form Ω_C which we wrote as $TN_{C,p,t} = T_p C_t \oplus \text{Hor}_{C,p,t}$ where $p \in C_t$. The second decomposition comes from the structure of \mathbb{C}^2 -bundle over K and the choice of α_C . Any vector in $T_{[x,z]}N_C$ can be expressed as the projection of $u^\# + v \in T_{(x,z)}(P_C \times \mathbb{C}^2)$, where $u^\#$ is the unique lift of a vector $u \in T_{p_C(x)}K$ so that $\alpha_C(u^\#) = 0$ and $v \in T_z\mathbb{C}^2$.

The main purpose of introducing Ω_N is that the parallel transport maps for the fibration F preserve the fibres of the normal bundles N_C and N_D viewed as vector bundles over K . More precisely, we claim that $\text{Hor}_C \subset T^{\text{vert}}N_C$, $\text{Hor}_D \subset T^{\text{vert}}N_D$ and $\text{Hor} \subset T^{\text{vert}}N$.

We will prove this for N_C , the proofs for N_D and N are the same. Recall that $\text{Hor}_C = \{v \in TC : \Omega|_C(v, w) = 0 \text{ for all } w \in TC_t\}$, where in our case we have $\Omega|_C = p_C^*\omega_{12} + \kappa(d\langle\mu, \alpha_C\rangle + \omega_{\mathbb{C}^2})$. Take $u_1, u_2 \in T_{p_C(x)}K$ and lift them in unique way to $u_1^\#, u_2^\#$ on $T_x P_C$ so that $\alpha_C(u_i^\#) = 0$. Let $v_1, v_2 \in T_z\mathbb{C}^2$ be vertical vectors, and project $u_1^\# + v_1$ and $u_2^\# + v_2$ to $T_{[x,z]}N_C$, then we have

$$\Omega|_C(u_1^\# + v_1, u_2^\# + v_2) = \omega_{12}(u_1, u_2) + \kappa(\langle\mu(z), d\alpha_C(u_1^\#, u_2^\#)\rangle + \omega_{\mathbb{C}^2}(v_1, v_2))$$

Now, in order to show that $\text{Hor}_C \subset T^{\text{vert}}N_C$, we need to prove that if $u_1^\# + v_1 \in \text{Hor}_{C,[x,z]}$ then $u_1^\# = 0$. Assume otherwise and take $u_2 \in T_{p_C(x)}K$ such that $\omega_{12}(u_1, u_2) \neq 0$, now consider its horizontal lift $u_2^\#$. Note that $u_2^\# \in TC_t$ since in the Morse-Bott tubular neighborhood F is given by its Hessian, and by the Morse-Bott lemma

the derivative of the Hessian of F along horizontal vectors is zero. Now, we have $\Omega|_C(u_1^\# + v_1, u_2^\#) = \omega_{12}(u_1, u_2) + \kappa(\langle \mu(z), d\alpha_C(u_1^\#, u_2^\#) \rangle)$. We claim that by restricting to a smaller neighborhood of K if necessary (by letting λ be smaller), we can ensure that $\Omega|_C(u_1^\# + v_1, u_2^\#) \neq 0$. which contradicts the assumption $u_1^\# + v_1 \in \text{Hor}_C$. Hence it follows that $u_1^\# = 0$ and $\text{Hor}_C \subset T^{\text{vert}}N_C$. To see that $\kappa(\langle \mu(z), d\alpha_C(u_1^\#, u_2^\#) \rangle)$ is small when restricted to a neighborhood of K , observe that $\mu(0) = 0$ (in fact we also have $d\mu(0) = 0$), so in a neighborhood of K this expression will be small. Exactly the same argument shows that $\text{Hor}_D \subset T^{\text{vert}}N_D$ and $\text{Hor} \subset T^{\text{vert}}N$.

Step5: Since the parallel transport respects the normal fibres to K it suffices to show that $V_{L_1} \circ \bar{V}_{L_2} = V_{L_2} \circ \bar{V}_{L_1}$ at each vertical slice of the normal bundle N . Therefore, without loss of generality suppose that K is a point, then around $K = \{0\}$ we can find holomorphic coordinates associated to complex normal bundles $N_C = \mathbb{C}^2$ with coordinates (w_C, z_C) , $N_D = \mathbb{C}^2$ with coordinates (w_D, z_D) such that $F(w_C, z_C, w_D, z_D) = (w_D^2 + z_D^2, w_C^2 + z_C^2)$ and $\Omega_N = \kappa_2^i(dw_C \wedge d\bar{w}_C + dz_C \wedge d\bar{z}_C + dw_D \wedge d\bar{w}_D + dz_D \wedge d\bar{z}_D)$. It is now easy to see that $V_{L_1} \circ \bar{V}_{L_2} = V_{L_2} \circ \bar{V}_{L_1}$. Indeed an explicit calculation of the parallel transport shows that over $\alpha[0, 1/2]$ the set of points collapsing to C_λ is given by

$$\{(w_D, z_D, w_C, z_C) : w_C^2 + z_C^2 = \lambda, w_D^2 + z_D^2 = w_D\bar{w}_D + z_D\bar{z}_D \in \alpha[0, 1/2]\}$$

and over $\alpha[1/2, 1]$ the set of points collapsing to $K = \{0\}$ is given by

$$\{(0, 0, w_C, z_C) : w_C^2 + z_C^2 = w_C\bar{w}_C + z_C\bar{z}_C \in \alpha[1/2, 1]\}$$

It follows that

$$V_{L_1} \circ \bar{V}_{L_2} = \{(w_D, z_D, w_C, z_C) : w_C^2 + z_C^2 = w_D^2 + z_D^2 = w_C \bar{w}_C + z_C \bar{z}_C = w_D \bar{w}_D + z_D \bar{z}_D = \lambda\}$$

Clearly, this expression is symmetric so does not change if we instead used the path β . Hence we conclude that $V_{L_1} \circ \bar{V}_{L_2} = V_{L_2} \circ \bar{V}_{L_1}$.

Step6: (nearly symmetric case) Suppose $(\omega, \omega_1, \omega_2, \omega_{12})$ are nearly symmetric Kähler forms and $n = 2$. We will construct a Kähler form Ω on the total space of $F : \text{Hilb}_{D^2 \times D^2}^2(X) \rightarrow D^2 \times D^2$ such that its restrictions to the regular fibres of F are nearly symmetric. Furthermore, as before Ω will be the associated symplectic form $\kappa(\omega_{\mathbb{C}^2} \oplus \omega_{\mathbb{C}^2})$ on the tubular neighborhood $N_C \oplus N_D = \mathbb{C}^2 \oplus \mathbb{C}^2$ of $K = \{0\}$.

First, pick Ω on $\text{Hilb}_{D^2 \times D^2}^2(X)$ such that $\Omega|_N = \Omega_N$ in a holomorphic Morse neighborhood of $K = \{0\}$ as in Proposition B.0.5. Let $\epsilon > 0$ be sufficiently small so that the image of N under F includes $D^2(\epsilon) \times D^2(\epsilon)$, product of disks of radius ϵ . Let $r : D^2 \times D^2 \rightarrow D^2(\epsilon) \times D^2(\epsilon)$ be the scaling map that sends $(x, y) \rightarrow (\epsilon x, \epsilon y)$. Now, we use r to first pullback the fibration $f : X \rightarrow D^2 \times D^2$, to get a new fibration on X_ϵ , denoted by $r^*f : X_\epsilon \rightarrow D^2 \times D^2$. These two fibrations are diffeomorphic however the pull-back complex structure r^*J on the new fibration differs from the original one. Namely, one could obtain the fibration r^*f as in the construction of the fibration f in Step 1, if one started with an almost complex structure j on Σ which is sufficiently stretched along the vanishing cycles L_1 and L_2 . Thus, passing to the pullback fibration has the effect of stretching the complex structure j along the curves L_1 and L_2 on the initial datum. More precisely, recall the construction of the fibration f from the data (Σ, j, L_1, L_2) as in Step 1, involves first constructing

the standard box neighborhood:

$$U = \{x \in \mathbb{C}^2 : |q(x)| \leq 1, \|x\|^4 - |q(x)|^2 \leq c(j)\}$$

where $q : \mathbb{C}^2 \rightarrow \mathbb{C}$ given by $(a, b) \rightarrow a^2 + b^2$ and identifying holomorphically the fibre of $\tilde{q} : (pr_1^*U) \sqcup (pr_2^*U) \rightarrow D^2 \times D^2$ above $(1, 1)$ with a cylindrical neighborhood of L_1 and L_2 in Σ (where pr_1 and pr_2 are projections to components of $D^2 \times D^2$) and the constant $c(j)$ is determined according to this identification. Note that the circles L_1 and L_2 are identified in each U with the set $q(x) = \|x\|^4 = 1$. Now, the fibre of $r^*\tilde{q}$ above $(1, 1)$ (i.e. the fibre of \tilde{q} above (ϵ, ϵ)) is biholomorphic to a cylindrical neighborhood of L_1 and L_2 in (Σ, j') where the complex structure j' on Σ is obtained from j by an appropriate stretching.

Now, the relative Hilbert scheme of the fibration r^*f is given by the pull back r^*F . Therefore, we can consider the Kähler form $r^*\Omega$ on $\text{Hilb}_{D^2 \times D^2}(X)$, where the latter now denotes the relative Hilbert scheme of the fibration r^*f .

The advantage of this construction is that we can now ensure that the holomorphic Morse neighborhood $N = U \times U \subset \mathbb{C}^2 \times \mathbb{C}^2$ of $K = \{0\}$ for the fibration r^*F can be constructed as the pull-back of the holomorphic Morse neighborhood for the fibration F hence its projection to $D^2 \times D^2$ is onto (here U denotes the standard box neighborhood as above with j sufficiently stretched along L_1 and L_2). Thus, the whole construction of $V_{L_1} \circ \bar{V}_{L_2}$ takes place in the neighborhood N and the form $r^*\Omega = \omega_{\mathbb{C}^4}$ in this neighborhood. Furthermore, in the normal neighborhood coordinates the fibration r^*F is given by $(w_C, z_C, w_D, z_D) \rightarrow (w_C^2 + z_C^2, w_D^2 + z_D^2)$ as before. Moreover, the above identification of $L_1 \times L_2$ translates in these coordinates

to:

$$L_1 \times L_2 = \{(w_D, z_D, w_C, z_C) : w_C^2 + z_C^2 = w_D^2 + z_D^2 = 1, w_C \bar{z}_C = \bar{w}_C z_C, w_D \bar{z}_D = \bar{w}_D z_D\}$$

It is straightforward now to check that this agrees point-wise with the expression of $V_{L_1} \circ \bar{V}_{L_2}$ calculated in Step 5 :

$$V_{L_1} \circ \bar{V}_{L_2} = \{(w_D, z_D, w_C, z_C) : w_C^2 + z_C^2 = w_D^2 + z_D^2 = w_C \bar{w}_C + z_C \bar{z}_C = w_D \bar{w}_D + z_D \bar{z}_D = 1\}$$

Therefore, we conclude that $V_{L_1} \circ \bar{V}_{L_2} = L_1 \times L_2$ for the almost complex structures j on Σ sufficiently stretched along L_1 and L_2 and the Kähler form on $\text{Sym}^2(\Sigma)$ which is the restriction of Ω_N to the fibre of r^*F over $(1, 1)$. For any other nearly symmetric form on $\text{Sym}^2(\Sigma)$ in the same cohomology class as the restriction of Ω_N , one applies Moser's lemma to obtain a connecting symplectomorphism and by carefully choosing the Moser primitives such that the flux of the resulting Lagrangian isotopy is zero, one obtains Hamiltonian isotopic $V_{L_1} \circ \bar{V}_{L_2}$ and $L_1 \times L_2$. It is here that the hypothesis of nearly symmetric forms is essential so that the resulting Lagrangian obtained by flowing $L_1 \times L_2$ is the product of the images of L_1 and L_2 under the flow separately. This completes the proof. \square

Corollary B.0.7. *Let (Σ, j) be a Riemann surface and L_1, \dots, L_k embedded disjoint curves on Σ . Let σ be an element of the permutation group of a finite set with k elements. Then,*

$V_{L_1} \circ V_{L_2} \circ \dots \circ V_{L_k}$ and $V_{L_{\sigma(1)}} \circ V_{L_{\sigma(2)}} \circ \dots \circ V_{L_{\sigma(k)}}$ are Hamiltonian isotopic in $\text{Sym}^n(\Sigma) \times \text{Sym}^{n-k}(\Sigma_{L_1 L_2 \dots L_k})$ for $-\omega \oplus \omega_{12\dots k}$, where ω and $\omega_{12\dots k}$ are Kähler forms lying in cohomology classes $([\omega], [\omega_{12\dots k}]) = (s\eta_\Sigma + t\theta_\Sigma, s\eta_{\Sigma_{L_1 L_2 \dots L_k}} + t\theta_{\Sigma_{L_1 L_2 \dots L_k}})$ for $s, t > 0$.

Furthermore, for $n = k$, if ω is nearly symmetric for a complex structure j on Σ sufficiently stretched along L_1, \dots, L_k , then $V_{L_1} \circ V_{L_2} \circ \dots \circ V_{L_k}$ is Hamiltonian isotopic to $L_1 \times L_2 \times \dots \times L_k$ in $(\text{Sym}^k(\Sigma), \omega)$.

Proof. The proof follows exactly the same steps as in the case of $k = 2$ when one considers the degenerations over $D^2 \times \dots \times D^2$ (k times). At the end of each step in the proof of Theorem B.0.4, we indicated how the proof generalizes to this case. □

Bibliography

- [1] **Y Ai, T Peters** *The twisted Floer homology of torus bundles* (2008)
arXiv:0806.3487
- [2] **S Akbulut, Ç Karakurt** *Every 4-Manifold is BLF* (2008)
arXiv:0803.2297
- [3] **VI Arnold** *The theory of Singularities and Its Applications* (1991) Scuola
Normale Superiore, Pisa
- [4] **D Auroux, S K Donaldson, L Katzarkov** *Singular Lefschetz pencils*,
Geom. Topol. 9 (2005) 1043–1114
- [5] **R I Baykur** *Existence of broken fibrations*, Int. Math. Res. Not. IMRN
(2008) Art. ID rnn101, 15 pp
- [6] **F Bourgeois, Y Eliashberg, H Hofer, K Wysocki, E Zehnder** *Com-
pactness results in symplectic field theory*, Geom. Topol. 7 (2003) 799–888
- [7] **K Cieliebak, K Mohnke** *Symplectic hypersurfaces and transversality in
Gromov-Witten theory*, J. Symplectic Geom. 5 (2007), 281–356

- [8] **S K Donaldson, I Smith** *Lefschetz pencils and the canonical class for symplectic four-manifolds*, *Topology* **42** (2003) 743–785
- [9] **Y Eliashberg, N M Mishachev** *Wrinkling of smooth mappings and its applications. I*, *Invent. Math.* **130** (1997) 345–369
- [10] **D T Gay, R Kirby** *Constructing Lefschetz-type fibrations on four-manifolds* *Geom. Topol.* **11** (2007) 2075–2115
- [11] **R E Gompf, A I Stipsicz** *4-Manifolds and Kirby Calculus* *Graduate Studies in Mathematics* **20**, Amer. Math. Soc. (1999)
- [12] **M Hutchings** *An index inequality for embedded pseudoholomorphic curves in symplectizations* *J. Eur. Math. Soc. (JEMS)* **4** (2002) 313–361
- [13] **S Jabuka, T Mark** *Product formulae for Ozsváth Szabó 4-manifold invariants*, *Geometry & Topology* **12** (2008), 1557–1651
- [14] **A Juhász** *Holomorphic discs and sutured manifolds* *Algebraic & Geometric Topology* **6** (2006), 1429–1457
- [15] **P Kronheimer, T Mrowka** *Knots, sutures and excision* arXiv:0807.4891
- [16] **P Kronheimer, T Mrowka** *Monopoles and three-manifolds* Cambridge University Press (2007)
- [17] **Y Lekili, T Perutz** *A 3-manifold invariant via holomorphic quilts* In preparation.
- [18] **R Lipshitz** *A cylindrical reformulation of Heegaard Floer homology* *Geometry & Topology* **10** (2006) 955–1096

- [19] **R Lipshitz, P Ozsváth, D Thurston** *Bordered Heegaard Floer homology* arXiv:0810.0687
- [20] **G Liu, G Tian** *Floer homology and Arnold conjecture*, J. Differential Geom. **49** (1998) 1–74
- [21] **K Luttinger, C Simpson** *A normal form for the birth/flight of closed self-dual 2-form degeneracies* ETH preprint, unpublished, 1996
- [22] **C Manolescu, C T Woodward** *Floer homology on the extended moduli space* arXiv:0811.0805
- [23] **J McCleary** *A user's guide to spectral sequences*, Cambridge University Press (2001)
- [24] **M B Morin** *Formes canoniques des singularités d'une application différentiables* Comptes Rendus Acad Sci Fr. 260 (1965) 6503–6506
- [25] **Y Ni** *Sutured Heegaard diagrams for knots* Algebraic & Geometric Topology **6** (2006) 513–537
- [26] **P Ozsváth, Z Szabó** *Holomorphic disks and topological invariants for three-manifolds* Annals of Mathematics **159** (2004) 1027–1158
- [27] **P Ozsváth, Z Szabó** *Holomorphic disks and 3-manifold invariants: properties and applications* Annals of Mathematics **159** (2004) 1159–1245
- [28] **P Ozsváth, Z Szabó** *Holomorphic disks, link invariants and the multi-variable Alexander polynomial* Algebraic & Geometric Topology **8** (2008) 615–692

- [29] **P Ozsváth, Z Szabó** *Holomorphic triangles and invariants for smooth four-manifolds*, Adv. Math. **202** (2006) 326–400
- [30] **T Perutz** *Zero-sets of near-symplectic forms* J. Symplectic Geom. 4 (2006) 237–257
- [31] **T Perutz** *Lagrangian matching invariants for fibred four-manifolds:I* Geometry & Topology **11** (2007) 759–828
- [32] **T Perutz** *Lagrangian matching invariants for fibred four-manifolds:II* Geometry & Topology **12** (2008) 1461–1542
- [33] **T Perutz** *A symplectic Gysin sequence* arXiv:0807.1863
- [34] **T Perutz** *Hamiltonian handleslides for Heegaard Floer homology* Proceedings of 14th Gökova Geometry-Topology Conference (2008) 15–35
- [35] **J Rasmussen** *Floer homology and knot complements* PhD thesis, Harvard University (2003).
- [36] **D Salamon** *Seiberg-Witten invariants of mapping tori, symplectic fixed points, and Lefschetz numbers*, Proceedings of 6th Gökova Geometry-Topology Conference. Turkish J. Math. **23** (1999), no. 1, 117–143
- [37] **O Saeki** *Elimination of definite fold* Kyushu J. Math. 60 (2006) 363–382
- [38] **S Sarkar, J Wang** *An algorithm for computing some Heegaard Floer homologies*, to appear in Ann. Math. , arXiv:math.GT/0607777
- [39] **P Seidel** *A long exact sequence for symplectic Floer cohomology*, Topology **42**(2003), 1003–1063.

- [40] **P Seidel** *Floer homology and the symplectic isotopy problem*, D. Phil thesis, University of Oxford, 1997.
- [41] **C H Taubes** *Gr=SW: Counting curves and connections* J. Differential Geom.52 (1999) 453–609
- [42] **M Usher** *The Gromov invariant and the Donaldson–Smith standard surface count* Geom. Topol. 8 (2004) 565–610
- [43] **G Wasserman** *Stability of unfoldings in space and time* Acta Math 135 (1975) 58–128
- [44] **K Wehrheim, C T Woodward** *Functoriality for the Lagrangian correspondences in Floer theory* (2007) arXiv:0708.2851
- [45] **Z Wu** *Perturbed Floer homology of some fibred three-manifolds* Algebraic & Geometric Topology **9** (2009) 337–350